TRAJECTORY AND GUIDANCE ANALYSIS

COMET AND CLOSE-APPROACH ASTEROID MISSION STUDY

FINAL REPORT

VOL. 3

PHILCO

A SUBSIDIARY OF Ford Motor Company

WESTERN DEVELOPMENT LABORATORIES

3875 FABIAN WAY • PALO ALTO, CALIFORNIA

WDL-TR2366
2 January 1965

TRAJECTORY AND GUIDANCE ANALYSIS

COMET AND CLOSE-APPROACH ASTEROID MISSION STUDY

FINAL REPORT

VOLUME 3

Contract JPL 950870
under NAS 7-100

Prepared by

PHILCO CORPORATION
A Subsidiary of Ford Motor Company
WDL Division
Palo Alto, California

Prepared for

Jet Propulsion Laboratory
Pasadena, California

FOREWORD

This document is the final report of work performed on Trajectory and Guidance Analysis by the WDL Division of the Philco Corporation during the Comet and Close-Approach Asteroid Mission Study for the Jet Propulsion Laboratory under Contract JPL 950870. The report covers work performed during the period 2 July 1964 to 2 January 1965.

ACKNOWLEDGMENT

The work in this volume has been performed by Reece Jensen with contributions by Professor Leland E. Cunningham of the University of California to the section on the Preacquisition Phase of a Comet Mission.

SUMMARY

All well-known, short-period comets were surveyed to determine those best suited for a fly-by mission in the time period 1967-1975. The comets selected for additional study, primarily on the basis of required injection energy, were then investigated in more detail to determine guidance requirements, recovery problems and other trajectory characteristics. The guidance problem led to the requirement of performing a preliminary study to define better the orbit of a comet by the use of past observational data. The recovery problem resulted in a requirement for the generation of a comet ephemeris for approximately one year before launch. Analysis of the comet ephemeris together with predicted magnitude data resulted in a possible recovery date for each of the comets. From the accumulated data on each comet, a single mission was selected for comparison with the Mariner-C Mars mission.

A fly-by mission to one of the close-approach asteroids was also investigated. The asteroid Eros was chosen for this mission primarily on the basis of size and energy requirements.

TABLE OF CONTENTS

LIST OF ILLUSTRATIONS

LIST OF TABLES

SECTION 1

OBJECTIVES AND REQUIREMENTS

1.1 OBJECTIVES

The objectives of this investigation were to study the feasibility of comet missions within the time span of 1967-1975. The short-period, well-known comets were surveyed as possible candidates. A major goal of this undertaking was to uncover the problems pertinent to comet missions and pose solutions to these problems. A final objective was to study the feasibility of using an Atlas/Agena boosted Mariner-C spacecraft for any of the comet missions analyzed.

SECTION 2

MISSION SURVEY

2.1 MISSION CONSTRAINTS

To establish boundaries on the analysis, a set of mission constraints was generated to limit the scope of the analysis to comets and launch periods that are commensurate with current vehicle development and existing launch facilities. A list of the imposed trajectory constraints used for selective purposes is as follows:

1.	Launch period:	1967-1975
2.	Booster vehicles available:	a) Atlas/Agena b) Atlas/Centaur
3.	Spacecraft available for Atlas/Agena:	Mariner-C
4.	Launch pad:	AMR
5.	Range safety consideration:	$90^{\circ} < AZ_L < 114^{\circ}$
6.	Hyperbolic excess speed at arrival:	< 15 km/sec.
7.	Time-of-flight limit:	< one year
8.	Communication distances at arrival:	< 2 A.U.
9.	Terminal miss error:	5000 km to 10,000 km

2.2 COMET SURVEY

The preliminary portion of this study was devoted to conducting a general survey of possible comet targets for the time span under consideration, 1967-1975. From results of previous studies [JPL, 1964; STL, 1963], a table of comets to be considered was generated. Using

this table as a starting point, the possibilities occurring each year were analyzed in more detail by using the WDL Quick-Look Program [Philco, 1964]. The results of studying each comet as a potential mission candidate led to evaluating the energy requirements as a function of launch date. Using the energy requirement as a criteria, the comets were segregated into two groups. The first group consisted of comets which were beyond reasonable energies for the given launch vehicles. The second group contained all comets that might make a reasonable mission.

Additional analysis was conducted on the second group to select the strongest possible candidates for comet missions. The results of this analysis are presented in Table 2-1. The realistic comet missions for the time span of interest are shown according to booster requirements, Atlas/Agena and Atlas/Centaur. The five possible missions in the first two rows of the table were those selected for extensive investigation and evaluation. The groups of comets labeled "potential missions requiring additional investigation" contain some relatively high energy missions ($C_3 > 20$ km/sec^2).

2.3 TRAJECTORY CHARACTERISTICS

During the process of scanning the various comets for potential missions, the general behavior of trajectory characteristics for comet missions was also determined. The interesting portions of the trajectory to be discussed are launch and encounter.

2.3.1 Earth-Departure Characteristics

The complete definition of earth-departure characteristics for a typical comet mission depends on two main parameters:

1. The magnitude of the hyperbolic escape velocity ($\vec{V}_{P/E}$)

Table 2-1 Comet Survey (52 Opportunities)

		1966	1967	1968	1969	1970	1971	1972	1973	1974	1975
Possible Missions Investigated in Detail	A/A					Pons-Winnecke			Tuttle-Giacobini-Kresak		
	A/C		Tempel(2)			Kopff				Brooks(2)	
Potential Missions Requiring Additional Investigation			Finlay	Perrine-Mrkos	Honda-Mrkos-Pajdusakova Faye	D'Arrest		Giacobini-Zinner		Finlay Forbes Encke	
Non-Realistic Missions Based on Energy Constraints *		Giacobini-Zinner Neujmin(1)	Arend Borrelly Brooks(2) Encke Forbes Griggs-Skjellerup Harrington Reinmuth Tuttle Tuttle-Giacobini-Kresak Wirtanen Wolf(1)	Schaumasse Schwassman-Wachmann(2)	Coma- Sola Harrington-Abell	Johnson Whipple	Arend-Rigaux Daniel Encke Vaisala Wolf-Harrington Ashbrook-Jackson	Grigg-Skjellerup Neujmin(3) Tempel(2)	Reinmuth (1)	Borrelly Harrington Honda-Mrkos-Pajdusakova Reinmuth(2) Schwassman-Wachmann(1) Schwassman-Wachmann(2)	Perrine-Mrkos Arend

* Poor Earth Position or r_p Too Large

2. The declination of the asymptote to the escape hyperbola measured W.R.T. the earth equatorial plane (DAO).

In turn, the first of the two quantities specified above ($\vec{V}_{P/E}$) is a function of the desired time of flight or heliocentric transfer angle (Ψ) (see Figure 2-1), the latitude (LAT) and radial distance (R_F) of the comet at arrival and the earth-comet phase relationship for the comet and launch date being considered (φ). Hence, the functional relationship may be stated as follows:

$$|\vec{V}_{P/E}| = f_1(\Psi, LAT, R_F, \varphi) \qquad (2\text{-}1)$$

Similarly, the second parameter governing the departure characteristics, namely DAO, may also be expressed as a function of the same parameters:

$$DAO = f_2(\Psi, LAT, R_F, \varphi) \qquad (2\text{-}2)$$

To best see how the individual parameters composing f_1 and f_2 affect $\vec{V}_{P/E}$ and DAO, it is instructive to study the geocentric injection energy curves shown in Figures A-1 through A-5 in Appendix A. First, the time-of-flight or transfer angle dependence is readily seen to be that of changing from one parabolic-shaped energy curve to another with a different minimum. The effect of the comet latitude at arrival for a given time-of-flight curve is to cause the energy to be a minimum when the latitude is near zero, as shown in Figure 2-2. The radial distance of the target at perihelion sets the energy level requirements. This statement is only partially valid because the comet inclination and initial phase also enter into the energy requirements. Figure 2-3 is a representative plot showing the trend of energy requirements as a function of perihelion distance.

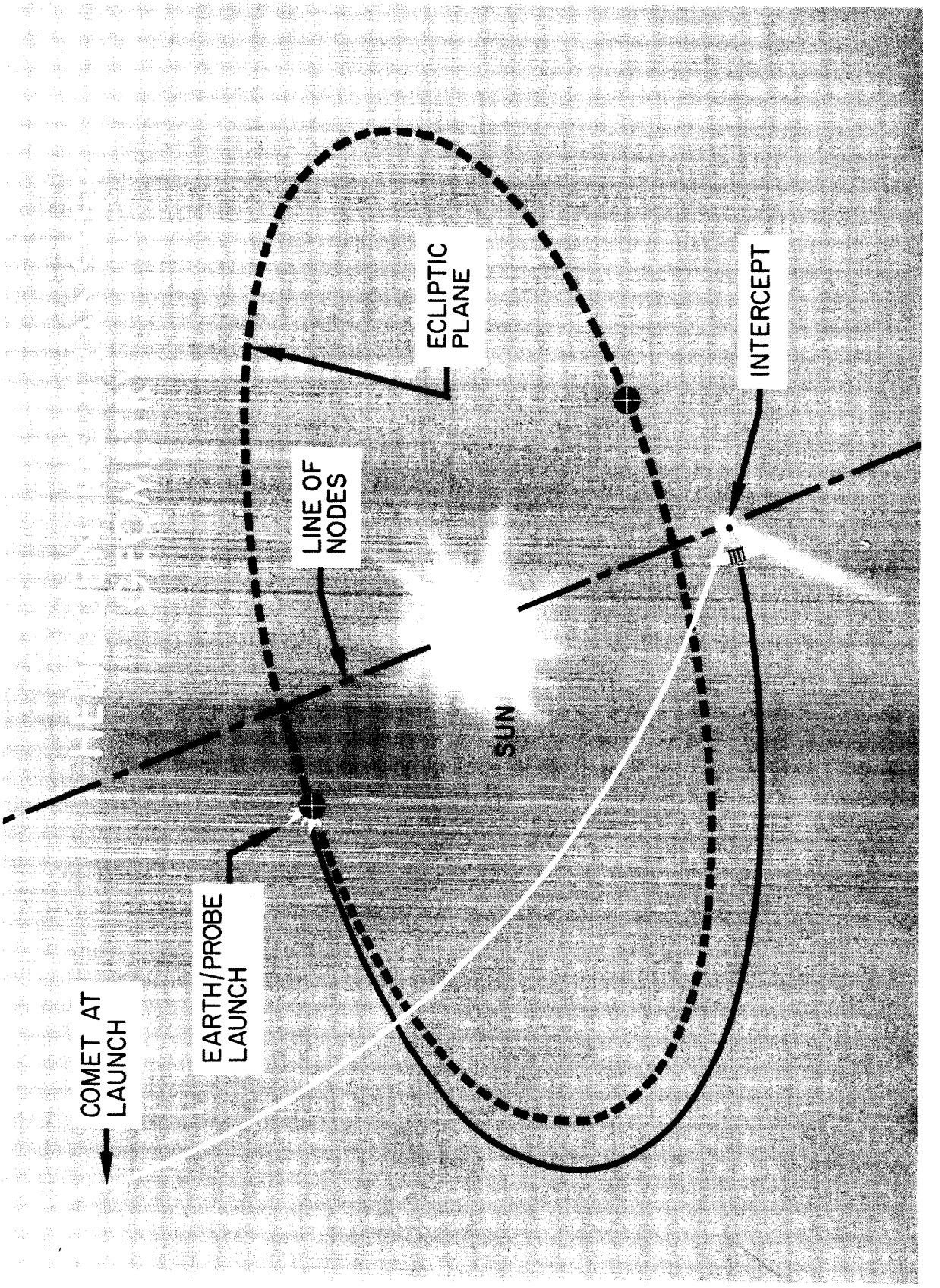
COMET AT LAUNCH
EARTH/PROBE LAUNCH
LINE OF NODES
ECLIPTIC PLANE
SUN
INTERCEPT

Fig. 2-1

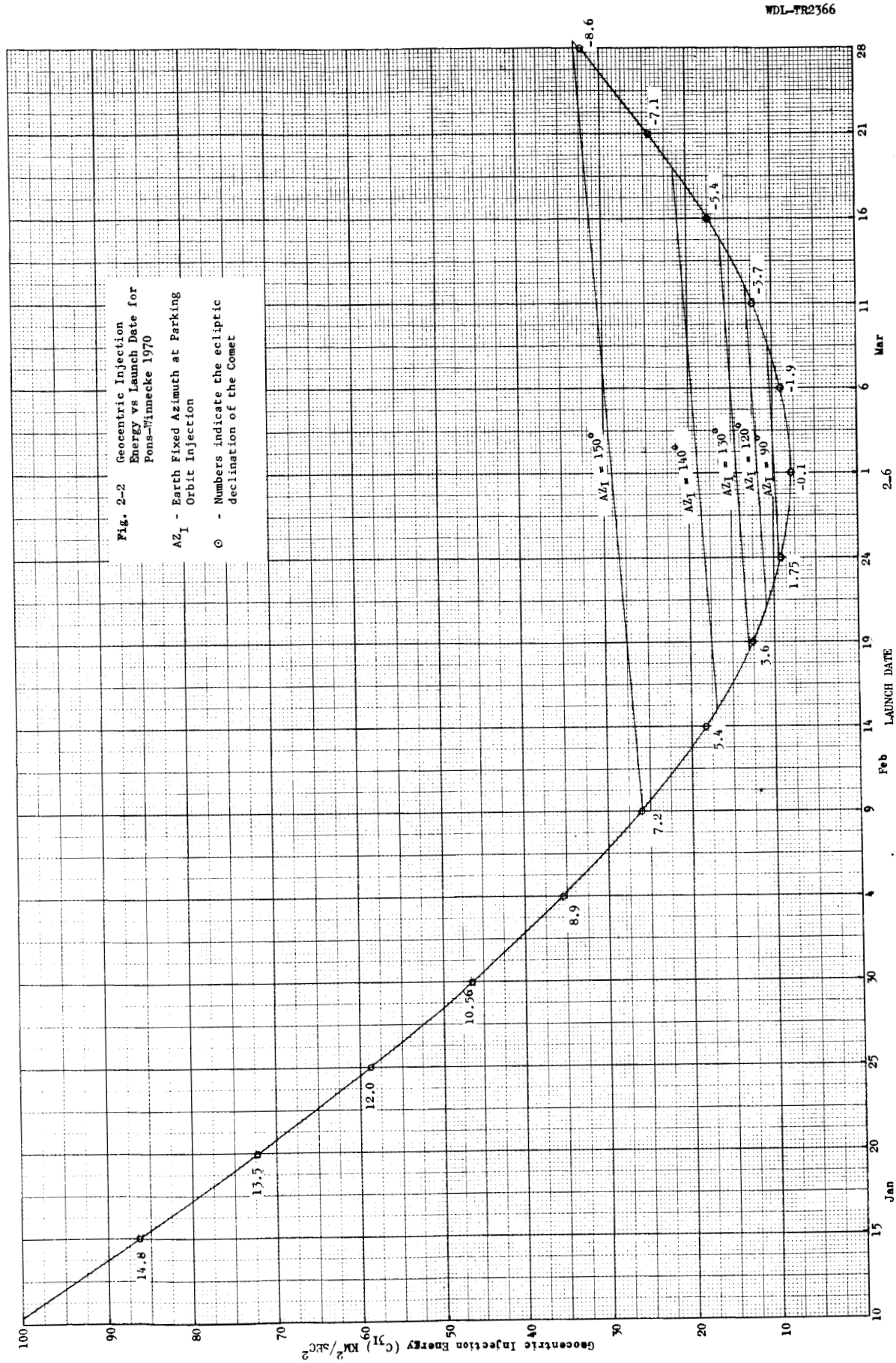
Fig. 2-2 Geocentric Injection Energy vs Launch Date for Pons-Winnecke 1970
AZ_I - Earth Fixed Azimuth at Parking Orbit Injection
⊙ - Numbers indicate the ecliptic declination of the Comet
Geocentric Injection Energy (C_{3I}) KM^2/SEC^2
LAUNCH DATE
Jan
Feb
Mar
AZ_I = 150°
AZ_I = 140°
AZ_I = 130°
AZ_I = 120°
AZ_I = 90°
-8.6
-7.1
-5.4
-3.7
-1.9
-0.1
1.75
3.6
5.4
7.2
8.9
10.56
12.0
13.5
14.8

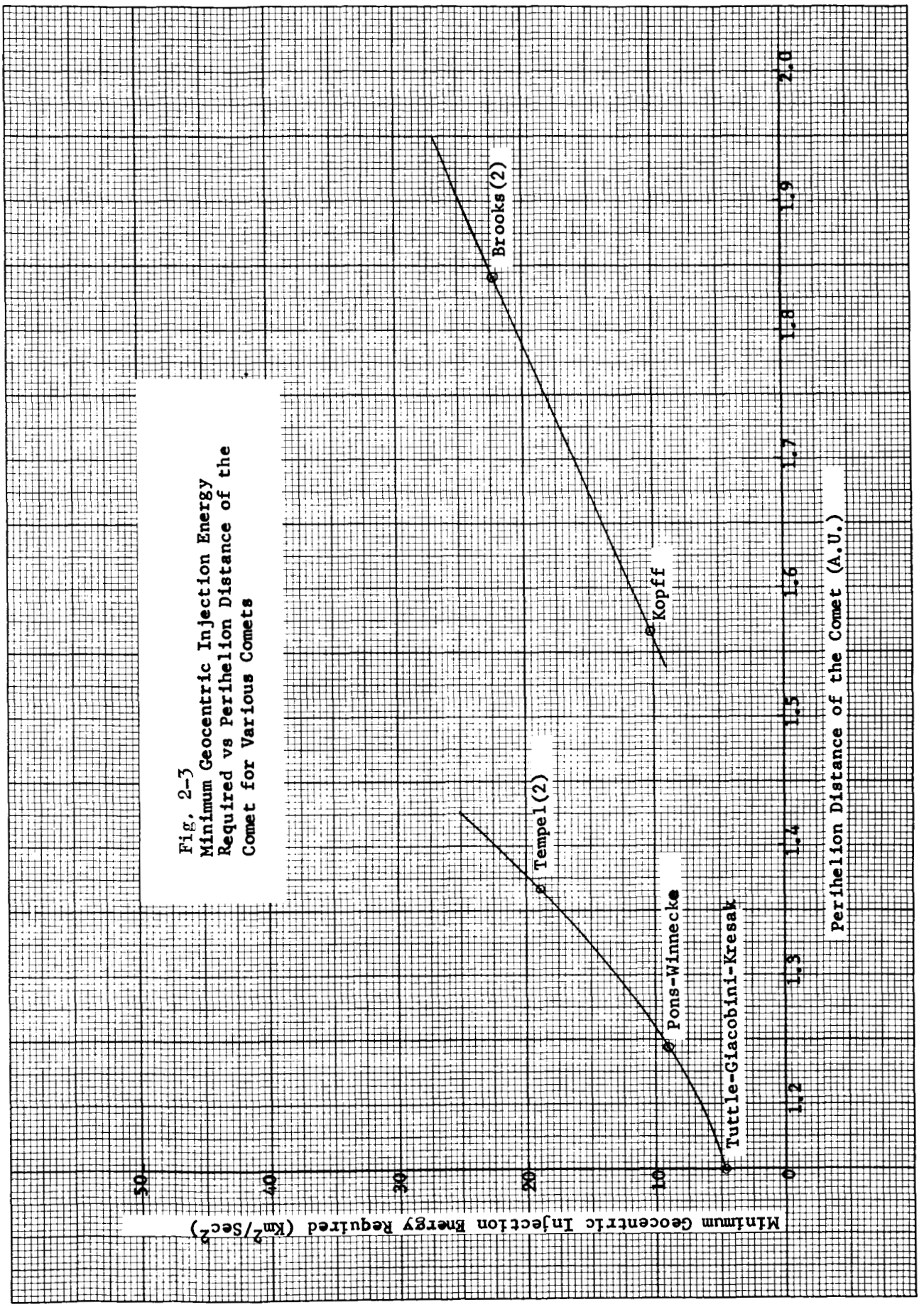

Fig. 2-3
Minimum Geocentric Injection Energy
Required vs Perihelion Distance of the
Comet for Various Comets

Probably the most important feature to observe in the energy curves is that of the shape of the curves and the amount of overlap between successive time-of-flight curves. Take, for example, Pons-Winnecke with very sharp energy curves and little overlapping of successive curves. The sharpness of the curves depicts the amount of time the comet spends between the reasonable latitude bounds. In other words, the inclination of the comet orbit dictates the shape of the curves. The squeezing together or stretching out depends primarily on the proximity of the perihelion of the comet orbit to that of the earth's orbit. If the comet perihelion were tangent to the earth's orbit, there would be a large number of transfer angles and, hence, launch dates which would provide low injection energies. Hence, a broad low-energy curve would result, as is somewhat the case for Pons-Winnecke (1970). The functional dependence on the earth-comet phase relationship is, in reality, an overriding parameter which must be favorable for the comet to be considered as a possible target.

In the case of the second parameter governing the launch characteristics (DAO), it is most important to say that the comet latitude at arrival is the governing factor for this parameter. This can be seen by observing Figure 2-2 which shows for Pons-Winnecke a single energy curve with target-latitude points at arrival superimposed. Also shown are lines of constant launch azimuth. From this curve, it is possible to select an upper bound on the latitude of the target at arrival $\pm 3^{o}$ and, hence, describe the DAO and the launch azimuth required. On Figure 2-2 the lines of constant launch azimuth are defined by the magnitude of the asymptote to the outgoing hyperbola (DAO) and the launch site latitude and launch azimuth. The relationship between the parking orbit plane and the outgoing asymptote is more clearly shown in Figure 2-4. If the escape direction defined by DAO lies outside the cone generated by revolving the parking orbit plane around the earth's axis, then a solution is possible. In the case of most comet missions, the asymptote swings quite rapidly between the two boundaries of the cone; hence, the noticeably small number of launch days for a given time of flight.

FIG. 2-4 PARKING ORBIT LAUNCH GEOMETRY

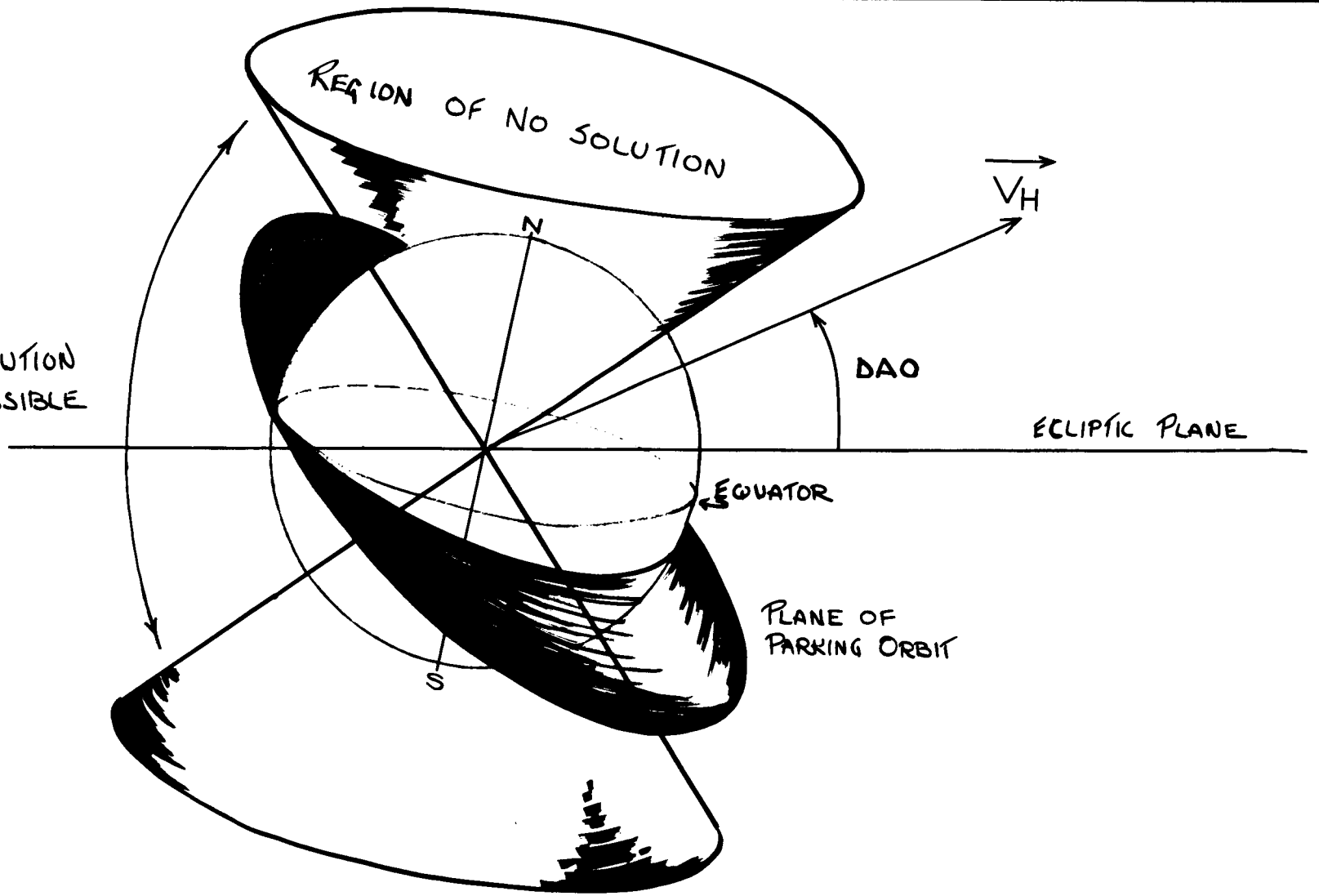

Typical plots of DAO are shown for Type I and Type II* comets in Figures 2-5 and 2-6. A significant point to bring out is that any extended launch window must take into consideration the motion of the asymptote. Hence, motion in launch date is more or less along the minimum-energy envelopes for range-safety controls to be satisfied. This condition does not necessarily apply as stringently to the Class-I comets (low inclination). It is also significant to note that following the minimum-energy envelopes as a function of launch date is equivalent to maintaining a fixed date of arrival. Namely, the arrival date is that of the comet nodal crossing or close thereto.

2.3.2 Arrival Geometry

The arrival geometry is best described in a coordinate system moving with the comet and defined as follows:

Along the velocity direction - $$\hat{V}_C = \frac{\vec{V}_C}{|\vec{V}_C|} \qquad (2\text{-}3)$$

Normal to the comet orbit plane - $$\hat{h}_C = \frac{\vec{R}_C \times \vec{V}_C}{|\vec{R}_C \times \vec{V}_C|} \qquad (2\text{-}4)$$

Approximately towards the sun if comet is at perihelion - $$\hat{R}_C = \hat{h}_C \times \hat{V}_C \qquad (2\text{-}5)$$

Where all quantities are given in sun-centered ecliptic coordinates.

The angular position of the incoming asymptote in this coordinate system is specified by RAI and DAI as shown in Figure 2-7. The magnitude

* Type I and Type II comets refer to low and high inclinations.

Fig. 2-5

Pons Winnecke 1969-70

Launch Date 7001.20
Inclination Angle 21.7°

Magnitude of the Declination of the Outgoing Asymptote vs Launch Date for Various Times of Flight

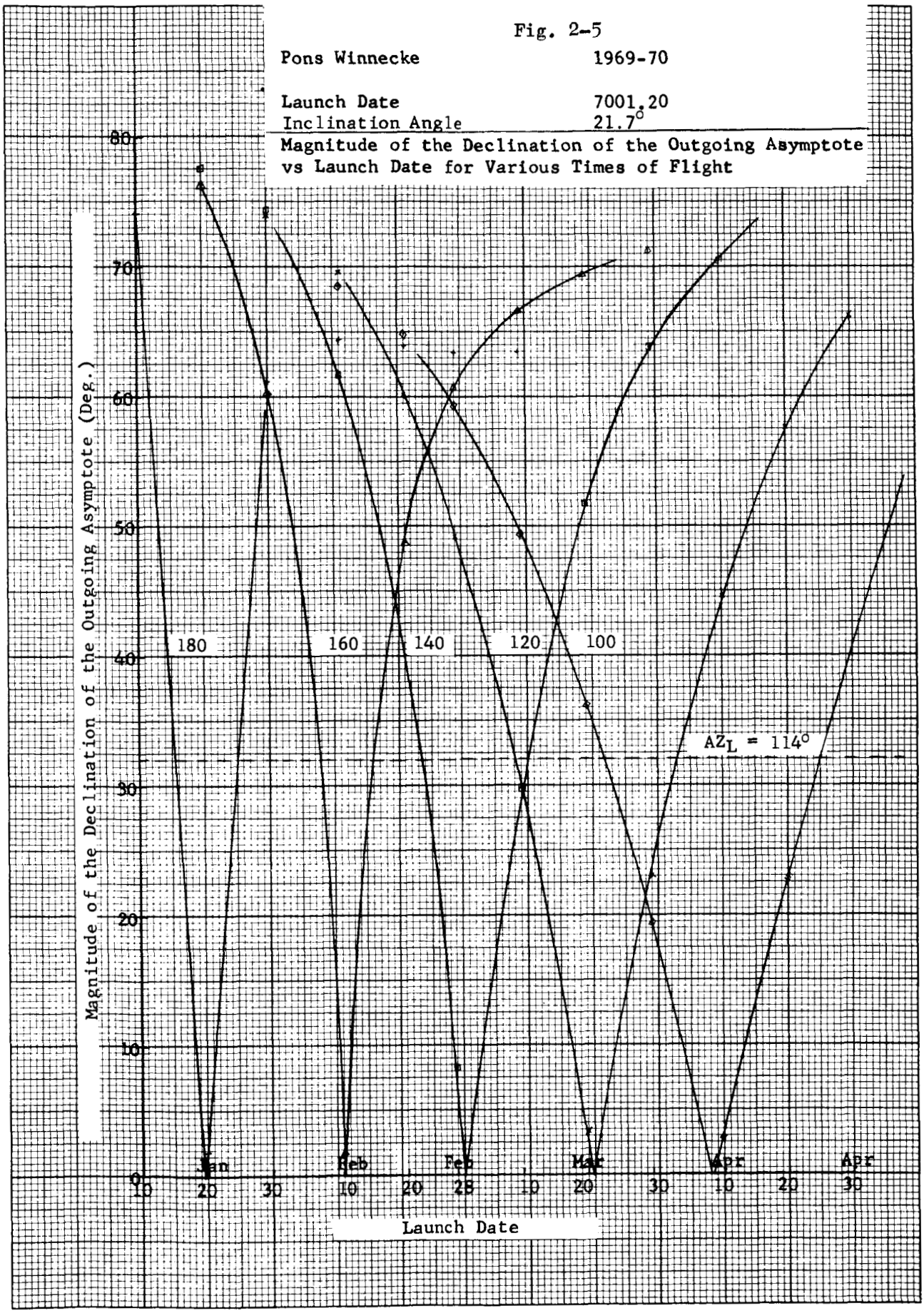

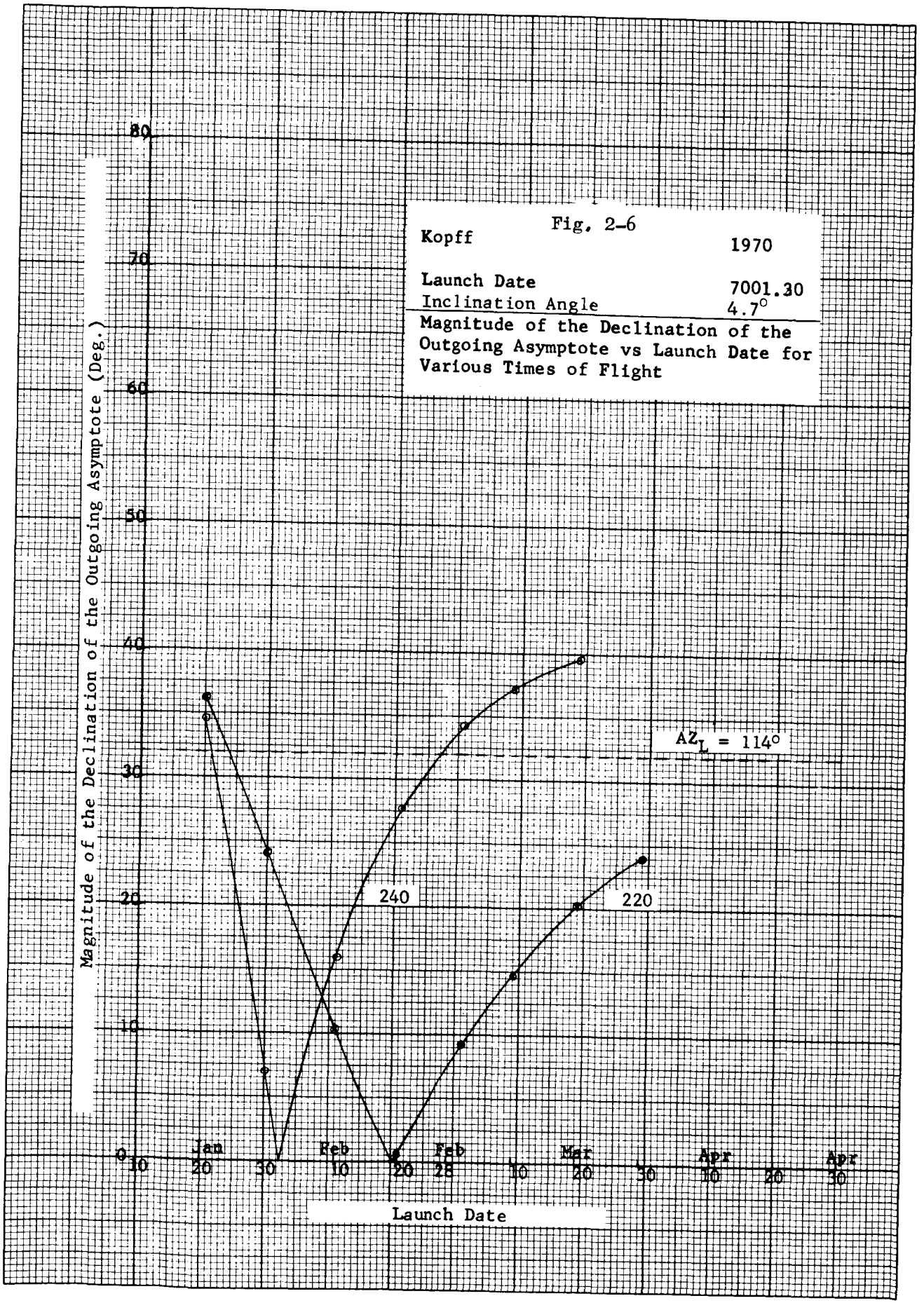
Fig. 2-6
Kopff 1970
Launch Date 7001.30
Inclination Angle 4.7°
Magnitude of the Declination of the Outgoing Asymptote vs Launch Date for Various Times of Flight
Magnitude of the Declination of the Outgoing Asymptote (Deg.)
80
70
60
50
40
30
20
10
0
AZ_L = 114°
240
220
Jan 20
30
Feb 10
20
Feb 28
Mar 10
20
30
Apr 10
20
Apr 30
Launch Date

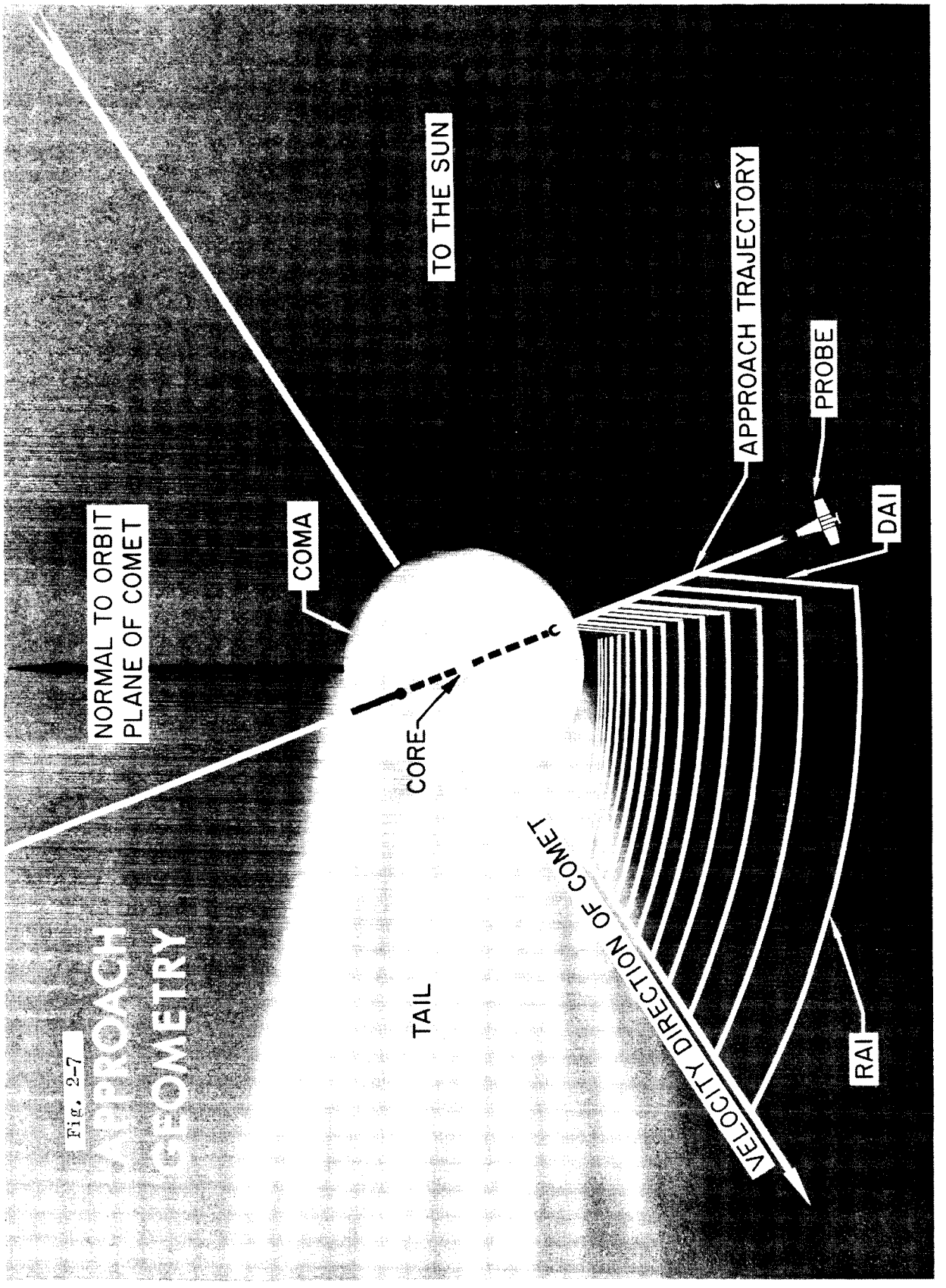
APPROACH GEOMETRY
NORMAL TO ORBIT PLANE OF COMET
COMA
TO THE SUN
APPROACH TRAJECTORY
PROBE
DAI
CORE
TAIL
VELOCITY DIRECTION OF COMET
RAI

Fig. 2-7

of the hyperbolic approach speed as well as the RAI and DAI are shown in Figures A-6 through A-10 in Appendix A for the various comets. The probe generally approaches the comet from the direction the comet is moving. Alternatively, one can say the comet overtakes the probe. The approach geometry is capable of limited adjustment by using time-of-flight and launch date as control parameters.

The main advantage in adjusting the arrival characteristics appears to be in minimizing the approach velocity (V_H) and/or controlling the direction of approach to suit experimental requirements.

2.3.3 Encounter

To achieve the scientific goals of the mission, the intercept should be adjusted such that the comet-vehicle-sun-earth relations are all best suited for the desired encounter geometry. The planar relations at encounter are essentially fixed and only small variations in the spacecraft velocity direction can be achieved by adjusting launch date and injection energy (see Figures A-6 to A-10) Hence, the only control variables remaining are the magnitude and direction of the $\vec{B}$. The $\vec{B}$ vector can be rotated about the $\vec{S}$ vector as desired. In the case of the comet Pons-Winnecke, where RAI is small (4^o), the approach geometry appears as shown in Figure 2-8 for a choice of this $\vec{B}$ along $\hat{T}$. The selection of the target point P has been made on the basis that the spacecraft will pass between the sun and comet and, at the point of closest approach to the comet, the spacecraft will be as near the sun-comet line as possible. Furthermore, the distance of the point P from the comet, $|\vec{B}|$, should be large enough such that errors in the second velocity correction will not allow encounter to take place on the shady side of the comet. The terminal dispersion figure is indicated by the circle around P. A particular set of $\vec{B}\cdot\hat{T}$ and $\vec{B}\cdot\hat{R}$ would be selected for each launch date throughout the launch period. This process is similar to that used on the Mars missions. However, any change in comet uncertainties at some time during the mission will tend to change the target parameters, $\vec{B}\cdot\hat{T}$ and $\vec{B}\cdot\hat{R}$. Hence, a continuous computation of the target point is necessary before accomplishing corrective maneuvers.

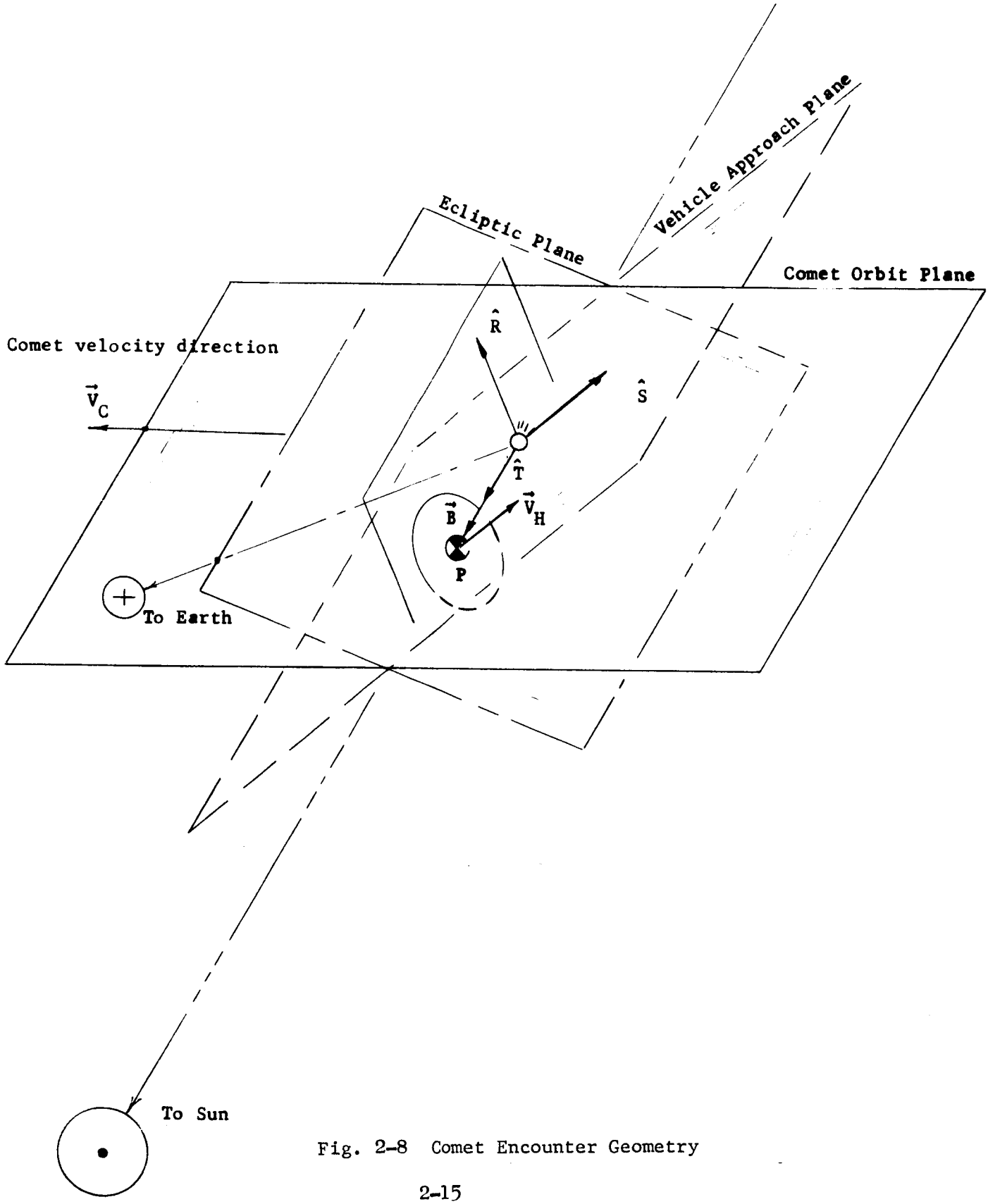

Fig. 2-8 Comet Encounter Geometry

It will be of interest to note the change in knowledge of the comet between recovery and launch shown in Table 4-1 of Section 4. This change in the target vector, as a function of time before launch, amounts to a requirement for instantaneous targeting capability from the booster guidance system. The terminal uncertainty ellipse of the comet at perihelion is in different directions for each of the comets. For the case of near opposition, the uncertainty in the comet position in the radial direction is determined by the A.U.-to-km conversion. For the case of the earth being at quadrature, the most poorly defined error in the comet's position will be distributed between the intrack and radial directions. In any case, the error in the radial direction will be determined from the previous measurements taken and will not exceed 1000 km, which corresponds to determining the perihelion distance in A.U.'s to the 6th significant figure rounded off.

The particular comet of interest should be thoroughly investigated before launch to determine how the biasing of the final aiming point should take place to account for comet uncertainties at perihelion. If we assume the errors in the second velocity correction produce an elliptical dispersion pattern at encounter, then a biasing point to compensate for both the expected comet uncertainties and the second correction uncertainties is required.

SECTION 3

DETAILED TRAJECTORY DATA

3.1 TRAJECTORY CHARACTERISTICS

Each of the five comets selected in Section 2 was investigated in detail according to basic trajectory characteristics, guidance sensitivity and comet sighting. The basic trajectory characteristics generated are the following:

a)	Geocentric injection energy v. launch date	: Figs. A-1 to A-5
b)	Hyperbolic approach velocity vs. launch date	: Figs. A-6 to A-16
c)	RT ascension and declination vs. launch date	
d)	Earth-comet-vehicle angle vs. time of flight	: Figs. A-11 to A-15
e)	Heliocentric trajectory profile	: Figs. A-16 to A-20
f)	Encounter trajectory profile	: Figs. A-21 to A-26

As discussed in Section 2, this information can be used to study the range of approach parameters and how launch windows are selected.

3.2 GUIDANCE PARAMETER

For purposes of guidance calculations, a guidance sensitivity parameter, $\left|\frac{\partial \vec{B}}{\partial \vec{V}}\right|$, was computed along trajectories of different flight times. This guidance parameter may be used to determine the effect of velocity additions at various positions along the trajectory. See Figures A-27 to A-31.

3.3 COMET SIGHTING

To study sighting problems of comets, the ephemeris of comet and earth were generated for one year prior to encounter. A latitude time history of the comet in the vicinity of perihelion also was generated to

understand the relation between perihelion and the crossing of the ecliptic plane. See Figures A-32 to A-41.

SECTION 4

PREACQUISITION PHASE OF A COMET MISSION

4.1 COMET ORBIT DETERMINATION

It has been concluded from all studies and investigations conducted to date that a preacquisition phase must be incorporated into a comet probe mission. Basically, a preacquisition phase, hereafter called Phase 0, is a detailed and thorough investigation of all available observational data for the particular comets of interest. A chronological search of all observations and plates, both reduced and unreduced, should be made with consideration to accuracies attained, equipment used, seeing conditions, reliability of the observer, and any other factors affecting the orbital elements of the comet in question. Some of the photographic plates could be re-measured to assure the accuracies necessary for their utilization in calculating orbital elements. Having accumulated all worthwhile data related to the comets of interest, a numerical fitting and weighting process would be used to fit data from apparition to apparition. Orbit fitting would include three and possibly four or five apparitions, if data were available. This type of work can best be accomplished by an astronomer in the field who is familiar with the data, the observers, and the possible sources of error in the past data. As an indication of the number of observations made and the type of accuracies attained, brief histories of four of the comets under consideration are presented in the following discussion prepared by Dr. Cunningham [1964].

4.2 COMET OBSERVATIONAL DATA

4.2.1 Periodic Comet Tempel (2), 1873 II

Tempel's second periodic comet has been observed at thirteen apparitions since its discovery in 1873.

Apparition of 1946

This comet was not observed at its apparitions in 1935 and 1941. It approached Jupiter closely at its 1943 aphelion, and large perturbations to its orbit resulted. Beart and Henderson computed the approximate values of these, applied them to an earlier orbit of questionable validity and published (B.A.A. Handbook 1946) an ephermeris for 1946. Search with the aid of this ephemeris did not result in the recovery of the comet.

Van Biesbroeck (H.A.C. 745) recovered the comet 1946 May 1 immediately following the receipt of a previously unpublished orbit and ephemeris determined by Ramensky, who had computed his basic orbit from the three apparitions of 1920, 1925 and 1930, and who had taken into account all perturbations including the large ones by Jupiter in 1943.

Ramensky's elements represented the recovery position with residuals of -215", +7" in right ascension and declination, respectively. Cunningham (H.A.C. 747) removed the one in right ascension by adopting a time of perihelion passage 0.07627 days (about 1.8 hours) later than predicted; a residual of only -2" then remained in declination. The ephemeris position by Beart and Henderson differed from the recovery position by about 8 degrees; their predicted time of perihelion passage required a correction of about 12 days. It is doubtful that the comet would have been recovered on the basis of their work.

Cunningham (H.A.C. 747) used the above change of 0.07627 days in the time of perihelion passage, a corresponding change in Ramensky's period and no change in his angular elements to provide a consistent set of elements and an ephemeris. Later (H.A.C. 765) he found that observations made two months after recovery had residuals of -18", -5" in right ascension and declination, respectively, and continued the ephemeris.

At the time of recovery the comet was in good observing position, was about two months before perihelion, and undoubtedly could have been

recovered somewhat earlier, if a correct ephemeris had been available. Van Biesbroeck (A.J. 54, 82) described the comet at recovery as a diffuse coma 10" in diameter and of magnitude 17. Closest approach to the Earth occurred 1946 August 20 at 0.635 A.U. Near this time observers estimated its brightness between magnitudes 8 and 11. The last known observation at this apparition was made 1947 January 15 by Van Biesbroeck, who estimated that the brightness had fallen to magnitude 17.

The following year Cunningham (H.A.C. 842) used most of the observations made during the current apparition to determine new elements; first-order perturbations by Jupiter were included. The root mean square of a single observation error was 2".1.

Apparition of 1951

Cunningham's elements wer used by Goodchild (B.A.A. Handbook 1951) to predict for this apparition. He included approximate perturbations by Jupiter and Saturn.

Cunningham recovered the comet 1951 February 3 with the 60" reflector of the Mount Wilson Observatory. It appeared stellar, magnitude 19.7. Its recovery was fully confirmed the following night with the same instrument. The predicted orbit left residuals of +92", -36" in the recovery position. The residual in right ascension was removed by adopting a time of perihelion passage 0.10858 days (about 2.6 hours) earlier than predicted; a residual of -3" remained in declination. A position by Johnson on 1951 August 29 had residuals of +13", -9" when the revised perihelion date was used. The orbit was not further revised at that time.

Recovery was made nearly 9 months before perihelion at a heliocentric distance of 2.75 A.U.; perihelion distance was 1.39 A.U. An unsuccessful search had been made the previous December and again in January with the same insturment. However, the geocentric distance was large and the position of the comet in the sky was far east just before dawn, and

so it is possible that under favorable circumstances the comet could have been recovered with the 60" a bit farther from perihelion than was the case at this apparition.

Observations were made each month with the 60" until perihelion, after which time the comet was too far west at the end of evening twilight. As late as June the comet still appeared perfectly stellar, although considerably brighter. In the following months diffuseness set in and increased rapidly. The photographs made with the 60" during the nine months of observation are capable of yielding accurate positions, but they have not yet been measured.

Apparition of 1956-57

Luss (B.A.A. Handbook 1956) made unstated revisions to the previous orbit, included approximate perturbations by Jupiter and Saturn, and provided elements and an ephemeris for 1956.

Van Biesbroeck (U.A.I.C. 1554) recovered the comet 1956 May 5 with the 82" reflector of the McDonald Observatory; magnitude 19. The predicted orbit left a residual of about one minute of arc in the recovery position. It was not revised.

Recovery was made nine months before perihelion at a heliocentric distance of 2.81 A.U.; perihelion distance was 1.37 A.U. Thus recovery was made at almost the same point in the orbit as in 1951. However, the reported brightness was much above the limit of the 82" or even the 60", and presumably the comet might have been recovered earlier, if the attempt had been made.

The comet quickly moved into and remained in a poor position in the sky. The only observations known for this apparition are those by Van Biesbroeck 1956 May 5-9.

Apparition of 1961-62

Marsden (B.A.A. Handbook 1961) used the elements by Luss for the previous apparition, included approximate perturbations by Jupiter and Saturn, and provided elements and an ephemeris for 1961.

Miss Roemer (U.A.I.C. 1757) recovered the comet 1961 March 19 with the 40" reflector of the U. S. Naval Observatory, Flagstaff Station. It was stellar in appearance, magnitude 20.5. She stated that a correction of +0.4 days to the predicted date of perihelion passage would well represent the recovery positions. This recovery was made 14 months before perihelion and at a heliocentric distance of 3.54 A.U. - far earlier than at any previous apparition. The comet was at opposition in a northern declination, and this coupled with the excellent sky in Flagstaff (which permits an exposure four times longer than on Mount Wilson) explain the earlier recovery with a smaller instrument.

The comet was well observed, reached magnitude 12, and was last observed by Miss Roemer 1962 December 20 at magnitude 20.1. Total period of observation was 21 months.

4.2.2 Periodic Comet Pons-Winnecke, 1819 III

The Pons-Winnecke periodic comet has been observed at sixteen apparitions since its discovery in 1819.

Apparition of 1951

Calway and Porter (B.A.A. Handbook 1951) provided elements and an ephemeris for this apparition. Perturbations by four planets were included. They based their prediction on a semi-definitive orbit by Porter (M.N. 109, 254, 1949) who used observations covering an arc of 126 days in 1945, and linked to a definitive orbit for the 1939 apparition.

Cunningham recovered the comet 1951 February 3 with the 60" reflector of the Mount Wilson Observatory. It appeared stellar, magnitude 19.7. The predicted orbit left residuals of +326", -141" in the recovery position. The residual in right ascension was removed by adopting a time of perihelion passage 0.2631 days earlier than predicted; a residual of -37" remained in the declination. No other revisions were made at that time, and observations near the time of perihelion passage 1951 September 8 had residuals of about 300".

Recovery was made 217 days before perihelion passage. The distance of the comet from the Sun at recovery was 2.61 A.U., and from the Earth 1.75 A.U. The observed magnitude 19.7 thus corresponds to an absolute magnitude of 16.4 for the comet's nucleus.

Apparition of 1957

The position of the comet relative to the Sun made observations during this apparition essentially impossible, and the comet was not recovered.

Apparition of 1963-64

Cunningham observed this comet for some nine months following his recovery of it in 1951. These observations were made the basis of a new orbit by Marsden (B.A.A. Handbook, 1963) who combined them with a few other observations, linked the mean motion back to 1945, and applied perturbations by Earth, Jupiter and Saturn to predict elements and an ephemeris for 1963-64.

Recovered by Miss Roemer (U.A.I.C. 1859) 1964 February 19, and confirmed by her on March 14 and 15. The predicted date of perihelion passage needed a correction of about +1.2 days. No improvement of the predicted orbit has yet been made. Perihelion was on 1964 March 23. The comet was too close to the Sun to have been recovered much earlier.

After perihelion it remained in good observing position, and is still under observation (most recent observation 1964 September 4).

4.2.3 Periodic Comet Kopff, 1906 IV

This comet was discovered in 1906, missed in 1912, and observed at each apparition since then.

Apparition of 1951

Predictions for this apparition were made by Beart and Julian (B.A.A. Handbook 1951) and by Kepinski (U.A.I.C. 1299). The starting orbit used by Beart and Julian was based in part on the 1945 ephemeris of Kepinski, who later stated (U.A.I.C. 1299) that a considerable correction was subsequently applied to those elements. However, the recovery position (see next paragraph) indicated a correction of -2.2 days to Kepinski's predicted date of perihelion passage, and a correction of only +0.4 days to that of Beart and Julian. Kepinski's earlier and later work on the orbit of this comet is far more accurate than the above, and his temporary low accuracy is fully explained by the loss of all of his work 1924-44 in the Warsaw insurrection of August 1944.

Jeffers recovered the comet 1951 April 12. He described it as not quite stellar, magnitude 18.7. Heliocentric distance was 2.35 A.U., geocentric distance 1.38 A.U. Thus the absolute magnitude of the nuclear condensation (rather than of the nucleus itself) was about 16.1.

Apparition of 1957-58

Predictions were made by Sumner (B.A.A. Handbook 1957) and by Kepinski (U.A.I.C. 1571, 1598, 1642). A close approach to Jupiter in 1954 produced large perturbations.

Van Biesbroeck announced the recovery of this comet 1957 February 20, but this proved to be incorrect.

Due to a poor observing position near the Sun, the comet was actually not recovered until 1958 June 25, when Miss Roemer observed it far east at the beginning of dawn. Not stellar, magnitude 18.8. She continued to observe it through 1958 October 8 at magnitude 20.8 (heliocentric distance 2.80, geocentric distance 1.85), and even photographed a trace of it 1958 December 4 at magnitude 21.5 (heliocentric distance 3.11, geocentric distance 2.34). These observations are consistent in yielding an absolute magnitude of 17.2 for the tiny nuclear condensation. This is 1.1 magnitudes fainter than the earlier estimate above, but the proper absolute magnitude to be used for a very early recovery may be still a little fainter yet.

The error in Kepinski's ephemeris was about 3', but the variations for converting this to an error in the time of perihelion passage are not immediately available.

Apparition of 1963-64

Predictions were made by Egerton, Ainslie and Calway (B.A.A. Handbook 1963) and by Kepinski (U.A.I.C. 1849). Their predicted times of perihelion passage differ by 2.65 days.

Recovered by Miss Roemer 1963 December 18. Not quite stellar, magnitude 18.8. Heliocentric distance 2.13 A.U., geocentric distance 2.76 A.U. Corresponding absolute magnitude is 15.0. The recovery was made at a point in the orbit a little nearer to perihelion than was the case in 1951 when the absolute magnitude was found above to be 16.1. All of the observations including those in 1958 made on the outward branch of the orbit agree in showing that the absolute magnitude changes with the position in the orbit even when the comet is far from perihelion. This result is also consistent with the non-stellar images that were always

noted by the observers.

The prediction by Kepinski proved to be far more accurate than the one by Egerton, Ainslie and Calway. The error in Kepinski's predicted time of perihelion passage was only 0.10 days.

This comet is still under observation (most recent 1964 August 30, magnitude 16) and will probably continue to be observed into the first part of 1965.

4.2.4 Periodic Comet Brooks (2)

Brooks' second short-period comet has been observed at each apparition except one since its discovery in 1889.

Apparition of 1946

Cripps (B.A.A. Handbook 1946) provided elements and an ephemeris for this apparition.

Jeffers (U.A.I.C. 1050) recovered this comet 1946 June 28 some two months before perihelion. Magnitude 18. The residuals from Cripps' prediction were +294", +84". Cunningham (H.A.C. 761) removed the one in right ascension by adopting a time of perihelion passage 0.1995 days earlier than the predicted one; a residual of only -1" remained in declination. Observations continued through November 1946.

Apparition of 1953

Goodchild (B.A.A. Handbook 1953) used Cunningham's elements of 1946, applied perturbations by Jupiter and Saturn, and provided elements and an ephemeris. The resulting elements were correct, but an error was made in the computation of the ephemeris. Porter, Harris and Wheel (U.A.I.C. 1400) provided a corrected ephemeris from the same elements.

Jeffers (U.A.I.C. 1410) recovered the comet 1953 June 18 again some two months before perihelion. Magnitude 18. The residuals from Goodchild's elements were +127", +35". Cunningham (H.A.C. 1237) removed the one in right ascension by adopting a time of perihelion passage 0.095 days earlier than the predicted one; a residual of only -1" remained in declination.

Apparition of 1960-61

Dubiago (B.A.A. Handbook 1959, U.A.I.C. 1736) applied perturbations by Jupiter and Saturn to give ephemerides for this apparition.

Recovered by Miss Roemer (U.A.I.C. 1736) 1960 August 4 about two months past perihelion. Magnitude 18. Last observed by her 1961 January 8 at magnitude 19.0 and February 9 at magnitude 20.2; described as not quite stellar. The first of these late positions gives an absolute magnitude of 16.1; the latter 16.6.

4.3 JUSTIFICATION FOR PHASE-0 STUDY

The task depicted for Phase 0 is a 6-month to one-year effort conducted at least 1 to 2 years after the last apparition. This time delay allows for collecting and reducing all data taken during the previous apparition.

The question: "Why accomplish a Phase-0 study?" has not been fully answered. Column 1 of Table 4-1 gives some indication of the realistic initial uncertainties that are expected for the comets if no prior orbit fitting work or integration is accomplished. It is true that these uncertainties can be reduced for a particular apparition if sufficient observations are made after acquisition. However, the complications of launching a month or two after acquisition means that the comet uncertainty is still likely to be large and would require large compensating velocity corrections. A more realistic approach is to use

Table 4-1 Predicted Comet Positional Uncertainties at Perihelion

Comet	Initial Acq. Uncertainty W/O Orbit Refinement	Initial Acq. Uncertainty With Orbit Refinement	Comet Uncertainty At Time Of Launch	Comet Uncertainty At Time of 1st Correction		Comet Uncertainty At Time of 2nd Correction *		Uncertainty At The Time of Arrival in KM ($\widehat{4}$ ")*
				30^d After Injection	60^d After Injection	40^d Before Arrival	20^d Before Arrival	
Tempel (2)	1.5^d	1^h	10^m	4^m	3^m	$\widehat{4\text{-}8}$ "	$\widehat{2\text{-}4}$ "	1200
Pons - Winnecke	4^d	3^h	30^m	10^m	7^m	$\widehat{4\text{-}8}$ "	$\widehat{2\text{-}4}$ "	1800
Kopff	1^d	2^h	30^m	10^m	7^m	$\widehat{4\text{-}8}$ "	$\widehat{2\text{-}4}$ "	5300
Brooks (2)	0.5^d	1^h	10^m	4^m	3^m	$\widehat{4\text{-}8}$ "	$\widehat{2\text{-}4}$ "	5800

* As viewed from the Earth.

existing data which contain sufficient accuracy to produce the predicted acquisition accuracies shown in column 2 of Table 4-1 [Cunningham, 1964]. As is evident from the remaining columns of the table, the guidance problem due to comet uncertainty is greatly diminished once the preacquisition analysis has been accomplished and incorporated into the mission plan.

Other factors in favor of a Phase 0 study are the following:

a. Reduced reliance on observatories, both before and after launch. (Probably one pair of observations would be made each new moon).

b. Capability to launch before the comet has been acquired. There is absolutely no reason that a launch could not take place before comet acquisition if a thorough Phase-0 study has been completed.

c. Reduced fuel expenditures due to both the smaller uncertainties of the comet and the possibility of earlier first and second corrections.

d. Possibility of mission failure because of the lack of observational data or because of adverse observational conditions (cloud over, etc.) is greatly reduced. The mission could be a partial success if only 3 or 4 observations were obtained.

4.4 UPDATING THE COMET ORBITAL ELEMENTS

After an initial set of orbital elements have been determined in a Phase 0 study they must be propagated by numerical integration to the epoch of perihelion desired. This problem of generating the orbital elements of the comets for the epochs of interest was investigated for two of the comets. In particular, the two comets, Tempel (2) and Kopff, were investigated by using orbital data for the apparitions in late 1950's (see Tables B-7 and B-8). The integration was initiated at this epoch and, hence, carried

forward approximately four apparitions (1978). The JPL Space Trajectory Program was used to carry out the integration. At the next apparition after initiating the integration, the results were compared with actually observed data to determine if the starting elements and the program produced expected results. The comparison is presented in Tables B-7 and B-8, and shows excellent agreement with observational data. It also shows that the starting orbital elements used by IITR for Kopff were not correct and, hence, the notable change in the date of perihelion passage in 1970 (4 days).

The results indicate that the orbital elements of the comets at any future epoch may be determined readily from current elements by numerical integration. However, the accuracy of future orbital elements is generally worse than the accuracy of the starting elements. The secular non-gravitational effects are not easily accounted for in the numerical integration. However, the existence of such non-gravitational forces on comet motions is a question yet to be fully explained and answered. The general consensus of opinion is that <u>if</u> these forces do exist, then they are extremely small ($\Delta T_p \leq 1^h$) and, most likely, act like a repetitive bias for each apparition.

SECTION 5

PRELAUNCH PHASE

5.1 COMET RECOVERY

An analysis of the comet motion before launch was conducted to determine possible recovery times for each comet target. The significant parameters considered in determining recovery times and positions are as follows:

a. Distance of comet from the earth

b. Distance of comet from the sun

c. Earth-sun-comet angle histories

d. Declination of the comet W.R.T. the equator

e. Prior recovery data pertaining to magnitudes and distances at which the comet was recovered

A pre-launch and post-launch ephemeris for each of the possible comet targets and earth are presented in Figures A-32 to A-36 in Appendix A. The positions of comet and earth are numbered consecutively for increasing date. Additional data for each of the numbered positions of the comet are provided in Tables B-1 to B-5 in Appendix B. As a general rule, recovery of the comet may not take place beyond 21st magnitude. However, with a Phase-0 study adequately accomplished, most of the comets could be recovered at 21st magnitude by the Mt. Palomar 200-inch or Mt. Hamilton 120-inch telescopes. For 20th magnitude observation the Mt. Wilson 100-inch telescope could be used together with the Flagstaff 40-inch telescope. In the case of Tempel (2), no problems are anticipated for a recovery at least three months before launch. The comet will be in excellent position for viewing and will be sufficiently

bright for detection on January 10, 1967. In the case of Pons-Winnecke, recovery is possible on December 1, 1969; this provides for more than one month of comet observation before launch on January 11, 1970. For comet Kopff, it is not likely that recovery can take place much before the middle of December 1969 (at 21st magnitude). Recovery at that time will allow 1.5 months of observation before launch. The Comet Tuttle-Giacobini-Kresak is a fainter comet than Kopff; however, the characteristics of this comet cause it to brighten up at fairly close distances to the sun. The result of the late brightening of this comet makes earlier recovery a fairly difficult problem. It is therefore unlikely that this comet will be recovered until three months after launch. Brooks (2) appears to be recoverable at approximately the same date the vehicle is to be launched. A summary of comet recovery lead times is shown in Table 5-1.

Table 5-1 Comet Recovery Table

COMET	PREDICTED DATE OF RECOVERY	PREDICTED DATE OF LAUNCH	LEAD TIME (MONTHS)
Tempel (2)	Jan. 10, 1967	Apr. 10, 1967	3
Pons-Winnecke	Dec. 1, 1969	Jan. 31, 1970	2
Kopff	Dec. 15, 1969	Feb. 1, 1970	1½
Tuttle-Giacobini-Kresak	Jan. 6, 1973	Oct. 5, 1972	-3
Brooks (2)	May 4, 1973	May 4, 1973	0

SECTION 6

GUIDANCE ANALYSIS

6.1 VEHICLE AND COMET ERROR PROPAGATION

The approach taken to compute the velocity requirements for a comet mission was to consider two separate sources of error. The first source of error considered was the booster. For purposes of consolidating the booster errors, the covariance matrix of injection errors (Λ_I) for the Atlas/Centaur was obtained [Elconin and Kohlhase, 1964]. The covariance matrix was expressed in an azimuth-independent plumb-bob coordinate system and is valid up to injection energies of 15 km^2/sec^2. The first operation was to transform the Λ_I matrix into the Cartesian coordinate system used for integration purposes. Hence, the transformation matrix [H] was computed where

$$[H] = \left[\frac{\partial \vec{X}_{INERTIAL}}{\partial \vec{Y}_{PLUMB-BOB}} \right]. \tag{6-1}$$

Then, the Λ_I matrix was transformed into inertial Cartesian coordinates as follows:

$$\Lambda_{I_{CARTESIAN}} = [H][\Lambda_I][H^T]. \tag{6-2}$$

Next, the injection covariance matrix was propagated along a reference spacecraft trajectory to the terminal point by using the transition matrix [Φ].

$$\Lambda_F = [\Phi_{t_I \rightarrow t_E}][\Lambda_I][\Phi_{t_I \rightarrow t_E}]^T, \tag{6-3}$$

where the matrix $\Phi_{t_I \to t_E}$ is expressed as follows:

$$[\Phi]_{t_I \to t_E} = \frac{\partial \vec{B}(t_E)}{\partial \vec{X}(t_I)} \tag{6-4}$$

and

$$\vec{B} = \begin{bmatrix} \vec{B} \cdot \vec{T} \\ \vec{B} \cdot \vec{R} \\ q \end{bmatrix}, \tag{6-5}$$

where q was selected to be any one of the terminal-control parameters desired:

$$q = (V_H, \text{SMA}, \text{ECC}, \text{LAN}, \text{INC}, \text{RCA}, C_3). \tag{6-6}$$

(Time of Flight was not used as a control parameter).
Λ_F is then the covariance matrix of the miss due to the booster ascent errors only.

The second error source to be considered in the calculation of velocity requirements was that of the comet uncertainty at arrival as determined at the time the spacecraft was launched. This error can be interpreted as an aiming error in the booster at launch; thus, the velocity requirement to null it may be computed.

To combine the booster ascent errors and booster aiming errors, we take the expression for the total miss at the target as follows:

$$\vec{X}_M = \vec{X}_V - \vec{X}_C \tag{6-7}$$

M - miss
V - vehicle
C - comet
X - total state.

Taking the expected value of the total miss,

$$E[\bar{X}_M \bar{X}_M^T] = E[(\bar{X}_V - \bar{X}_C)(\bar{X}_V - \bar{X}_C)^T]. \quad (6\text{-}8)$$

Expanding,

$$E[(\bar{X}_V - \bar{X}_C)(\bar{X}_V - \bar{X}_C)^T] = E[\bar{X}_V \bar{X}_V^T] + E[\bar{X}_C \bar{X}_C^T] - E[\bar{X}_V \bar{X}_C^T] - E[\bar{X}_C \bar{X}_V^T]. \quad (6\text{-}9)$$

However, there is no reason to assume any correlation between uncertainty in the vehicle's state at arrival and errors in estimating the comet's state. Thus,

$$E[\bar{X}_C \bar{X}_V^T] = E[\bar{X}_V \bar{X}_C^T] = 0 \quad (6\text{-}10)$$

Hence, the total covariance matrix of miss at arrival is the sum of the uncertainty due to the booster and that due to the comet:

$$\Lambda_E = \Lambda_F + \Lambda_C , \quad (6\text{-}11)$$

where

$$\Lambda_C = [\Phi_{t_{\bar{\Phi}} \rightarrow t_E}][\Lambda_{ACQ}][\Phi_{t_{\bar{\Phi}} \rightarrow t_E}]^T , \quad (6\text{-}12)$$

and Φ is similar to that previously described, except that it is generated along the comet reference trajectory. Λ_{ACQ} is the instantaneous covariance matrix of comet uncertainties at the time the vehicle is launched. Λ_C may be alternately specified in terms of variation in a single parameter, the date of perihelion passage (ΔT_p). Considering Λ_C as being computed in centered co-ordinate system at arrival. From equation (6-12), we have

$$\Lambda_C = \begin{bmatrix} \sigma^2_{\bar{B}\cdot\bar{T}} & \rho_{\bar{B}\cdot\bar{T},\bar{B}\cdot\bar{R}}\,\sigma_{\bar{B}\cdot\bar{R}}\,\sigma_{\bar{B}\cdot\bar{T}} & 0 \\ \rho_{\bar{B}\cdot\bar{R},\bar{B}\cdot\bar{T}}\,\sigma_{\bar{B}\cdot\bar{T}}\,\sigma_{\bar{B}\cdot\bar{R}} & \sigma^2_{\bar{B}\cdot\bar{R}} & 0 \\ 0 & 0 & 0 \end{bmatrix}, \qquad (6\text{-}13)$$

where the correlation between $\sigma_{\bar{B}\cdot\bar{T}}$ and $\sigma_{\bar{B}\cdot\bar{R}}$, namely $\rho_{\bar{B}\cdot\bar{T},\bar{B}\cdot\bar{R}}$, is very nearly unity. The matrix Λ_C may be computed at any time after all prior observational data has been included.

A third term contributing to Λ_E, due to orbit determination of the vehicle, has been omitted since it is small compared to Λ_F and Λ_C.

The minimum-velocity addition to compensate for Λ_E may be computed as follows. Let the velocity correction be given by

$$\dot{X}_G = \begin{pmatrix} a_{11} & a_{12} & a_{13} \\ a_{21} & a_{22} & a_{23} \\ a_{31} & a_{32} & a_{33} \end{pmatrix} \begin{pmatrix} \Delta\,\bar{B}\cdot\bar{T} \\ \Delta\,\bar{B}\cdot\bar{R} \\ \Delta\,A \end{pmatrix} = N\Delta M \qquad (6\text{-}14)$$

where

$$\Delta\,A = -\left[\frac{(a_{11}a_{13}+a_{21}a_{23}+a_{31}a_{33})\,\Delta\,\bar{B}\cdot\bar{T} + (a_{12}a_{13}+a_{22}a_{23}+a_{32}a_{33})\,\Delta\,\bar{B}\cdot\bar{R}}{a_{13}^2 + a_{23}^2 + a_{33}^2}\right] \qquad (6\text{-}15)$$

Writing $\Delta\,A$ in an alternate form,

$$\Delta\,A = -(\alpha\,\Delta\,\bar{B}\cdot\bar{T} + \beta\,\Delta\,\bar{B}\cdot\bar{R}), \qquad (6\text{-}16)$$

and taking the expected value of ΔM, we compute a new Λ_E:

$$\Lambda'_E = \begin{pmatrix} \sigma^2_{\bar{B}\cdot\bar{T}} & \rho_{\bar{B}\cdot\bar{T},\bar{B}\cdot\bar{R}}\,\sigma_{\bar{B}\cdot\bar{T}}\,\sigma_{\bar{B}\cdot\bar{R}} & -\alpha\sigma^2_{\bar{B}\cdot\bar{T}} - \beta\rho_{\bar{B}\cdot\bar{T},\bar{B}\cdot\bar{R}}\,\sigma_{\bar{B}\cdot\bar{R}}\,\sigma_{\bar{B}\cdot\bar{T}} \\ & \sigma^2_{\bar{B}\cdot\bar{R}} & \alpha\rho_{\bar{B}\cdot\bar{T},\bar{B}\cdot\bar{R}}\,\sigma_{\bar{B}\cdot\bar{T}}\,\sigma_{\bar{B}\cdot\bar{R}} - \beta\sigma^2_{\bar{B}\cdot\bar{R}} \\ & & \alpha^2\sigma^2_{\bar{B}\cdot\bar{T}} + \beta^2\sigma^2_{\bar{B}\cdot\bar{R}} + 2\alpha\beta\rho_{\bar{B}\cdot\bar{T},\bar{B}\cdot\bar{R}}\,\sigma_{\bar{B}\cdot\bar{T}}\,\sigma_{\bar{B}\cdot\bar{R}} \end{pmatrix} \quad \text{(Symmetric)} \tag{6-17}$$

The minimum-velocity correction is then

$$E[\dot{X}_G\,\dot{X}_G^T] = N\,\Lambda'_E\,N^T, \tag{6-18}$$

and

$$\sigma_{V\ RMS} = \left[\text{TRACE } E\,(\dot{X}_G\,\dot{X}_G^T)\right]^{\frac{1}{2}} \tag{6-19}$$

Plots of $\sigma_{V\ RMS}$ as a function of time of flight from injection are shown in Figures 6-1 to 6-3. Various combinations for the correlation coefficient $\rho_{\bar{B}\cdot\bar{T},\bar{B}\cdot\bar{R}}$ are shown. It should be noted that the contributions to $\sigma_{V\ RMS}$ by the Atlas-Centaur booster errors were 1σ values. For the comet Pons-Winnecke, Figure 6-2 indicates that it takes approximately 180 m/s to compensate for 1σ Atlas-Centaur errors plus 0.5 day variation in the date of perihelion passage.

6.2 GUIDANCE REQUIREMENTS

The amount of fuel required for midcourse guidance on a mission to Pons-Winnecke depends on the type of trajectory one selects. If a Type-II trajectory is utilized as previously discussed, then the launch may occur as early as 1 November 1969. However, it is unlikely that the

Case No.	Booster Errors	Comet Uncertainties
1	A/C Vehicle +	None
2	A/C Vehicle +	$\sigma_{\bar{B}\cdot\bar{T}} = 1.0 \times 10^6$, $\sigma_{\bar{B}\cdot\bar{R}} = 0$
3	A/C Vehicle +	$\sigma_{\bar{B}\cdot\bar{T}} = \sigma_{\bar{B}\cdot\bar{R}} = 1.0 \times 10^6$ Uncorrelated
4	A/C Vehicle +	$\sigma_{\bar{B}\cdot\bar{T}} = \sigma_{\bar{B}\cdot\bar{R}} = 1.0 \times 10^6$ Perfectly Correlated

Fig. 6-1 Expected First Midcourse Velocity Requirements

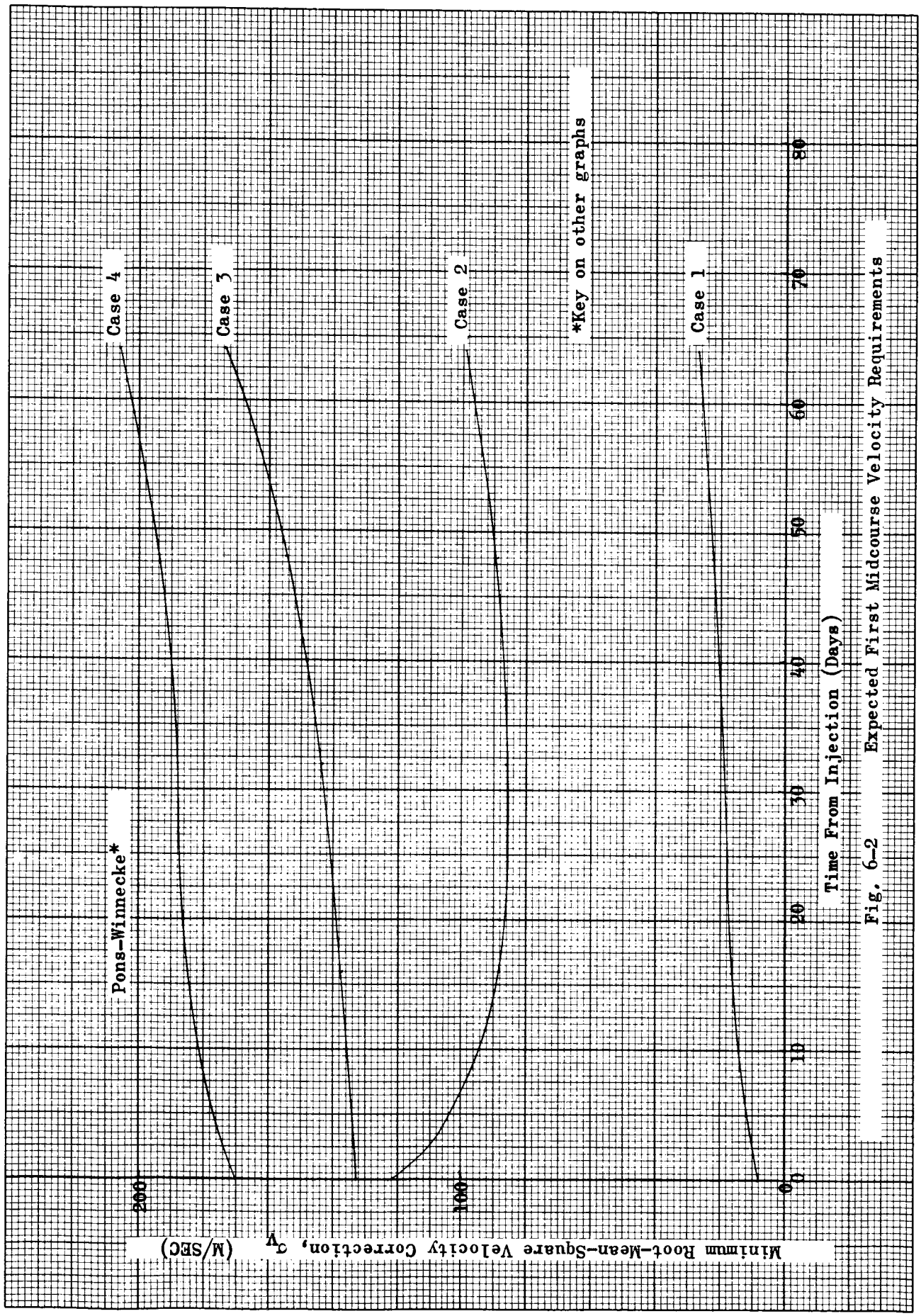

Fig. 6-2 Expected First Midcourse Velocity Requirements

Case No.	Booster Errors	Comet Uncertainties
1	A/C Vehicle +	None
2	A/C Vehicle +	$\sigma_{\overline{B}\cdot\overline{T}} = 1.0 \times 10^6$, $\sigma_{\overline{B}\cdot\overline{R}} = 0$
3	A/C Vehicle +	$\sigma_{\overline{B}\cdot\overline{T}} = \sigma_{\overline{B}\cdot\overline{R}} = 1.0 \times 10^6$ Uncorrelated
4	A/C Vehicle +	$\sigma_{\overline{B}\cdot\overline{T}} = \sigma_{\overline{B}\cdot\overline{R}} = 1.0 \times 10^6$ Perfectly Correlated

Fig. 6-3 Expected First Midcourse Velocity Requirements

comet will be recovered before 1 December 1969. Hence, the target vector used for launching will be derived from the pre-recovery studies conducted. The uncertainty in the location of perihelion is larger for this case (see Table 4-1); hence, the midcourse fuel requirements will be larger. For the case of a Type-I trajectory, the comet will have most likely been recovered and the comet perihelion time error will be considerably smaller, so less fuel will be required for velocity corrections. A summary table of the velocity requirements for the two types of trajectories to Pons-Winnecke is shown below.

Trajectory Type	1st Velocity Correction (m/sec)	2nd Velocity Correction (m/sec)	Total Velocity Change Required (m/sec)
I	70	6	76
II	110	10	120

6.3 GUIDANCE CALCULATIONS

To show how the guidance fuel requirements were ascertained, an example is carried out in detail. Consider the mission to Pons-Winnecke in 1970 and assume a pre-acquisition analysis has been accomplished. Constrain the error, at encounter due to guidance, to be 5000 km or less. Impose standard hardware uncertainties on the midcourse propulsion system. Given the above information, and assuming the state of the vehicle due to earth-based tracking is perfectly known, then the following statements can be made about the problem, referring to the encounter dispersion ellipse in Figure 6-4:

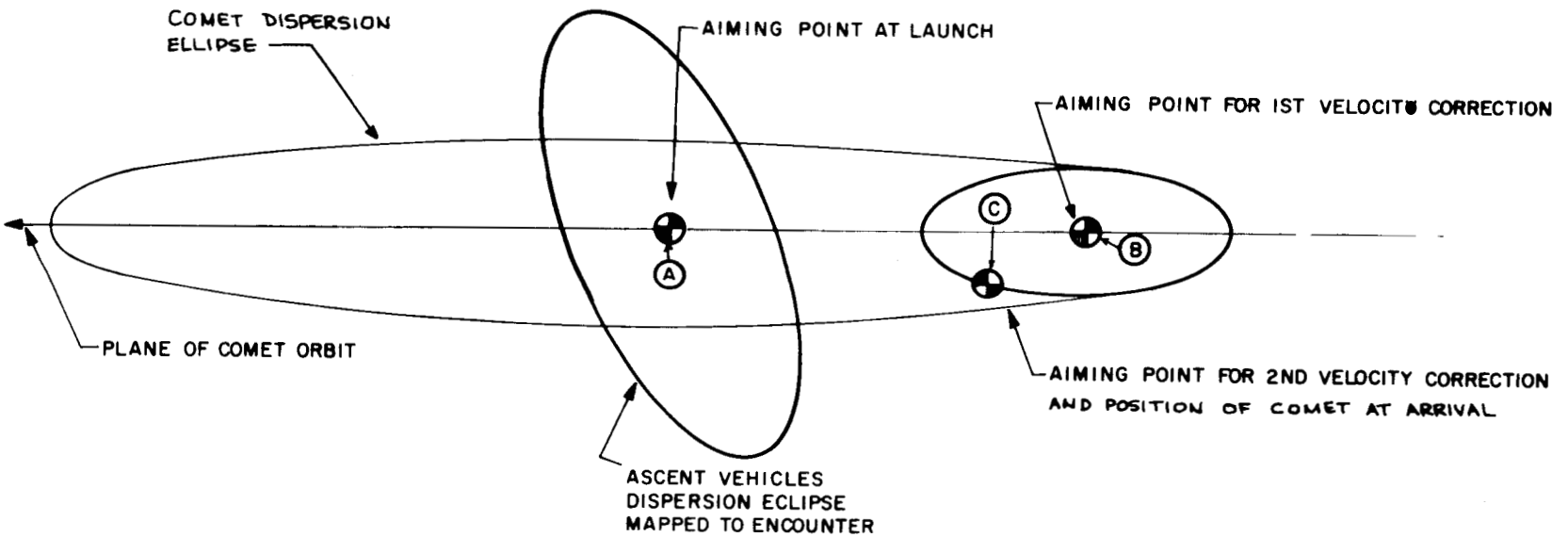

Fig. 6-4 Encounter Dispersion Ellipses

At Launch

a) At launch the vehicle should be targeted to the center of the comet dispersion ellipse (point A). The worst-case situation arises for the comet's true position ending up at either end of the ellipse.

b) The uncertainty in the time of perihelion passage for the comet is 30^m (from Table 4-1).

At First Velocity Correction

a) The comet's perihelion position is still not precisely defined. The aiming point for the first velocity correction is the center of the new dispersion ellipse (point B).

b) The velocity addition is intended to accomplish a translation of the aiming point from point A to point B and remove all boost ascent errors present in the trajectory.

c) The pointing error for the midcourse velocity addition is assumed to be 1^o.

d) The propulsion uncertainty for the midcourse motor is small compared to (c).

e) If 30^d is selected for the location of the correction, then the comet uncertainty in date of perihelion is 10^m (from Table 4-1).

At Second Velocity Correction

a) The uncertainty in the position of the comet at perihelion (4 arc seconds) may be neglected in calculating the shift of the target vector.

b) The upper bound imposed on the error at encounter (5000 km), together with the pointing error (1^{o}), determine when the second correction should take place.

c) The velocity addition is intended to shift the target vector from point B to point C and remove any velocity errors introduced by the first correction.

To determine the first velocity correction, given the time of execution 30^{d} after injection, we make use of Figures 6-1 to 6-3 and Figure 6-5. It is desired to remove the entire booster uncertainty due to the Atlas-Centaur and as much of the comet uncertainty as is possible. However, the comet position at arrival is uncertain to within 10^{m}. Hence, it is possible to remove only the difference between launch uncertainty and 30^{d} uncertainties, for this comet; this amounts to 10^{m}. In terms of an aiming-point concept, we have said that originally at launch the target vector was in the center of the dispersion ellipse of the comet uncertainties.

Now, at 30^{d}, we have a new aiming point with an associated uncertainty. Therefore, the first velocity correction will use as the aiming point the center of the new comet dispersion ellipse. It is important to remember that the second dispersion ellipse will always be contained in the first. Furthermore, the worst-case situation is when the second dispersion ellipse has shifted to either end of the first ellipse, as shown in Figure 6-4. This case for Pons-Winnecke amounts to a change in target vector centers of 10^{m}. Hence, with the aid of Figures 6-1 to 6-3 and 6-5, first velocity correction of 70 m/s is obtained (Figure 6-2 was generated using 1-σ booster errors). This includes sufficient fuel to remove all Atlas-Centaur uncertainties and shift the aiming point.

The next step is to estimate a position in time for the second velocity correction. If we select an upper bound for the magnitude of the

Fig. 6.5. Uncertainty in Position of Perihelion Passage vs. Uncertainty in Time of Perihelion Passage

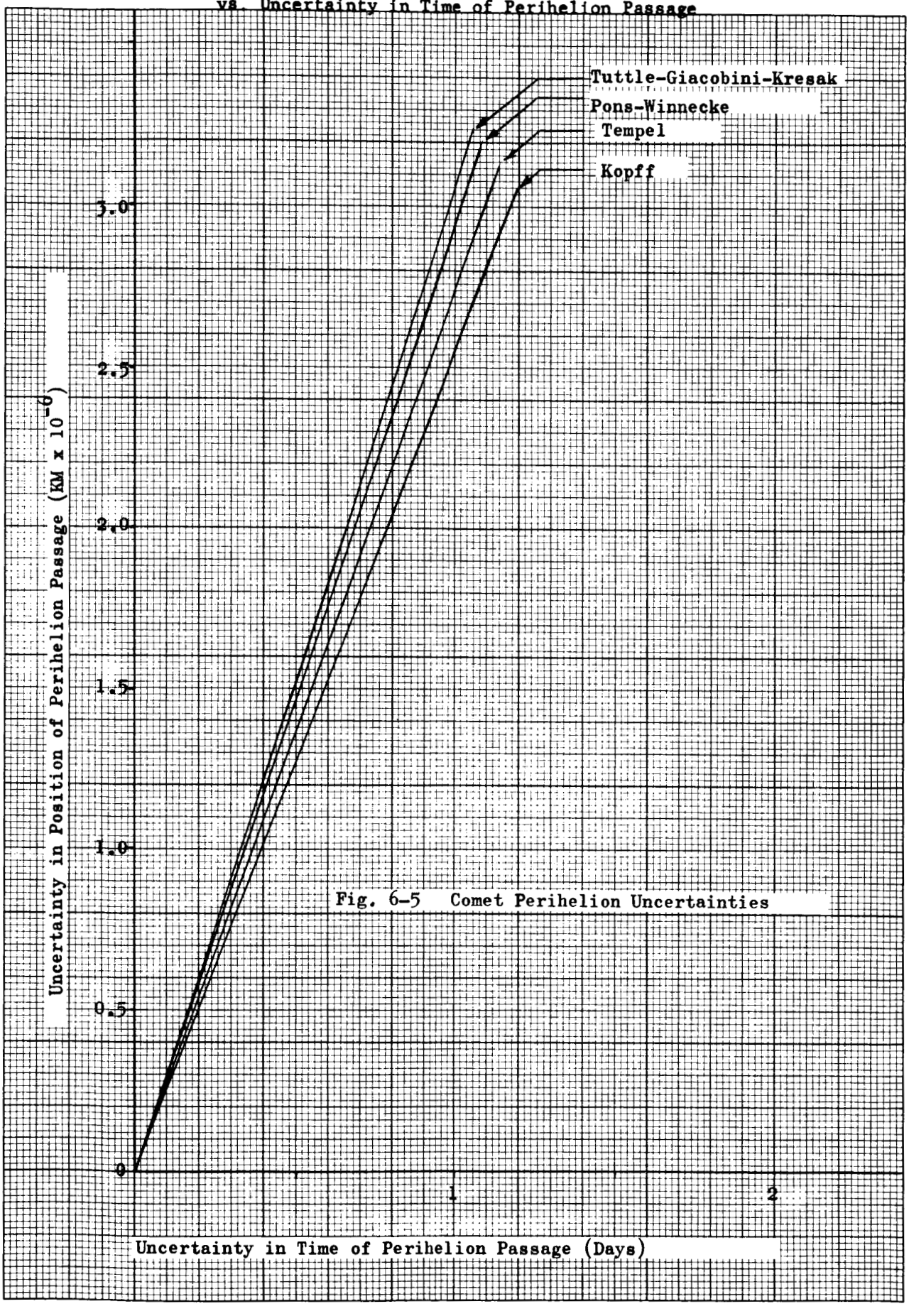

Fig. 6-5 Comet Perihelion Uncertainties

second correction of (ΔV_2) = 50 m/s, then the worst-case error in the second correction would be due to pointing.

$$\delta(\Delta V_2) = (50)\left(\frac{1}{57.3}\right) \cong 1 \text{ m/s}$$

Using $\delta(\Delta V_2)$, the maximum allowable miss of 5000 km, and Figure A28, we determine a minimum time for the second correction of 40 days before arrival.

Now it is also possible to assess the velocity required at the time of the second correction that will eliminate the error in the first correction. A ratio of the sensitivities at the two correction points is computed (m).

$$m = \frac{\left(\frac{\partial \vec{B}}{\partial \vec{V}}\right)_{t = 30^d \text{ after injection}}}{\left(\frac{\partial \vec{B}}{\partial \vec{V}}\right)_{t = 40^d \text{ before arrival}}} \qquad (6\text{-}20)$$

From Figure A28, $m \cong 4$. Using the error in the first correction and m, the portion of the second correction required to compensate for the error in the first correction may be computed

$$\Delta V_2 = m\left(\Delta V_1 \ \frac{1}{57.3}\right) \cong 5 \text{ m/s.}$$

Now, the portion of the second correction required to rotate the target vector or correct for comet uncertainties may be determined by using the comet uncertainty at the time of the second correction (4 arc seconds) and the comet uncertainty at the time of the previous correction (10 min.). Since the comet positional uncertainties at the time of the second correction are small, we assume that all the positional error in the trajectory at

arrival is eliminated. Hence,

$$\Delta V_2 = \left(\frac{\partial \vec{B}}{\partial \vec{B}} \right)_{t = 40^d \text{ before encounter}} \times 11{,}000 = 3 \text{ m/s.}$$

Combining the two portions of the second correction by root-sum squaring, we have

$$\Delta V_2 \cong 6 \text{ m/s}$$

Summing the two velocity corrections results in a total fuel requirement of

$$\Delta V_T = \Delta V_1 + \Delta V_2 = 76 \text{ m/s.}$$

If it is desired that time of flight be controlled, then the velocity requirements would most definitely be increased. An estimate of the increase in fuel requirements would be 30% to control time of flight as well as target-encounter distance.

SECTION 7

MARINER-C COMET PROBE

7.1 MARINER-C COMPARISON

Since the mission to Pons-Winnecke in 1969-1970 is the only one found which is suitable for using an Atlas/Agena launch vehicle and for accomplishing the scientific objectives, it was chosen for the comparison. The mission to Tuttle-Giacobini-Kresak in 1973 may be accomplished using an Atlas/Agena combination. However, the comet is faint and not recoverable for at least 3 months after launch (see Table 5-1). No earlier launches to periodic comets were discovered that might use an Atlas-Agena/Mariner-C combination. A mission to the comet Tempel (2) in 1967 looks favorable for an Atlas/Centaur launch. Similarly, missions to the comet Kopff (1970) and Brooks (2) (1973) fall into the Atlas/Centaur class.

7.2 LAUNCH PERIODS

The launch periods possible for a mission to Pons-Winnecke in 1969-1970 are shown in Figures 7-1 and 7-2. These figures are detailed energy curves for the two types of trajectories. Range-safety and energy limitations prohibit using a single time-of-flight curve for more than a few days of launch time. Tables of launch-heliocentric and comet-centered information were compiled for a typical 30-day launch window for each type of trajectory (see Tables 7-1 and 7-2). For an actual launch table more frequent time-of-flight changes would be utilized to eliminate the large jumps in energy. The net effect would be that of following the envelope of the energy curves instead of individual curves for a number of days.

Fig. 7-1. Detailed Energy Curves for Pons-Winnecke, Type II

Fig. 7-1 Detailed Energy Curves for Pons-Winnecke
TYPE II

Fig. 7-2. Detailed Energy Curves for Pons-Winnecke, Type I

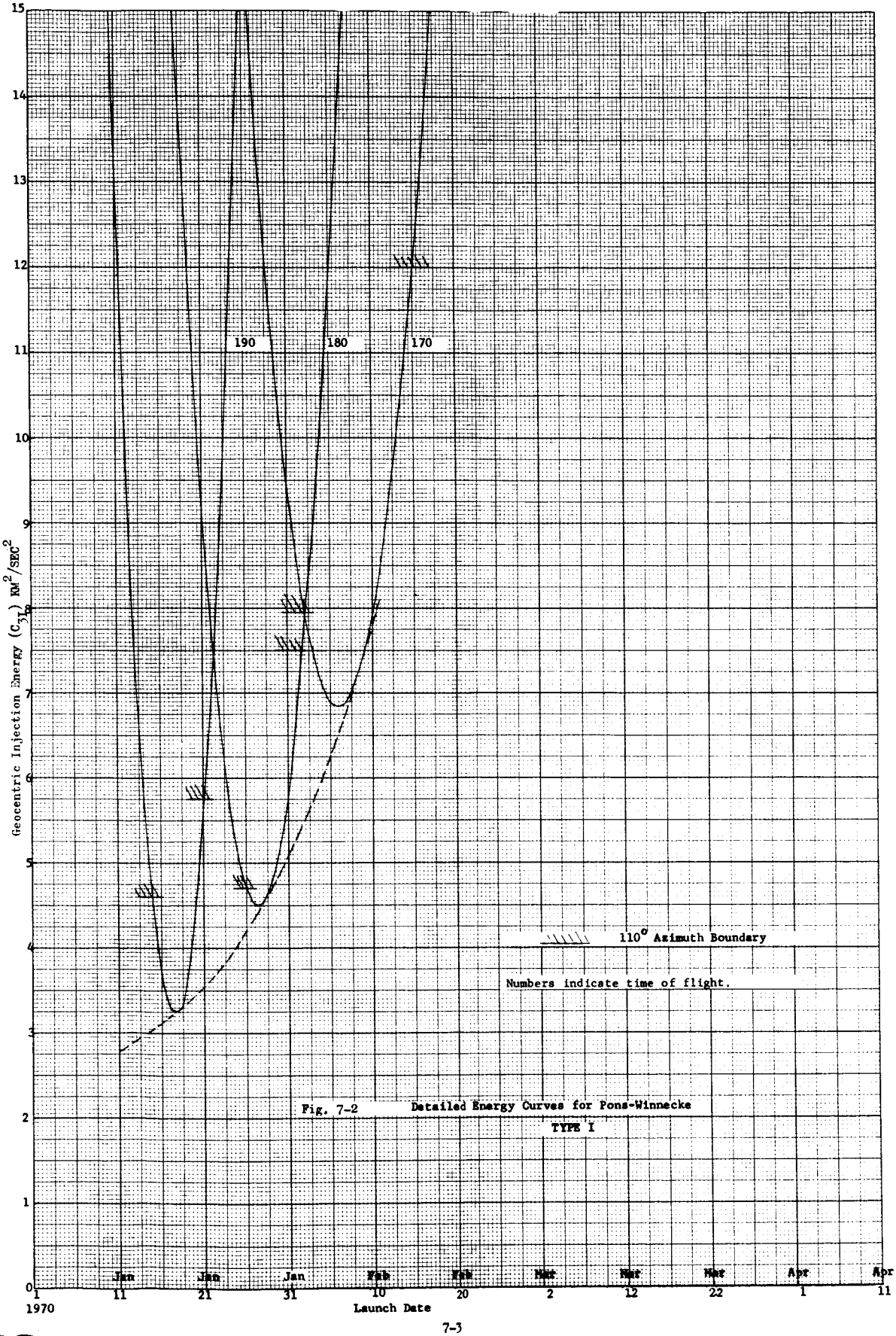

Fig. 7-2 Detailed Energy Curves for Pons-Winnecke
TYPE I

TABLE 7 - 1

TRAJECTORY CHARACTERISTICS - PONS-WINECKE 1969

(TYPE II)

	GEOCENTRIC PHASE		HELIOCENTRIC PHASE		
	No. of Launch Days	Range of Geocentric Injection Energy (km^2/sec^2)	Transfer Angle Range (deg.)	Inclination Angle Range (deg.)	Latitude of ' at Arriv (deg.)
Launch Date : 1 Nov - 3 Nov Time of Flight: 270 days Arrival Data : 29 Jul - 31 Jul	3	7.64 to 8.53	248.11 to 236.36	0.98 to 1.80	-0.82 to
Launch Date : 2 Nov - 15 Nov Time of Flight: 260 days Arrival Data : 21 Jul - 2 Aug	12	7.76 to 8.74	228.05 to 225.93	2.58 to 3.02	1.92 to -
Launch Date : 15 Nov - 25 Nov Time of Flight: 250 days Arrival Data : 23 Jul - 2 Aug	10	5.70 to 8.92	217.63 to 215.85	2.02 to 3.70	1.23 to -
Launch Date : 25 Nov - 30 Nov Time of Flight: 240 days Arrival Date : 23 Jul - 28 Jul	5	5.72 to 4.04	207.54 to 206.62	2.66 to 1.07	1.23 to
Launch Date : 1 Nov - 30 Nov Time of Flight: Arrival Date : 21 Jul - 2 Aug	30	4.04 to 8.92	206.62 to 248.11	0.98 to 3.70	-2.17 to

	COMACENTRIC PHASE					
Target Il	Hyperbolic Excess Velocity (km/sec)	Rt. Ascension of the Incoming Asymptote (deg.)	Declination of the Incoming Asymptote (deg.)	Total Resultant Approach Angle (deg.)	Communication Distance at Arrival ($\times 10^6$ km)	Sun-Probe Distance at Arrival (A.U.)
-1.50	14.58 to 14.45	11.33 to -12.61	-38.99 to -38.31	40.35 to 40.02	95.52 to 96.53	1.255 to 1.258
2.17	15.24 to 14.00	4.00 to -13.08	-41.57 to -37.33	41.73 to 39.24	92.47 to 97.63	1.248 to 1.261
2.17	15.19 to 13.61	-4.48 to -12.33	41.64 to -36.75	41.83 to 38.48	93.09 to 97.63	1.249 to 1.261
0.48	15.46 to 14.24	-3.58 to -7.63	-42.31 to -39.56	42.44 to 40.17	93.09 to 95.05	1.249 to 1.254
1.92	13.61 to 15.46	-13.08 to 11.33	-42.31 to -36.75	38.48 to 42.44	92.47 to 97.63	1.248 to 1.261

TABLE 7-2

(TYPE I) TRAJECTORY CHARACTERISTICS - PONS-WINNECKE 1970

	GEOCENTRIC PHASE		HELIOCENTRIC PHASE			
	No. of Launch Days	Geocentric Injection Energy (Km^2/Sec^2)	Transfer Angle (deg.)	Inclination Angle (deg.)	Latitude of Target at Arrival (deg.)	Hype Ve (k
Launch Date : 11 Jan Time of Flight : Arrival Data :	1	2.78				
Launch Date : 18 Jan Time of Flight : 190 days Arrival Data :	1	3.27	155.91	0.34	-0.14	
Launch Date : 28 Jan Time of Flight : 180 days Arrival Data :	1	4.54	145.77	0.24	-0.14	
Launch Date : 9 Feb Time of Flight : 170 days Arrival Date :	1	7.49	135.23	1.16	-0.82	
Total Range	29	2.78-7.49				

COMACENTRIC PHASE					
rbolic Excess locity m/sec)	Rt. Ascension of the Incoming Asymptote (deg.)	Declination of the Incoming Asymptote (deg.)	Total Resultant Approach Angle (deg.)	Communication Distance at Arrival (x 10^6 km)	Sun Probe Distance at Arrival (A.U.)
14.66	-5.11	-40.87	41.13	94.61	1.253
14.65	-5.28	-40.57	40.85	94.61	1.253
14.97	-7.16	-40.46	40.98	95.52	1.255

7.3 PAYLOAD CAPABILITIES

A Mariner-C mission to Mars and several possible missions to Pons-Winnecke are compared in Table 7-3. The Mariner-C payload capability is based on the actual launch weight of 565 lbs. (see Figure 7-3). The midcourse velocity capability of Mariner-C was based on 80 m/s as provided by JPL. In comparing the numbers presented in the table, it is evident that an Atlas/Agena-B/Mariner-C spacecraft combination can be used for a mission to Pons-Winnecke in either late 1969 or early 1970. It seems most likely that both opportunities would be considered (Type I and Type II) and hence improve the overall reliability of mission success by having two launch periods spaced only a month or so apart in time Figure 7-4.

Table 7-3 Mariner-C Comparison Chart for a Mission to Pons-Winnecke (1970)

COMPARISON QUANTITY	MARINER-C TO MARS	MARINER-C TO COMET PONS-WINNECKE Type I	Type II
Geocentric Injection Energy (C_3) (For 30 Day Launch Window) Km^2/Sec^2	10.2	2.8 - 7.5	4.0 - 8.9
Payload Capability to Achieve Injection Energy Requirements (lbs.)	565	630	578
Range of Flight Times to Encounter (Days)	220-250	200-170	270-240
Earth-Vehicle Communication Distance at Arrival (millions of Km.)	220-250	94-96	92-97
Relative Approach Velocities at Encounter (Km/Sec)	5-6	14.7-15.0	13.6-15.5
Midcourse Velocity Requirements with a Preacqusition Study (m/s)	80	80	120
Minimum Encounter Approach Distance (Km)	10,000-25,000	5,000-10,000	5,000-10,000

Fig. 7-3. Geocentric Injection Energy vs. Payload Capability for Advanced Atlas/Agena Vehicle

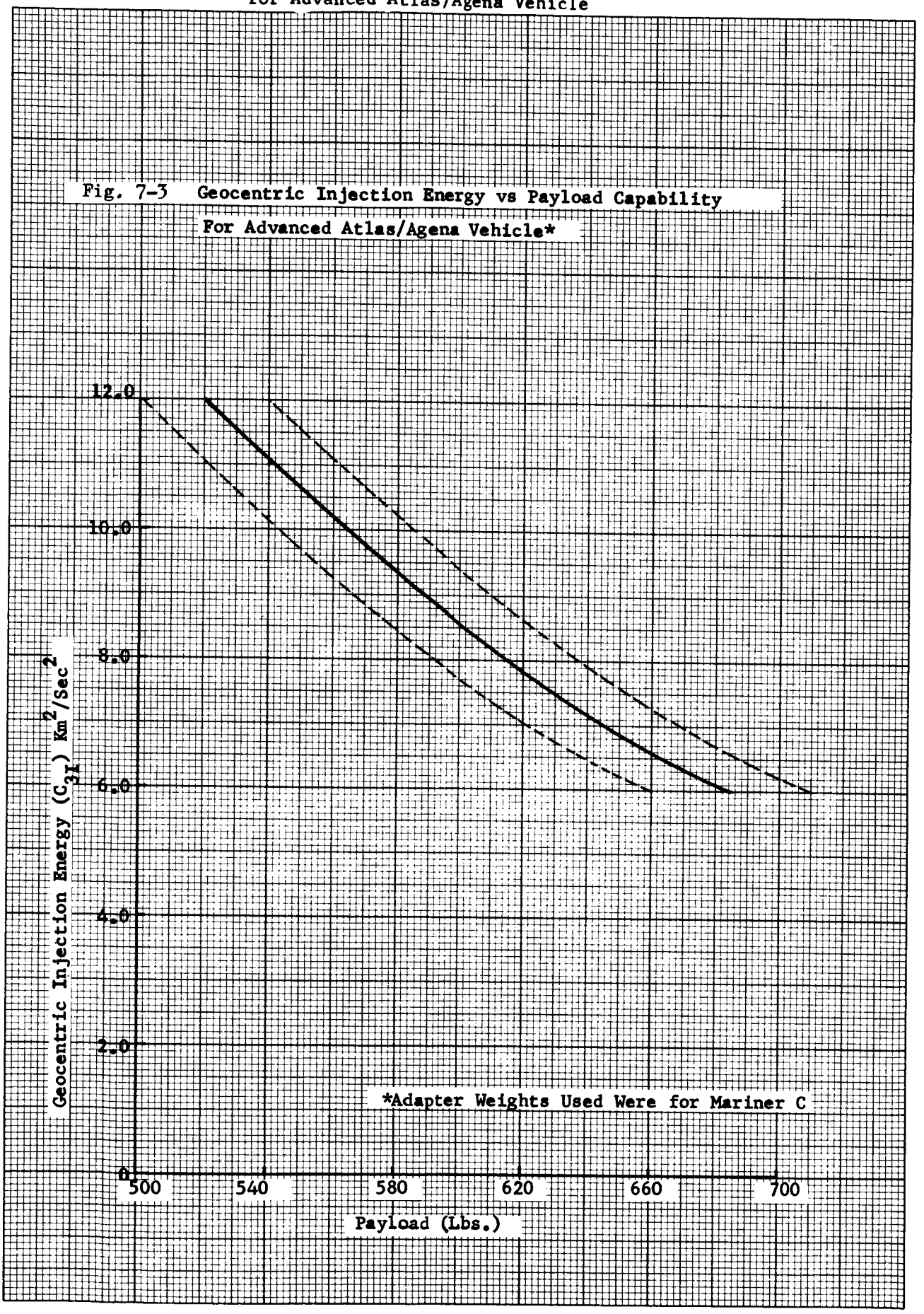

Fig. 7-4 Dual Launch Window Characteristics for a Mission to Pons-Winnecke

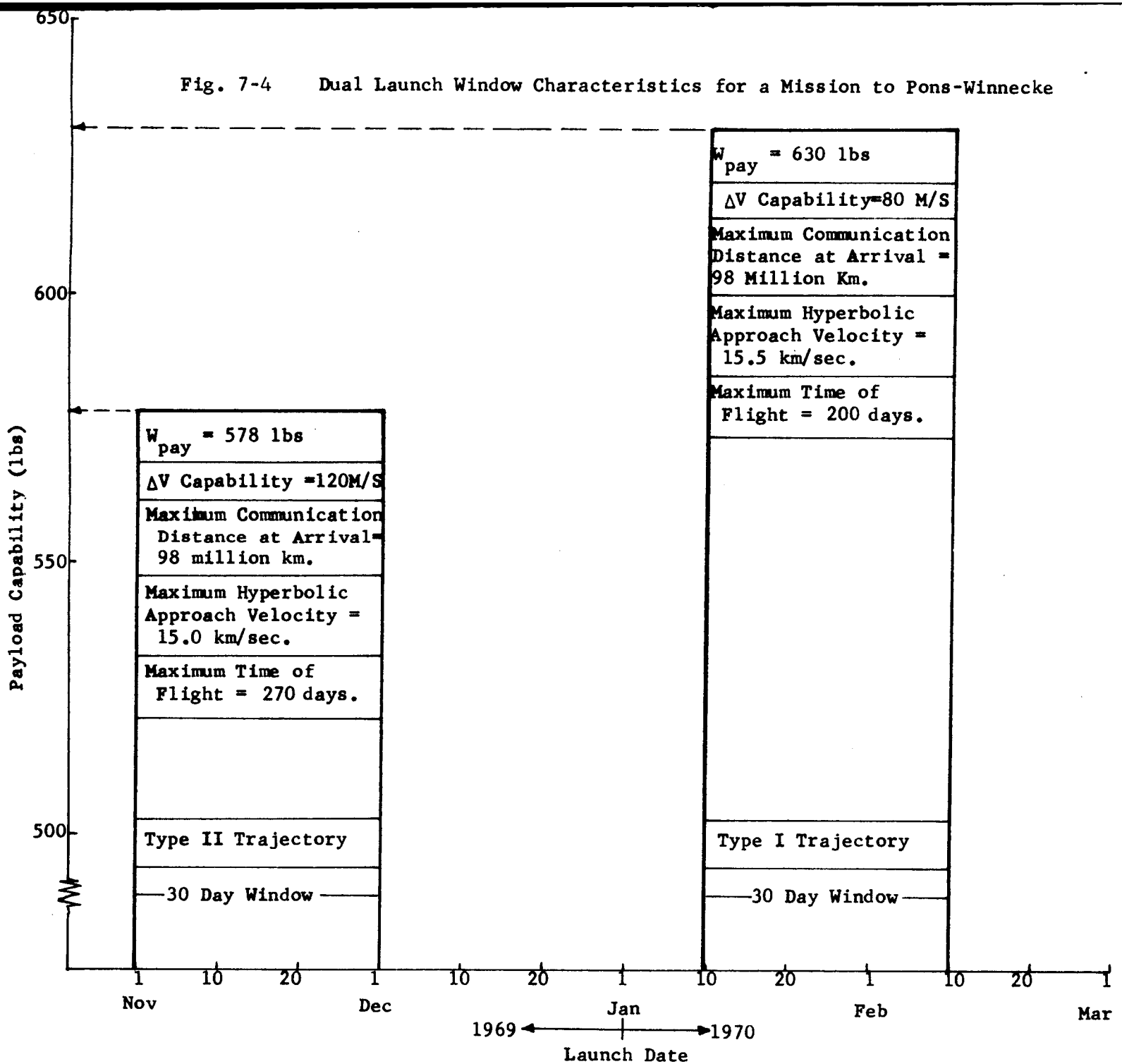

SECTION 8
CONCLUSIONS

8.1 MARINER-C COMET PROBE

The major conclusion derived from this study is that a launch to the comet Pons-Winnecke may be accomplished in the time period of late 1969 to early 1970 using an Atlas/Agena/Mariner-C combination. All aspects of the mission considered to be problem areas were investigated in detail to insure feasibility. Some special requirements of the mission resulting from these studies are as follows:

a. A Phase 0 study should most definitely be undertaken

b. Advantage should be taken of both Type I and Type II trajectories

c. Launch windows derived by following the envelope of minimum energy should be investigated to determine the influence on Atlas/Agena guidance setting requirements

d. Provisions for making accurate observations of the comet from observatories should be made well in advance of the expected recovery

8.2 ATLAS-CENTAUR COMET PROBES

Secondary comet missions to Tempel (2), Kopff and Brooks (2) may be accomplished with an Atlas/Centaur/Mariner-C class vehicle. Similar requirements apply to these comets as for Pons-Winnecke.

8.3 MISSION PLANNING FACTORS

Comet missions are somewhat different from planetary encounter missions. Significant changes in planning a comet mission are the following:

a. Comet orbits are very poorly defined compared to those of planets. This requires an additional effort before launch to improve the comet ephemeris to minimize guidance requirements.

b. Range-safety boundaries and launch-guidance settings change more rapidly due to the higher inclinations of some of the comets.

c. Approach velocities are generally higher due to the larger semi-major axis of the comet orbit.

It is not likely that any newly discovered comets will be suitable for consideration in the time span of interest. The likelihood of proper phasing between the earth and a "new" comet is very low and the lack of sufficient orbital data most likely preclude any such mission possibilities.

SECTION 9

CLOSE-APPROACH ASTEROID MISSION

9.1 ASTEROID SELECTION

The four close-approach asteroids Eros, Apollo, Hermes and Icarus were considered as possible targets for the asteroid mission. The results of a preliminary analysis of these asteroids and other work carried on by IITR [1964] resulted in discarding all the above asteroids except Eros as possible targets. Eros was selected primarily on the basis of size (8 x 22 km). The other asteroids are all about 1 km or smaller in size.

9.2 EROS TRAJECTORY CHARACTERISTICS

Trajectory characteristics for a mission to Eros in 1974 are presented in Appendix C. Energy requirements are quite reasonable, i.e., C_3 = 7.5 km^2/sec^2 for a 30-day launch window. Approach velocities are similar to a Mars mission, V_H = 4 to 6 km/sec. The communication distance for this mission is nearly constant and extremely low, C_D = 25 million km. Unlike most of the asteroids, Eros has its perihelion very near the descending node. This orbit characteristic accounts for the low energy and the relatively constant communication distance. The orbit ephemeris is much better defined than any of the comets. The asteroid is also visible a good portion of the time and hence sufficient data is or could be obtained to define the orbit to the required accuracy. As such, the guidance problem for a close-approach asteroid mission is not considered to be a problem area. The guidance problem mentioned above infers miss distances of the order of thousands of km and in no way touches on the problem of target impact.

9.3 ASTEROID MISSIONS

It seems logical to justify a mission to an asteroid, sometimes referred to in the literature as a gray rock, that one must set out to accomplish one of the following tasks:

1. Fly by at very close distance and obtain high-resolution TV pictures which could be used to analyze the surface character of the asteroid.

2. Obtain spectographic information which could result in analysis of the composition of the asteroid.

Both of the tasks mentioned above seem extremely difficult to achieve due to the small size of the asteroid and the solid character of its mass. However, a solution has been considered for accomplishing the second task. In order to conduct spectroscopic measurements on asteroidal surface material on a fly-by mission, an experiment is proposed which might be called the shotgun method. This experiment is outlined below.

9.4 SHOTGUN EXPERIMENT

The Shotgun Experiment consists of the following sequence of events:

1. Achieve a distance of closest approach of 100 to 300 km by using a triple-correction guidance scheme. Without a closed-loop guidance system, the minimum error can never be smaller than A.U. uncertainties.

2. At a specified time before arrival from the asteroid, separate a spinning payload from the spacecraft (see Figure 9-1).

3. Re-orient the spacecraft and retro-fire the spacecraft engine ($\Delta V \geq 100$ m/s). The spacecraft will then travel on a slower

Fig. 9.1 Spinning Particle Dispenser

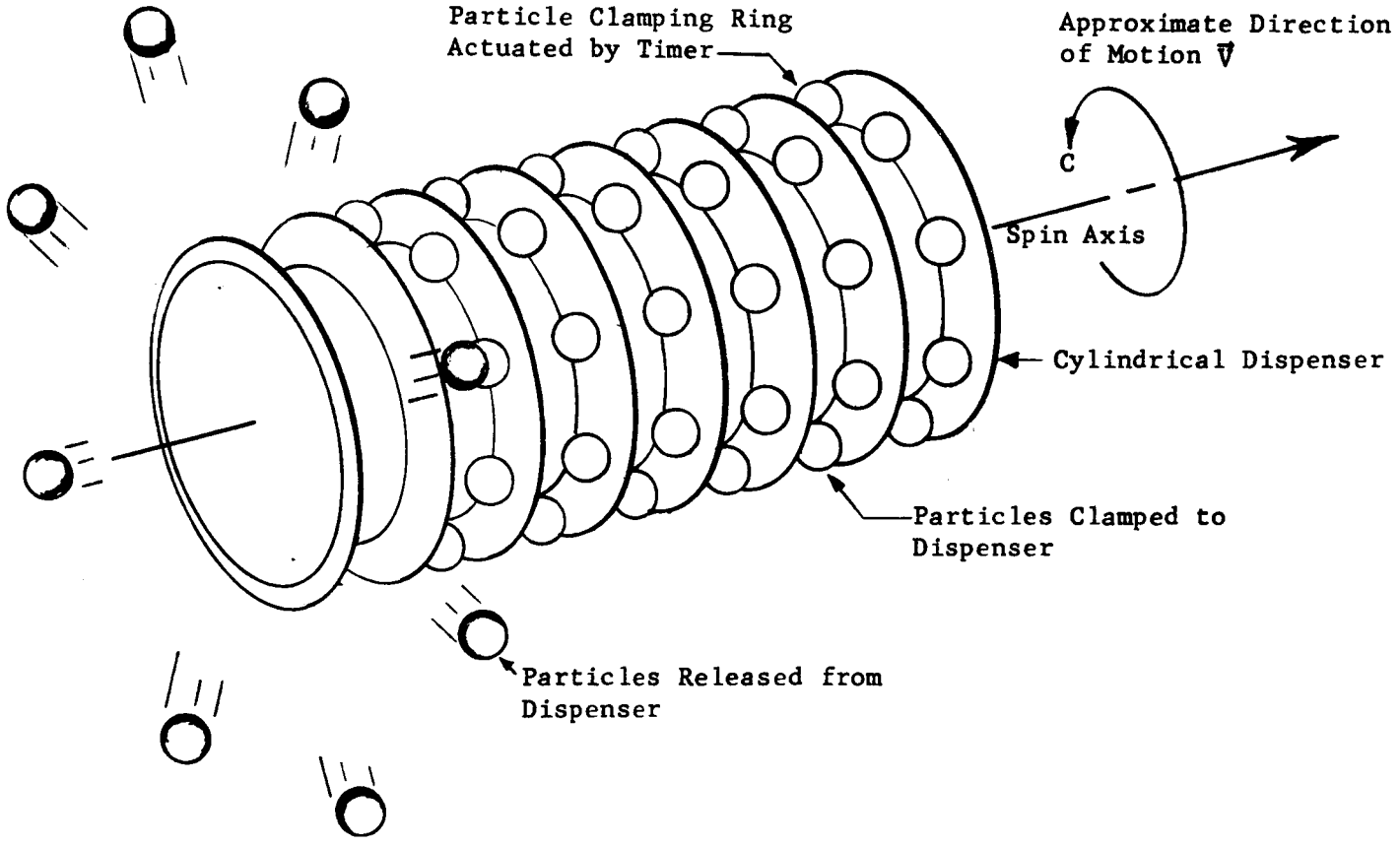

trajectory than the spinning payload.

4. At fixed-time increments, release rings of particles from the spinning payload. The net effect of the propagation of these particles is to create a cross-sectional area of particles such that at least one and preferably more will impact the asteroid. The size of these particles may be that of a ping-pong ball or smaller and the composition is such that a maximum cloud of asteroid material is created.

5. The spacecraft is equipped with a spectrograph which then analyzes the artificially created cloud of asteroid material. The small gravitational coefficient of the asteroid should allow the cloud to remain dispersed for a relatively long period of time.

No refined estimate of particle sizes, composition, etc., have been made, but a 100-lb. spinning payload should provide ample margin.

9.5 CONCLUSIONS

The Shotgun mission as briefly described herein seems to be a reasonable approach for obtaining good composition data for the asteroid Eros. A TV system could additionally be used if the total payload weight permitted.

SECTION 10

REFERENCES

Cunningham, Prof. L.E., University of California Astronomy Dept., Consultant to Philco-WDL on Comet and Close-Approach Asteroid Mission Study; September-October, 1964.

Elconin, T., Kohlhase, C. E., "Variation of Midcourse Maneuver Requirements with Injection Energy for Centaur Direct Ascent Trajectories", JPL, August 3, 1964.

Holdridge, D. B., "Space Trajectories Program for the IBM 7090 Computer"; JPL, Pasadena, California; TR 32-223; March 2, 1962.

Jet Propulsion Laboratory, "Comet and Close-Approach Asteroid Mission Study Reference Information", EPD 224; June 20, 1964.

Philco, "Programmer's Manual for Interplanetary Error Propagation Program", WDL; TR-2184; November 15, 1963.

Philco, "Programmer's Manual for Quick-Look Mission Analysis Program", WDL; TR-2217; January 24, 1964.

Porter, J. G., "The Orbits of Periodic Comets", JPL, TM 312-167; March 2, 1962.

"Reports on Progress of Astronomy", The Quarterly Journal of the Royal Astronomical Society," The Royal Astronomical Society; Burlington House, London; October, 1961; September, 1962; September, 1963.

Roemer, E., letter to R. Jensen re: Comet Initial Position Accuracies; August 7, 1964.

Space Technology Laboratories, Inc., Comet Intercept Study Final Report on NASw-414, 8668-6002-RU-000; March 28, 1963.

Narin, F. and Pierce, P., "Perturbation, Sighting and Trajectory Analysis for Periodic Comets: 1965-1975", IITRI Report No. T-7; July 22, 1964.

IIT Research Institute, "Digest Report Missions to the Asteroids"; Astro Sciences Center of IITRI, Chicago, Illinois; TRM-5 September, 1964.

APPENDIX A

COMET TRAJECTORY AND GUIDANCE CHARACTERISTICS

Tempel (2)	A1	A10	A11	A19		A27	A32	A37
Pons-Winnecke	A2	A8	A12	A16	A21 A22	A28	A33	A38
Kopff	A2	A7	A13	A17	A23 A24	A29	A34	A39
Tuttle-Giacobini-Kresak	A4	A9	A14	A20		A30	A35	A40
Brooks (2)	A5	A6	A15	A18	A25 A26	A31	A36	A41

Figure No.

A1 - A5	Geocentric Injection Energy vs. Launch Date
A6 - A10	Target Arrival Conditions (VH, DAI, LAT) vs. Launch Date
A11 - A15	Earth Target Vehicle Angle vs. Time of Flight
A16 - A20	Trajectory Profile in Ecliptic Plane
A21 - A26	Encounter Profile-Vehicle Centered
A27 - A31	Midcourse Guidance Parameter vs. Time to Go
A32 - A36	Prelaunch Comet Ephemeris
A37 - A41	Ecliptic Latitude of Comet vs. Date

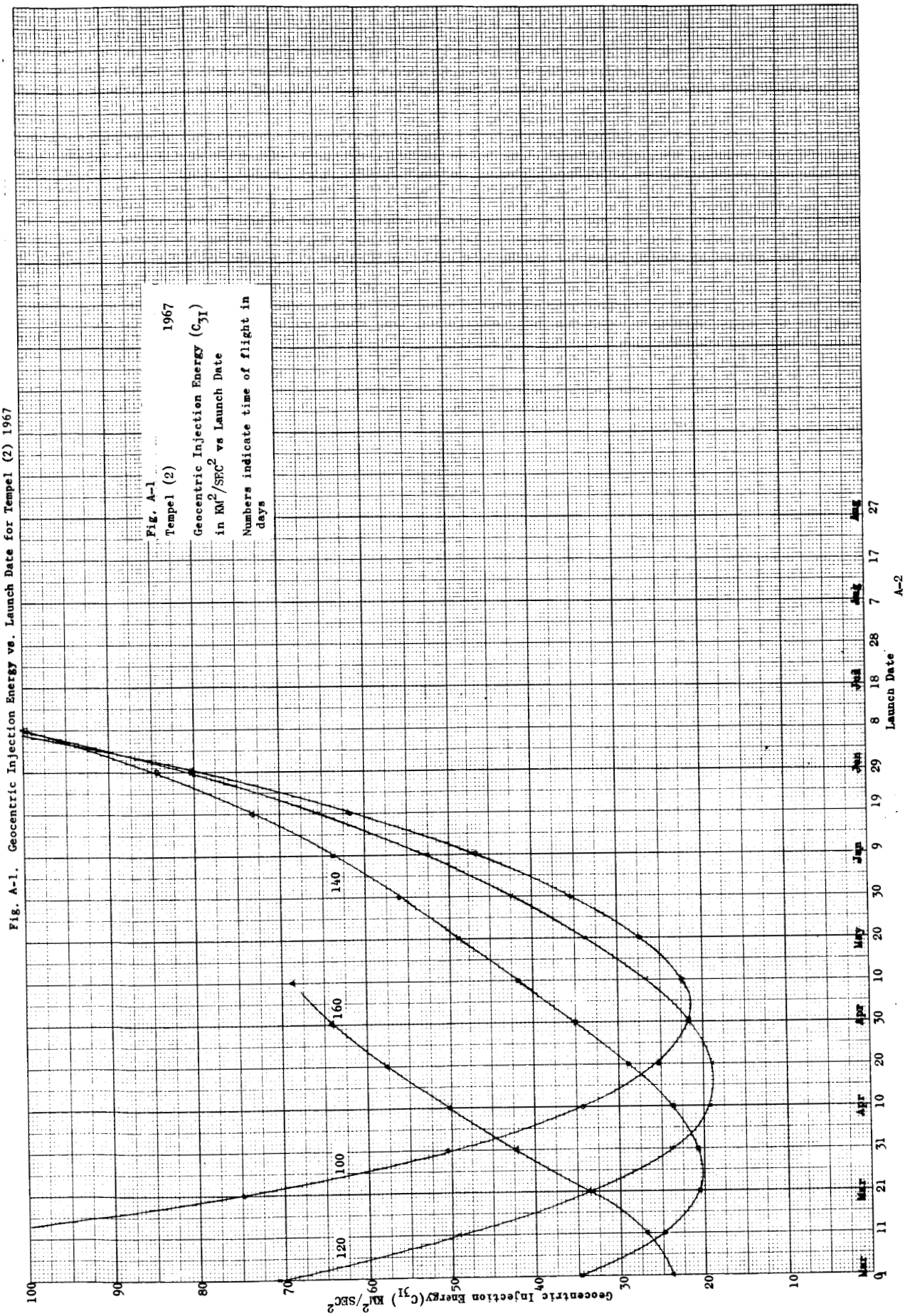

Fig. A-1. Geocentric Injection Energy vs. Launch Date for Tempel (2) 1967

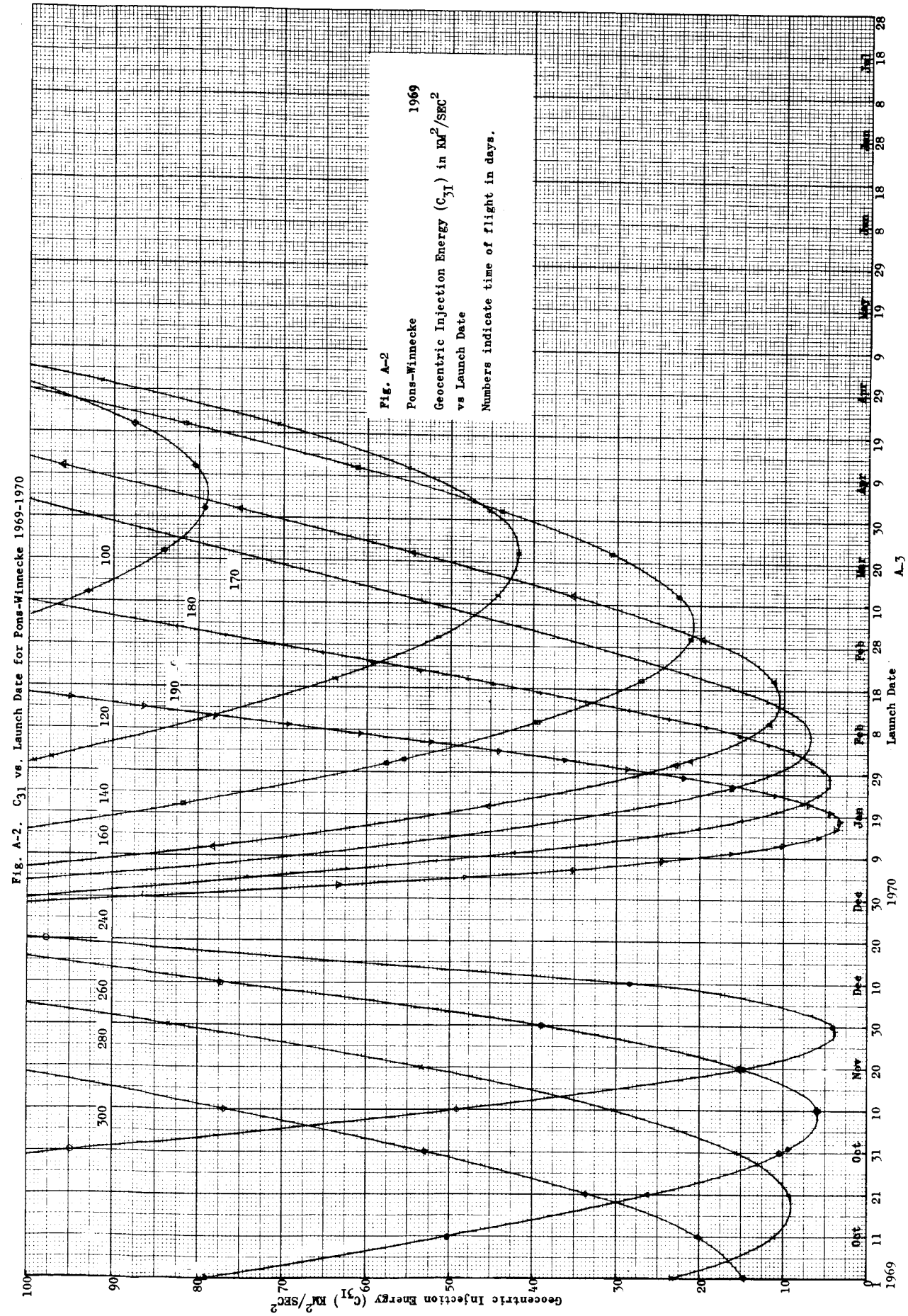

Fig. A-2. C_{3I} vs. Launch Date for Pons-Winnecke 1969-1970

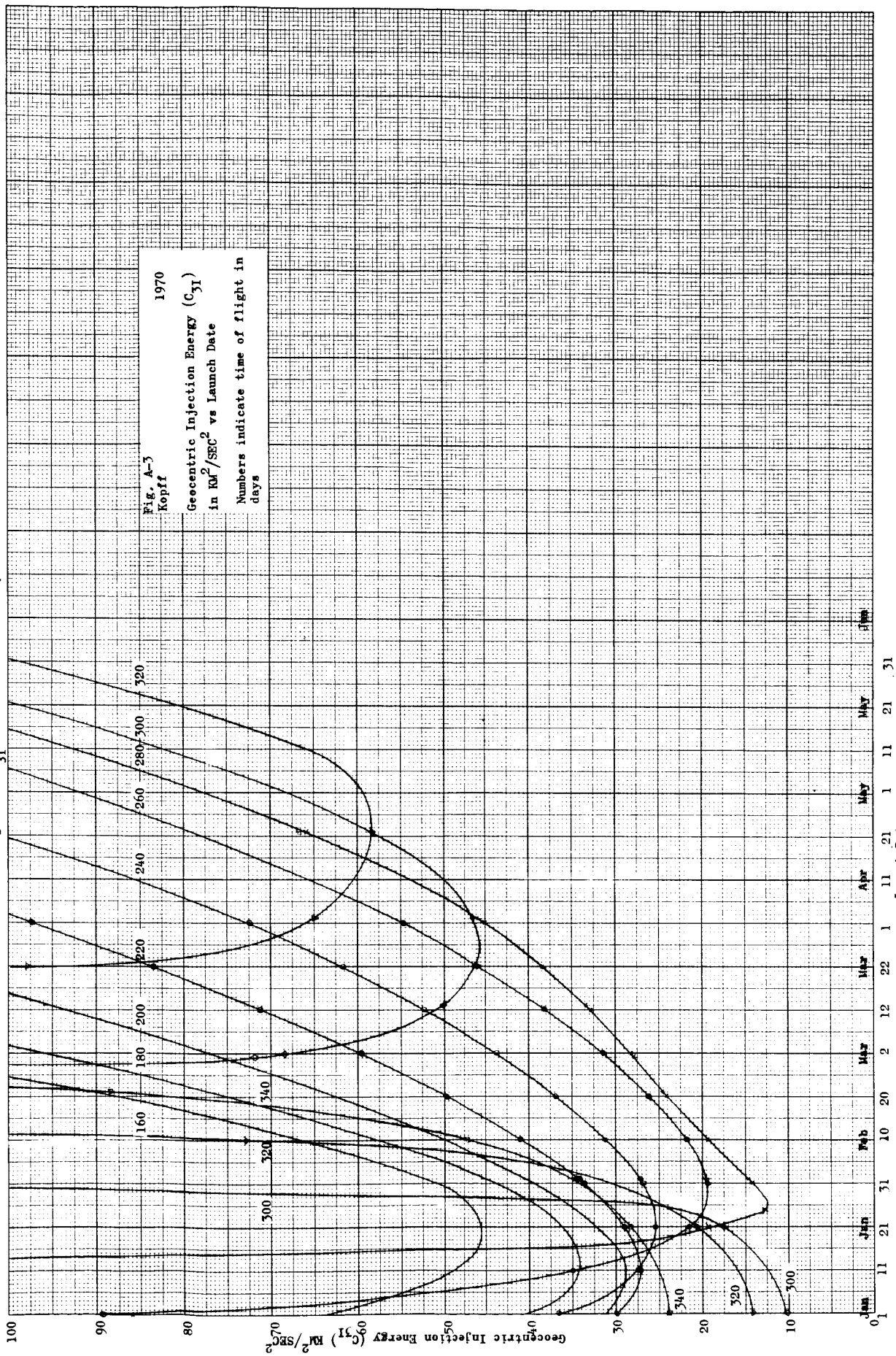

Fig. A-3. C_{31} vs. Launch Date for Kopff 1970

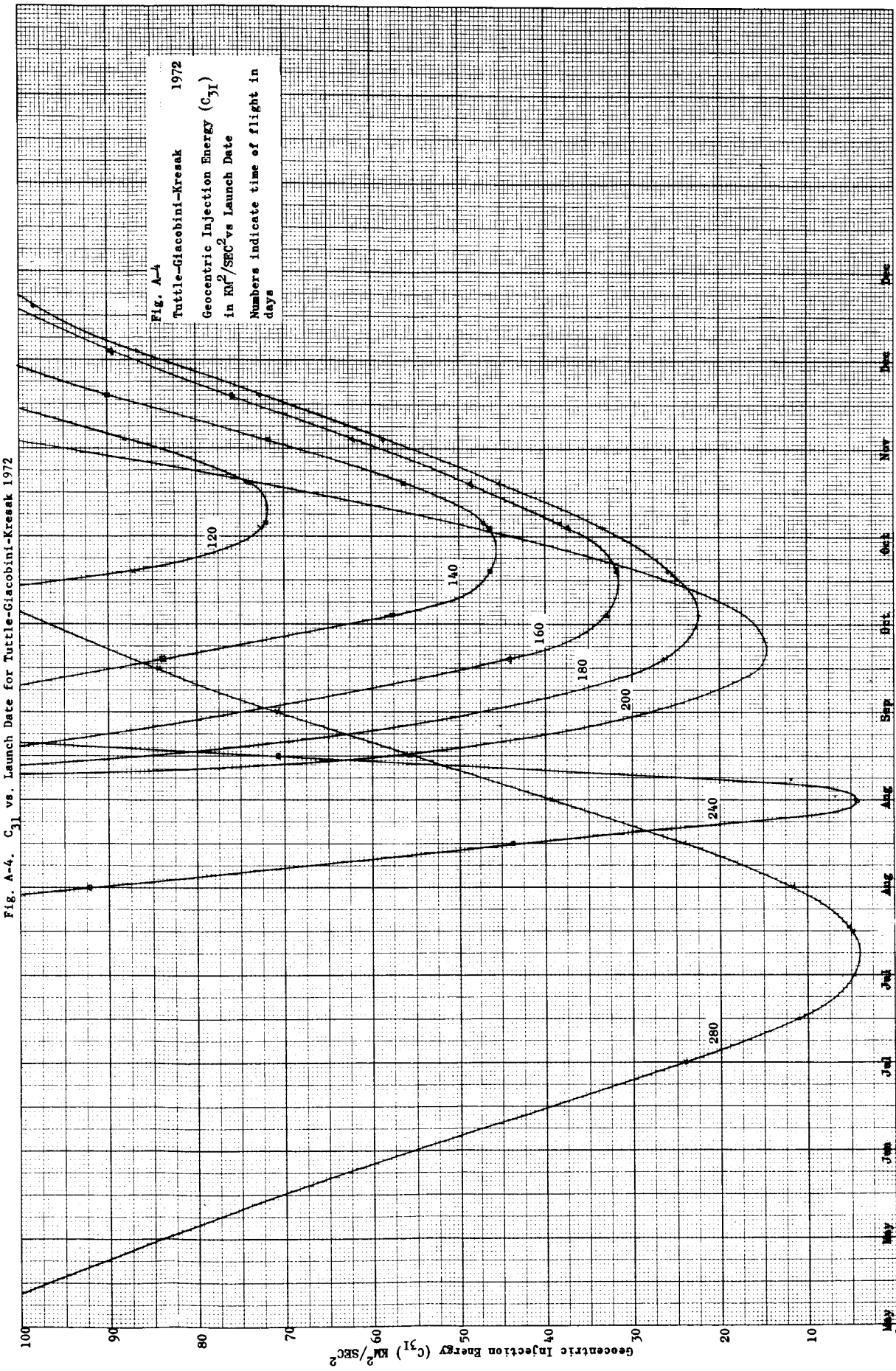

Fig. A-4. C_{3I} vs. Launch Date for Tuttle-Giacobini-Kresak 1972

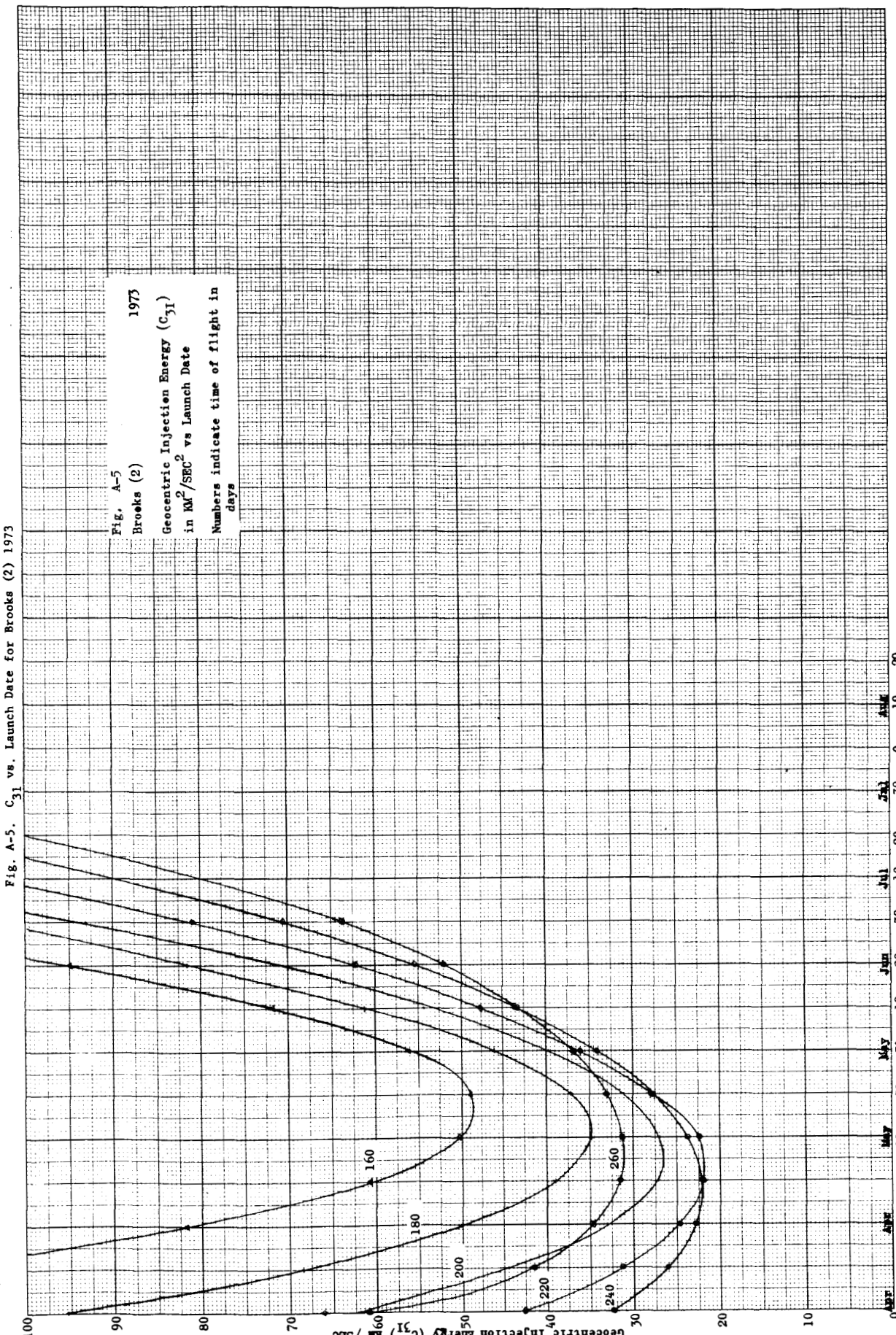

Fig. A-5. C_{3I} vs. Launch Date for Brooks (2) 1973

Fig. A-6. Hyperbolic Excess Speed at Arrival vs. Launch Date for Brooks

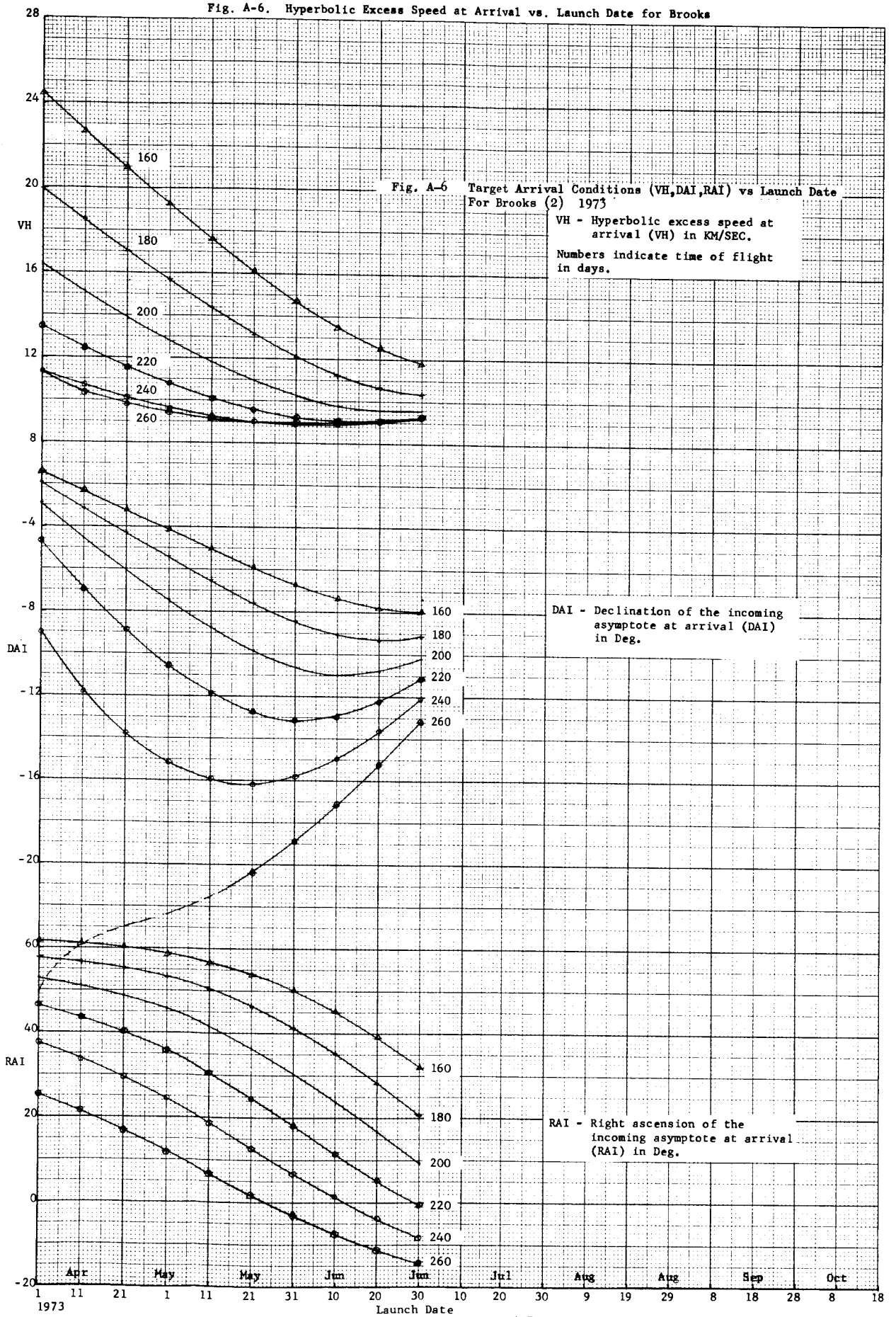

Fig. A-7. V_H vs. Launch Date for Kopff

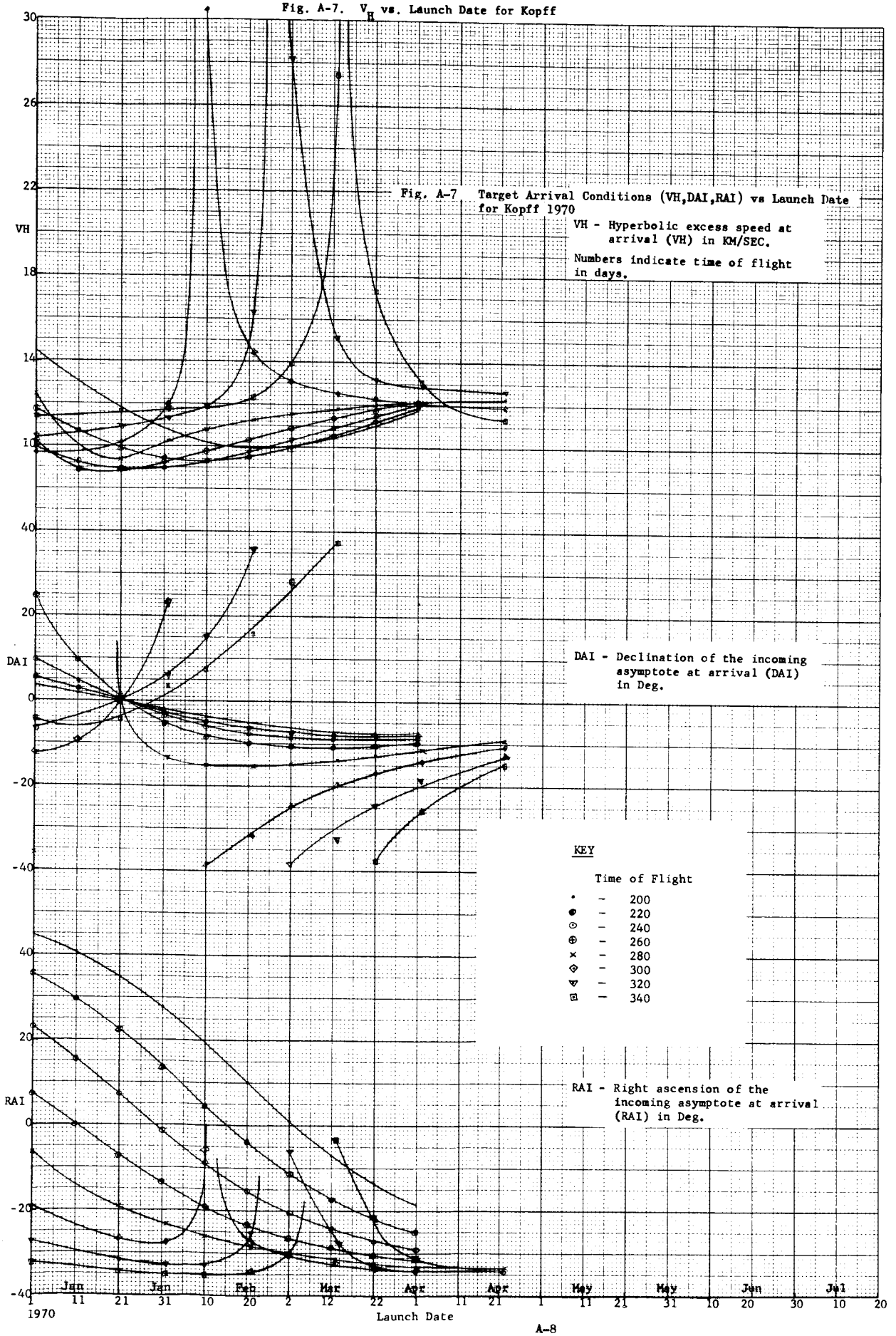

Fig. A-8. V_H vs. Launch Date for Pons-Winnecke

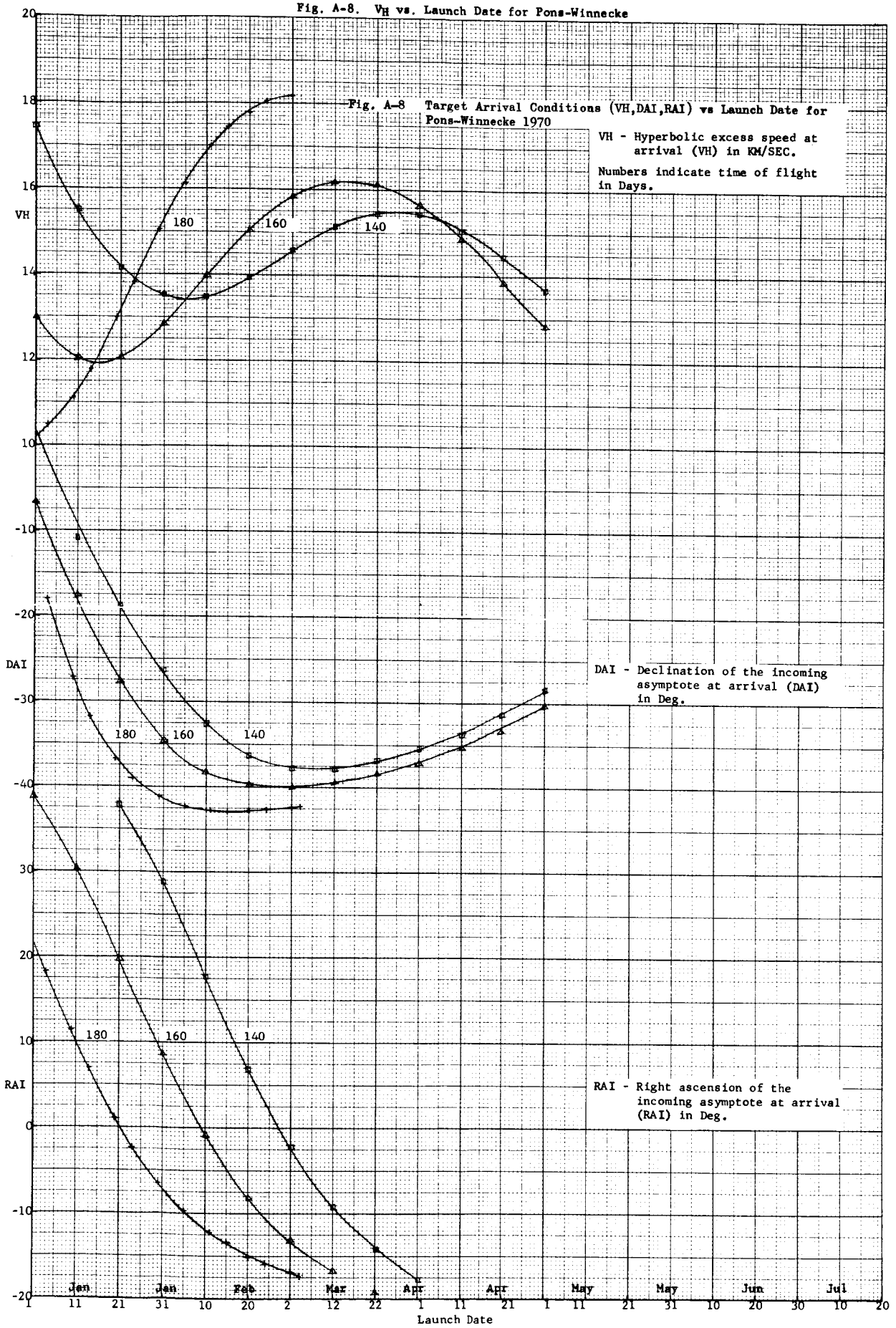

No Figure

Fig. A-10. V_H vs. Launch Date for Tempel (2)

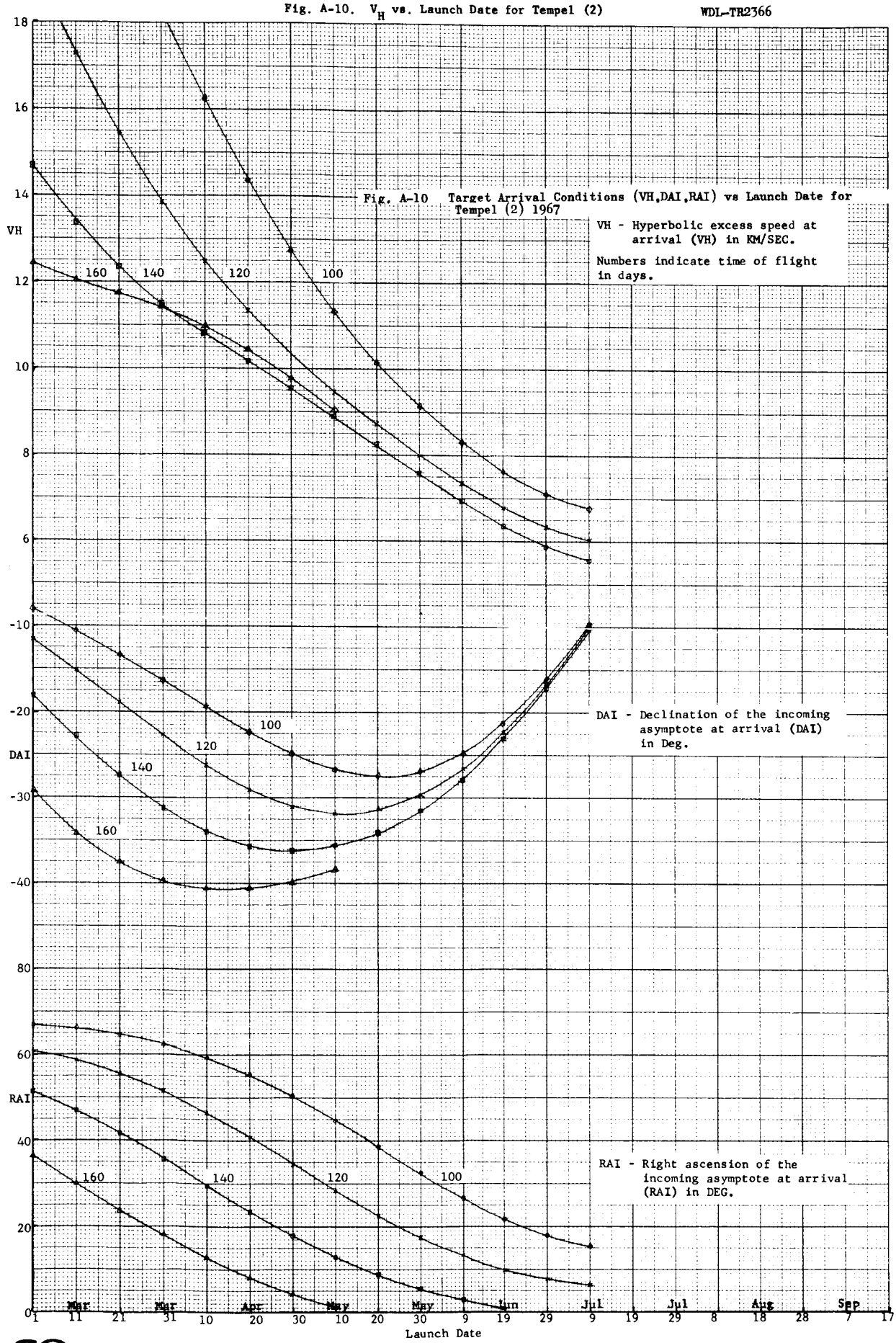

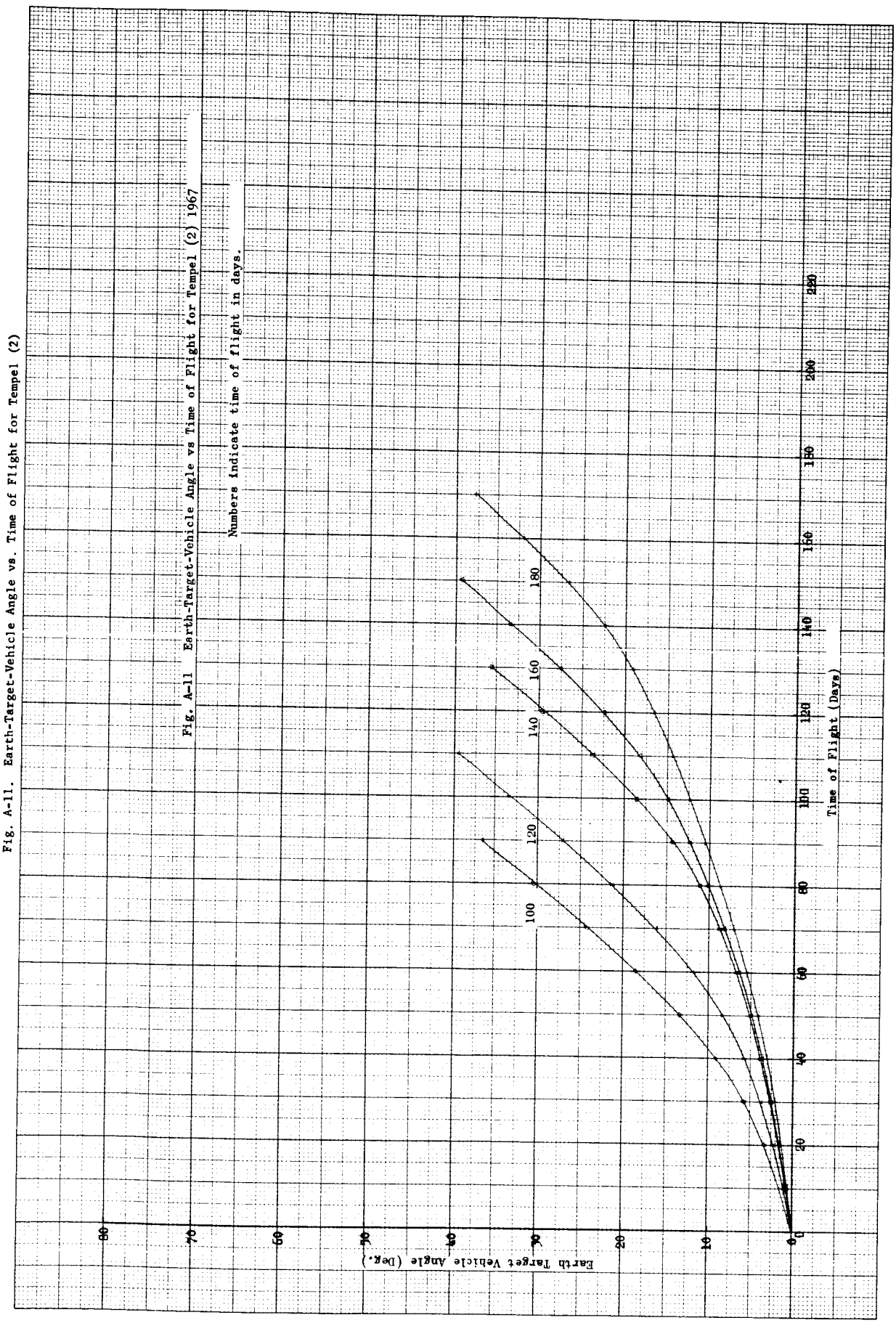

Fig. A-11. Earth-Target-Vehicle Angle vs. Time of Flight for Tempel (2)

Fig. A-11 Earth-Target-Vehicle Angle vs Time of Flight for Tempel (2) 1967

Numbers indicate time of flight in days.

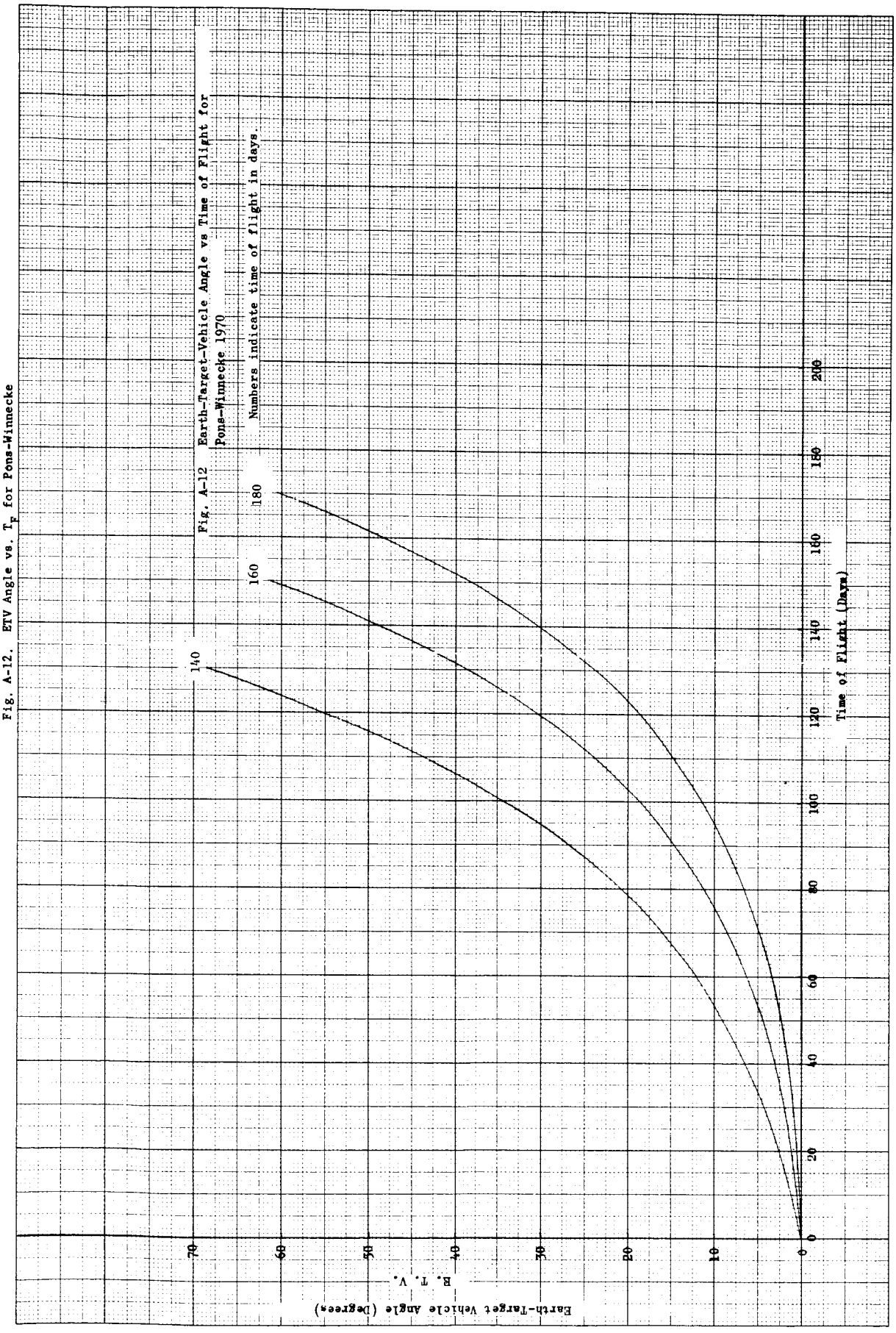

Fig. A-12. ETV Angle vs. T_F for Pons-Winnecke

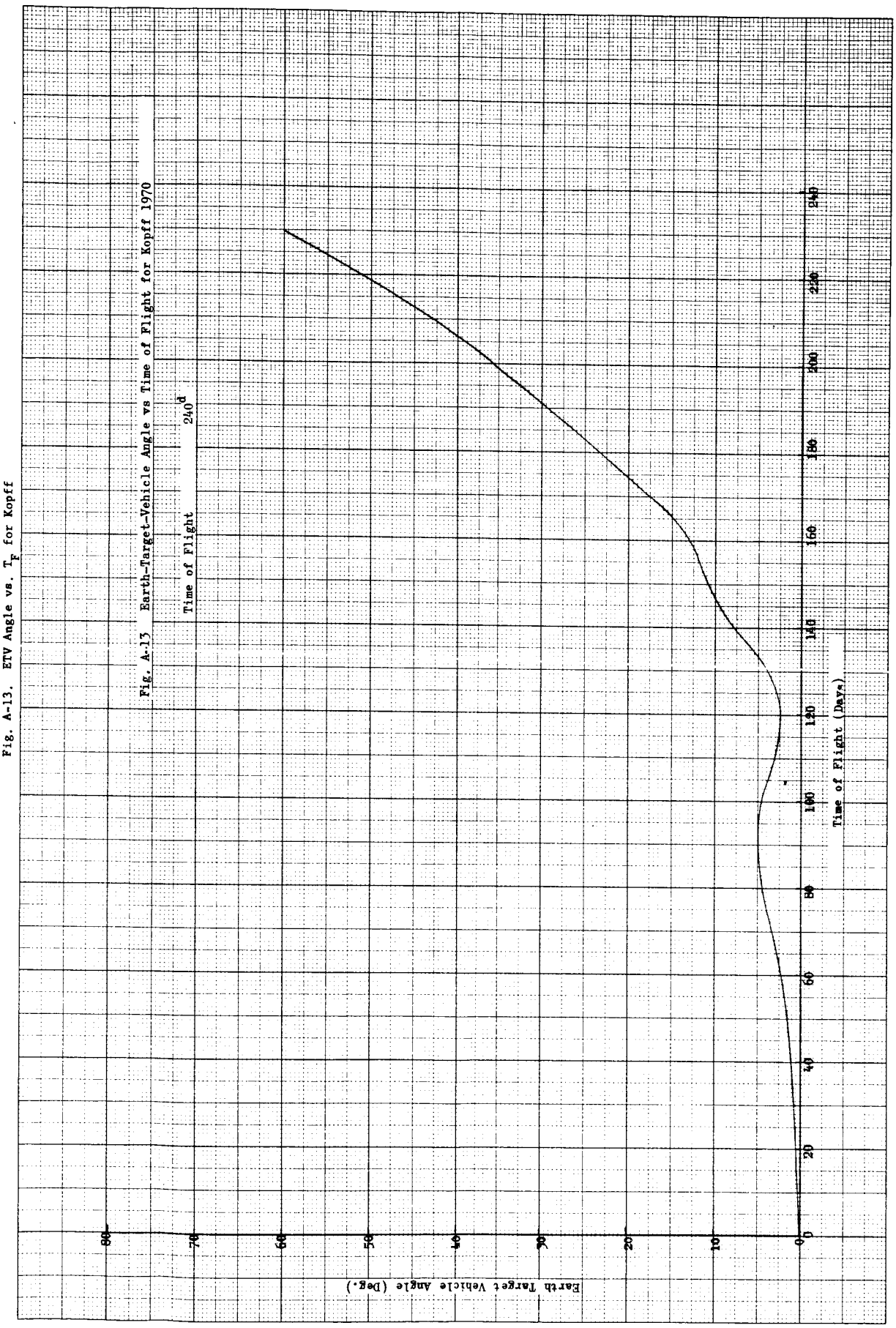

Fig. A-13 Earth-Target-Vehicle Angle vs Time of Flight for Kopff 1970

Time of Flight 240d

Fig. A-13. ETV Angle vs. T_F for Kopff

Fig. A-14. ETV Angle vs. T_F for Tuttle-Giacobini-Kresak

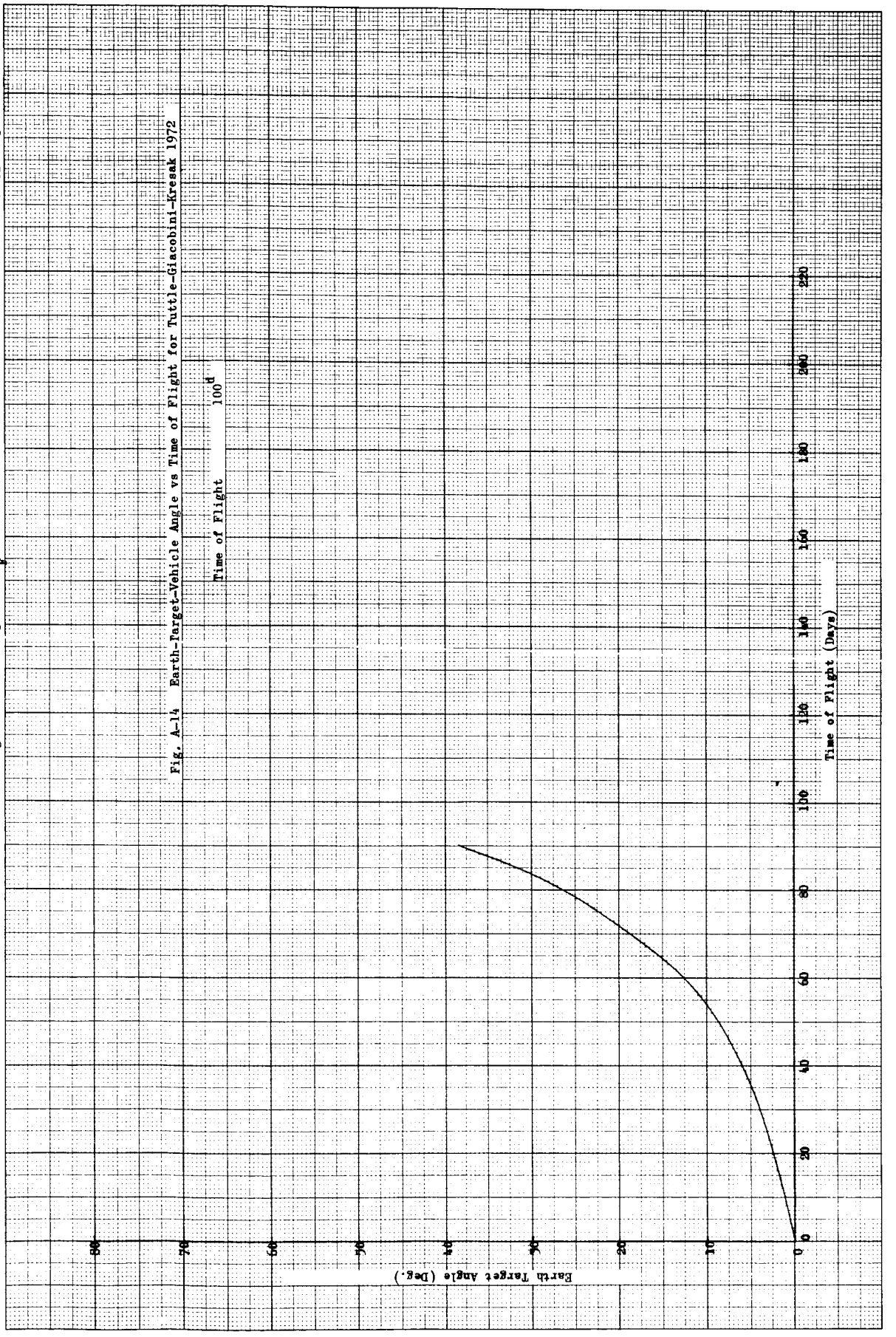

Fig. A-14 Earth-Target-Vehicle Angle vs Time of Flight for Tuttle-Giacobini-Kresak 1972

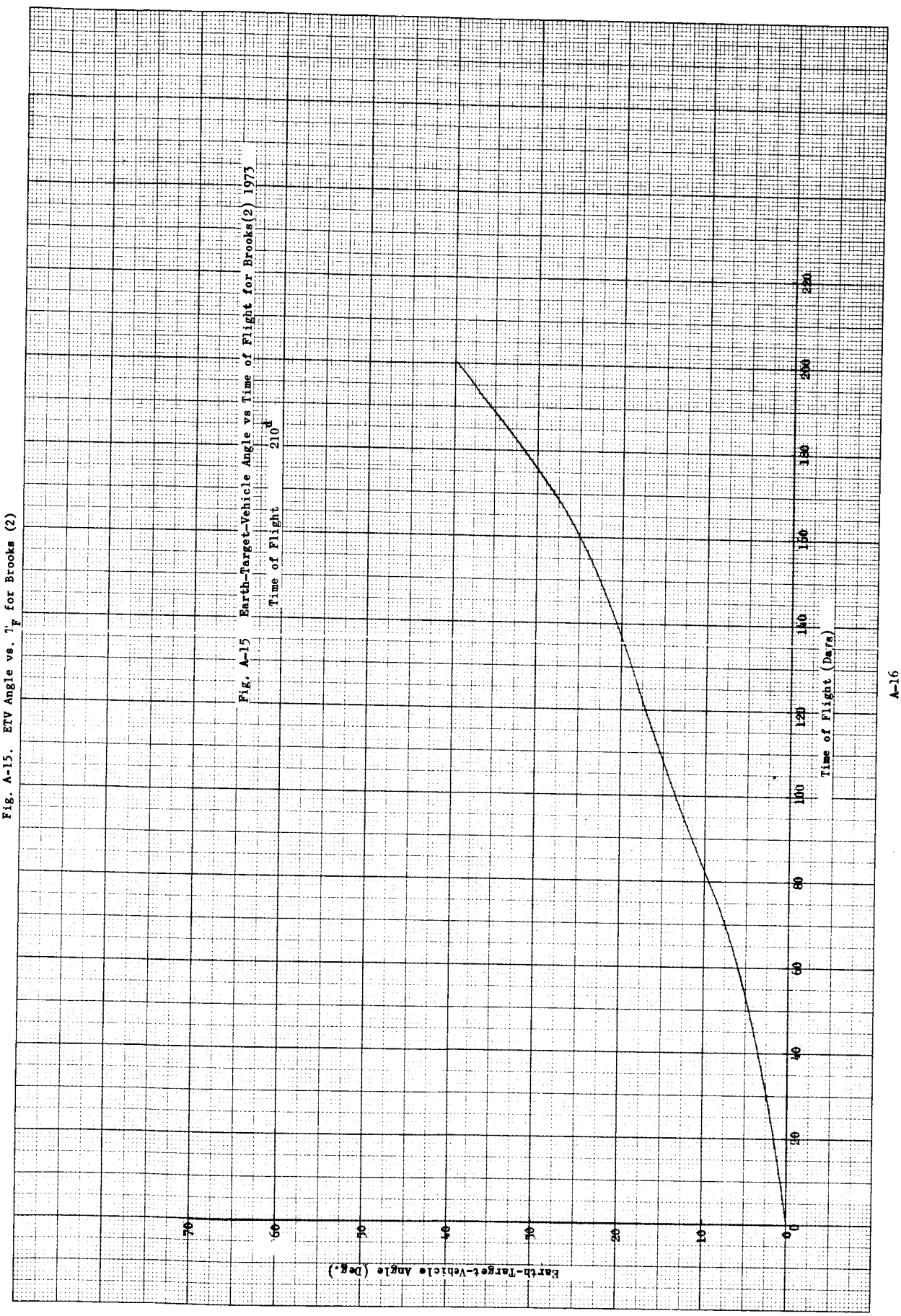

Fig. A-15 Earth-Target-Vehicle Angle vs Time of Flight for Brooks(2) 1973
Time of Flight 210d

Fig. A-15. ETV Angle vs. T_F for Brooks (2)

Fig. A-16. Ecliptic Plane Projection of Comet and Vehicle Trajectories for Pons-Winnecke

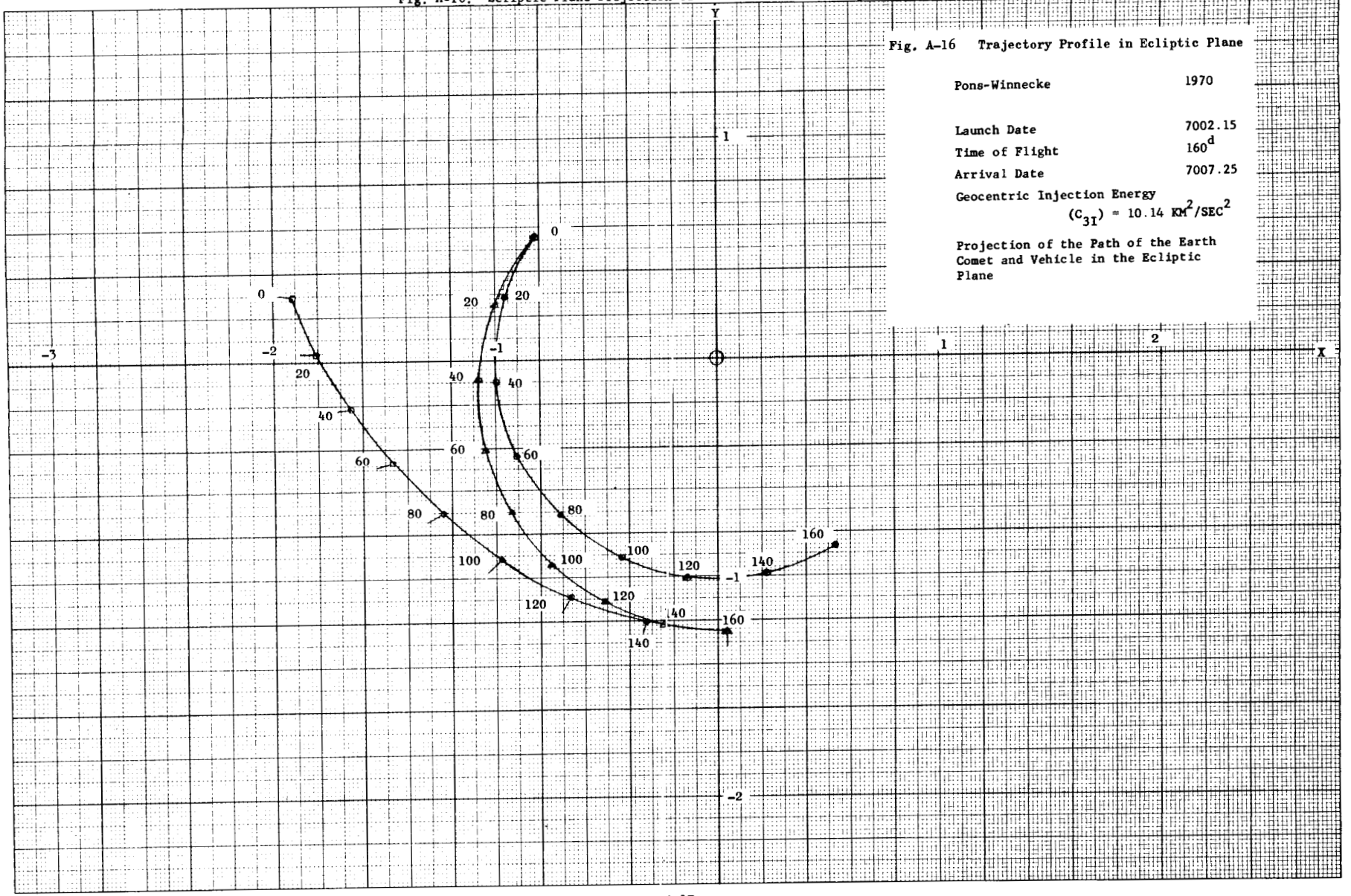

Fig. A-16 Trajectory Profile in Ecliptic Plane

Pons-Winnecke	1970
Launch Date	7002.15
Time of Flight	160^d
Arrival Date	7007.25

Geocentric Injection Energy
$(C_{3I}) = 10.14\ KM^2/SEC^2$

Projection of the Path of the Earth Comet and Vehicle in the Ecliptic Plane

WDL-TR2566

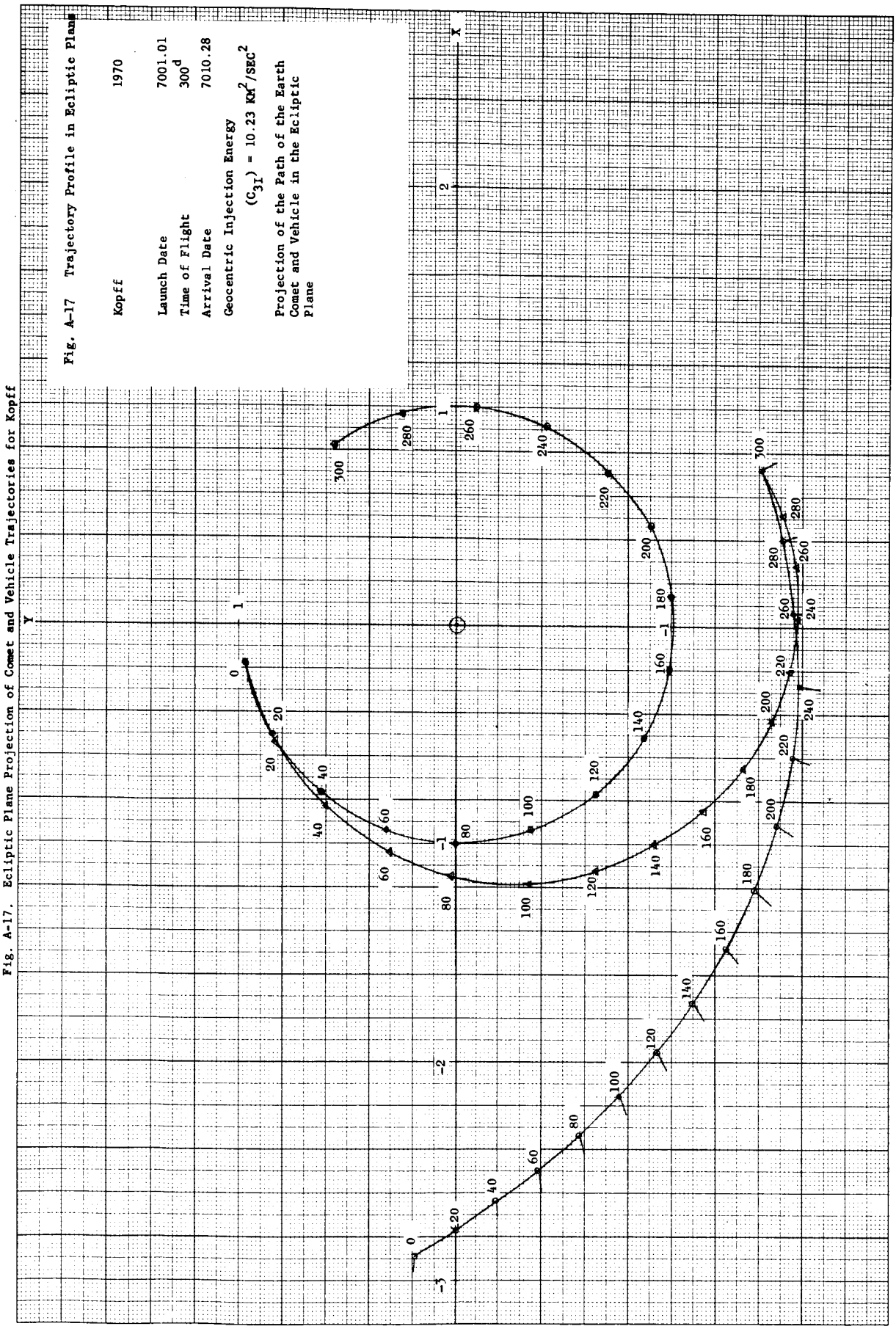

Fig. A-17. Ecliptic Plane Projection of Comet and Vehicle Trajectories for Kopff

Fig. A-18. Ecliptic Plane Projection of Comet and Vehicle Trajectories for Brooks (2)

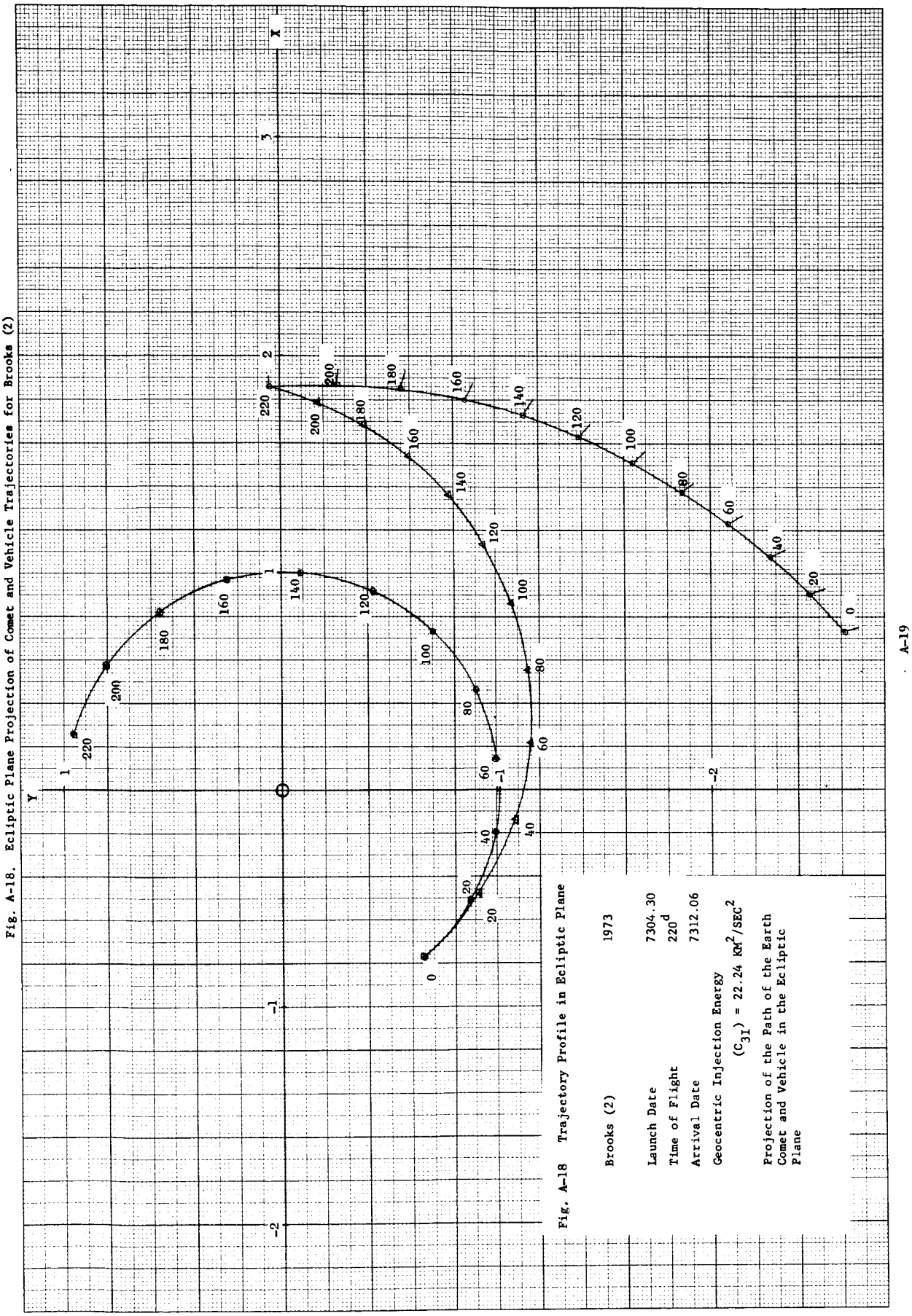

Fig. A-18 Trajectory Profile in Ecliptic Plane

Brooks (2)	1973
Launch Date	7304.30
Time of Flight	220^d
Arrival Date	7312.06
Geocentric Injection Energy $(C_{3I}) = 22.24\ KM^2/SEC^2$	

Projection of the Path of the Earth Comet and Vehicle in the Ecliptic Plane

Fig. A-19. Ecliptic Plane Projection of Comet and Vehicle Trajectories for Tempel (2)

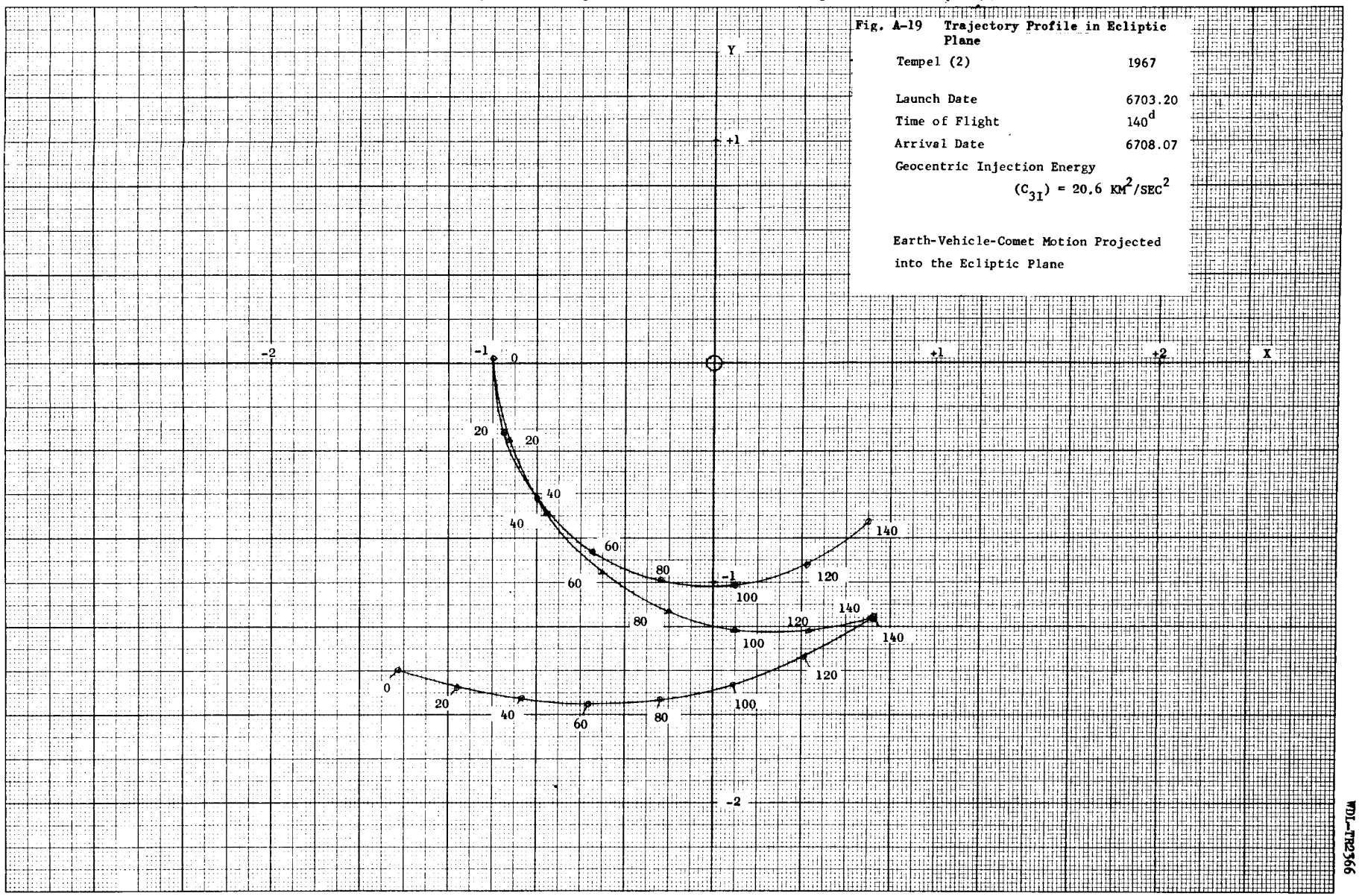

No Figure

Fig. A-21. In-the-Ecliptic Encounter Profile for Pons-Winnecke

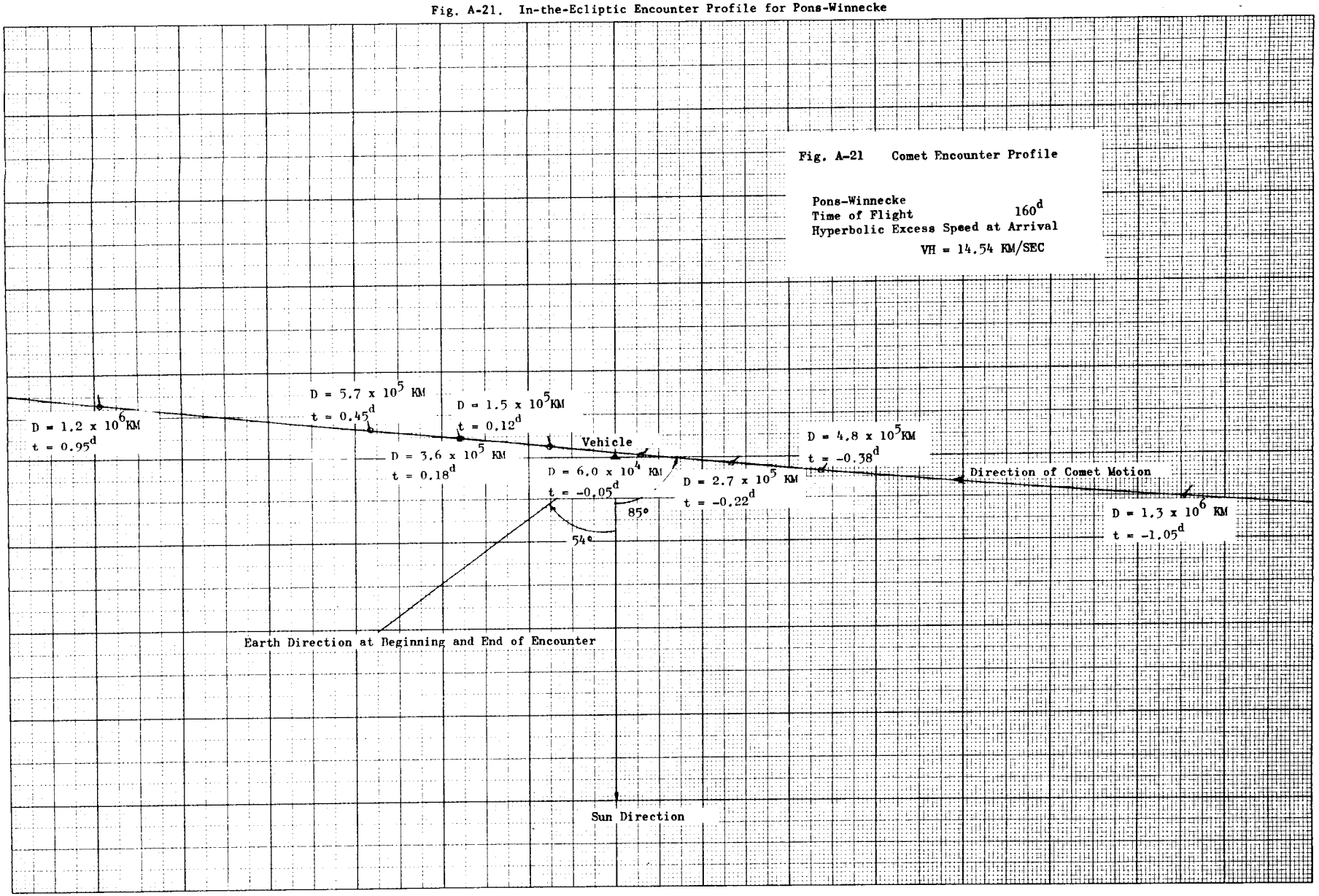

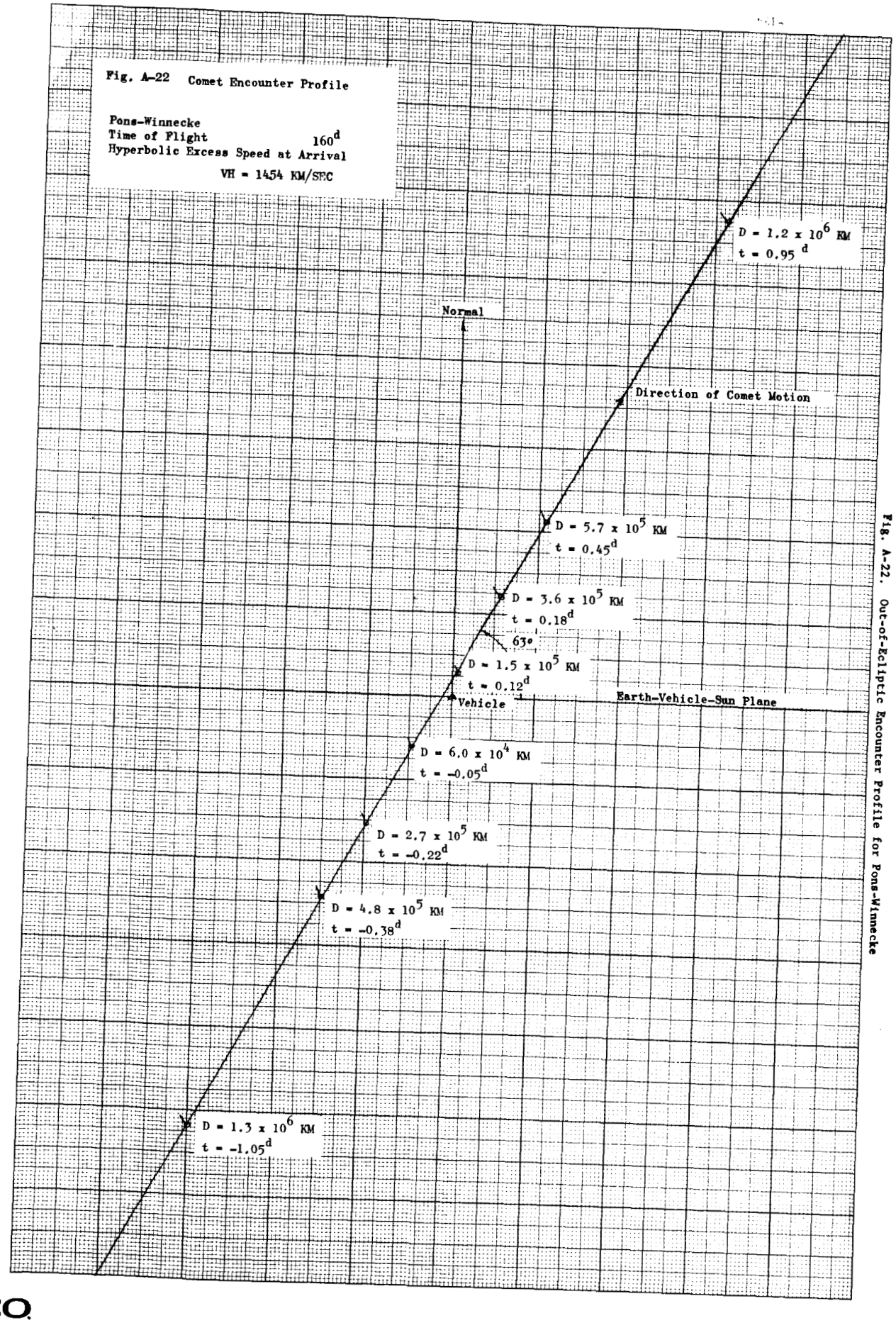

Fig. A-22. Out-of-Ecliptic Encounter Profile for Pons-Winnecke

Fig. A-23. In-the-Ecliptic Encounter Profile for Kopff

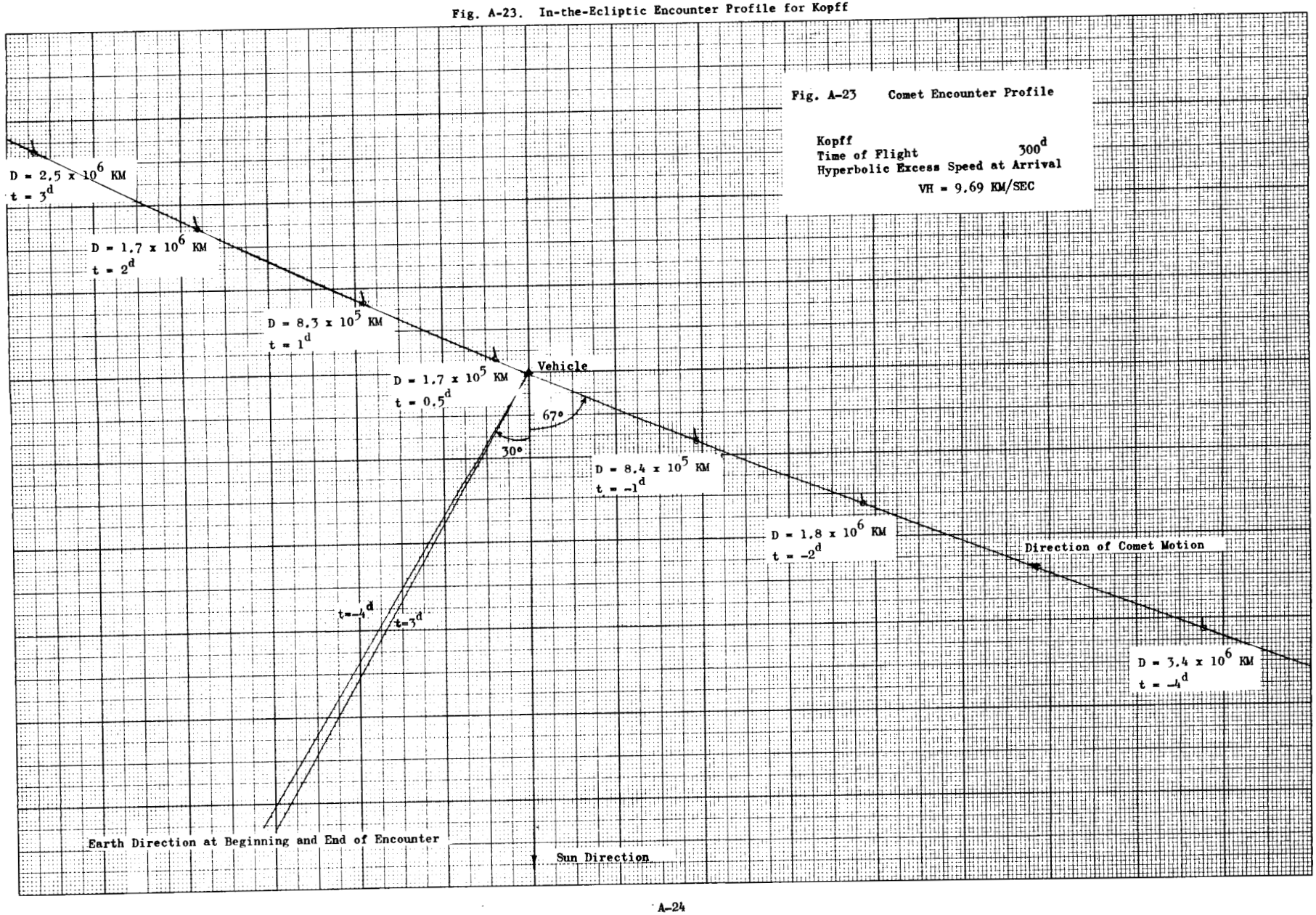

Fig. A-24. Out-of-Ecliptic Encounter Profile for Kopff

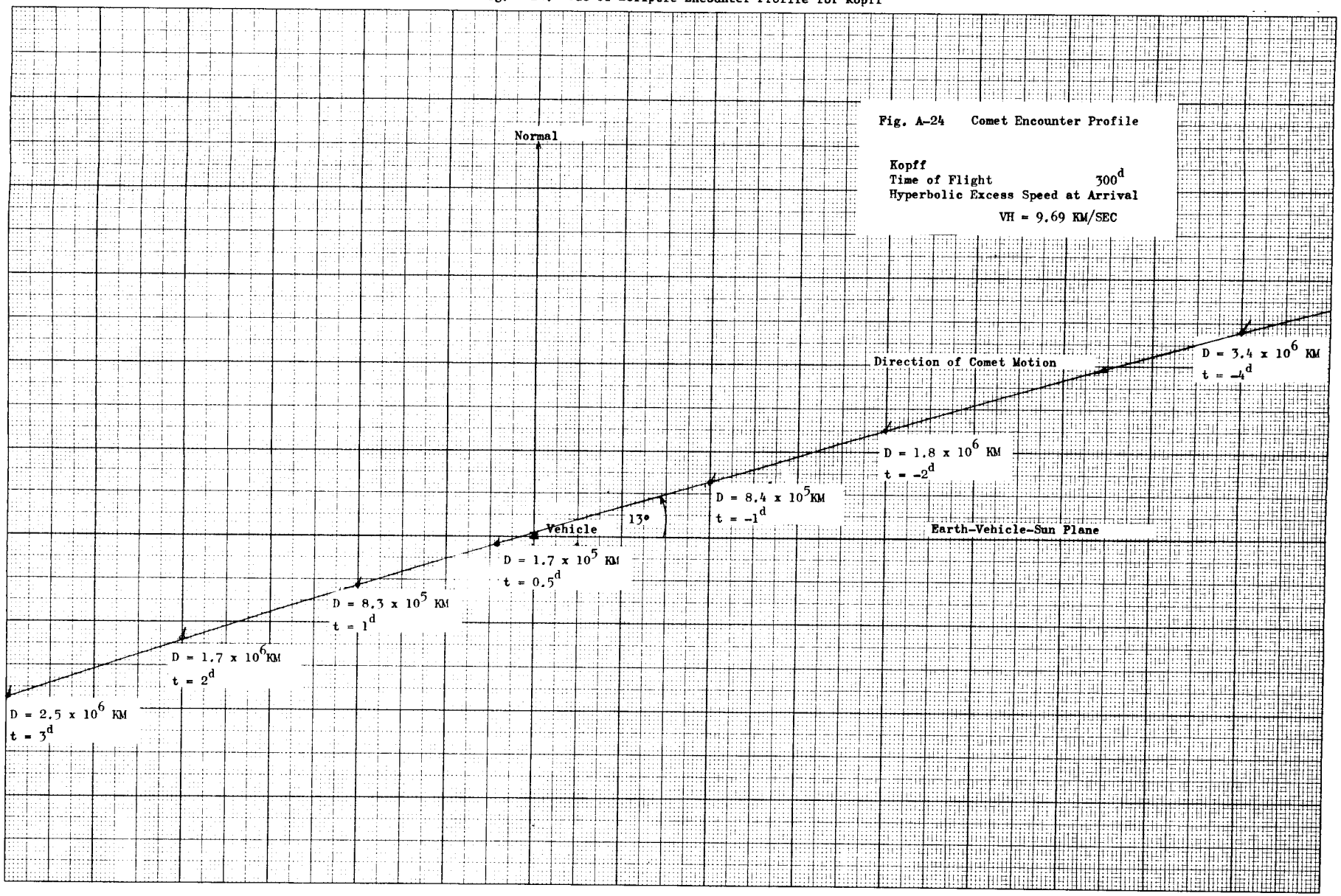

Fig. A-25. In-the-Ecliptic Encounter Profile for Brooks (2)

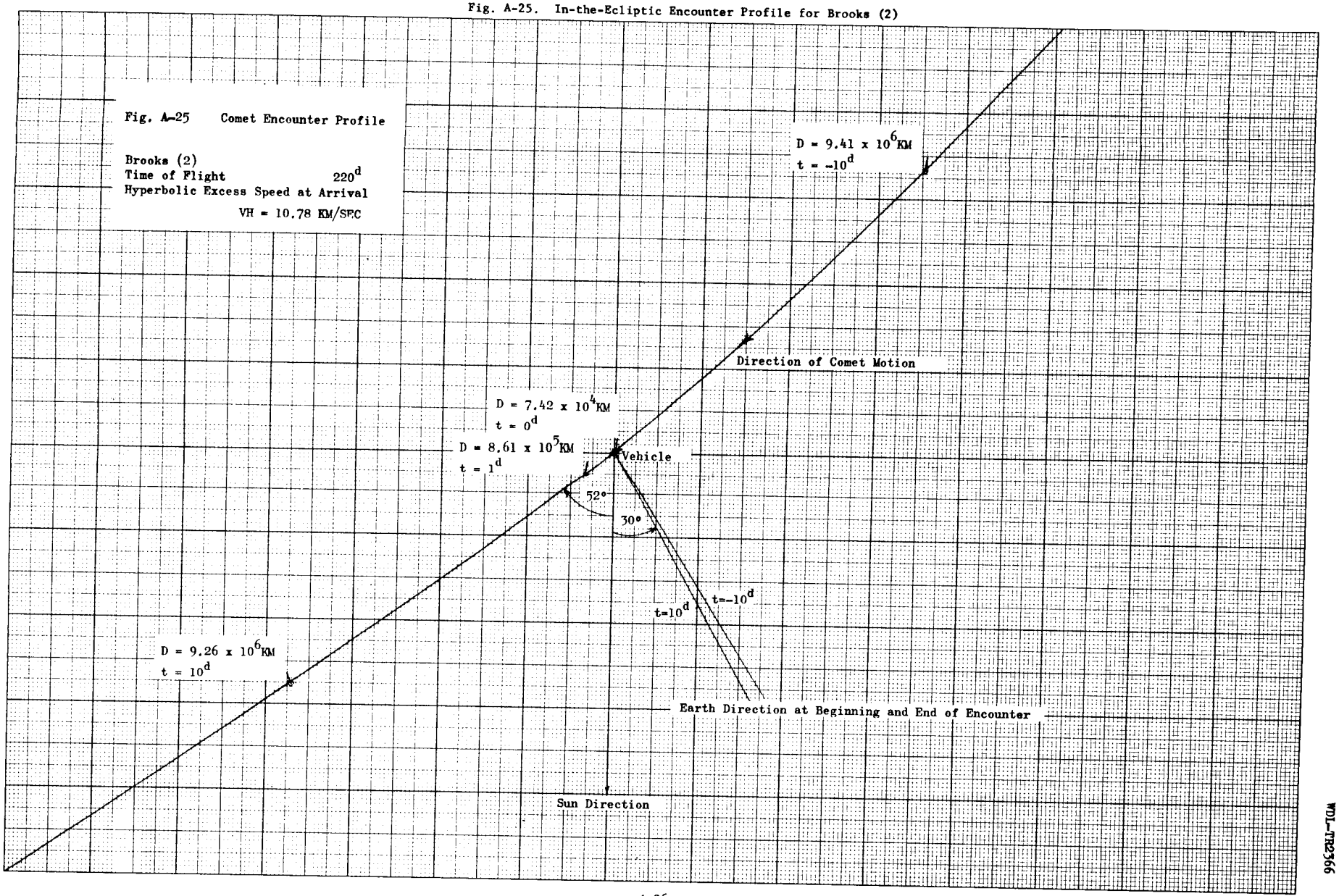

Fig. A-26. Out-of-Ecliptic Encounter Profile for Brooks (2)

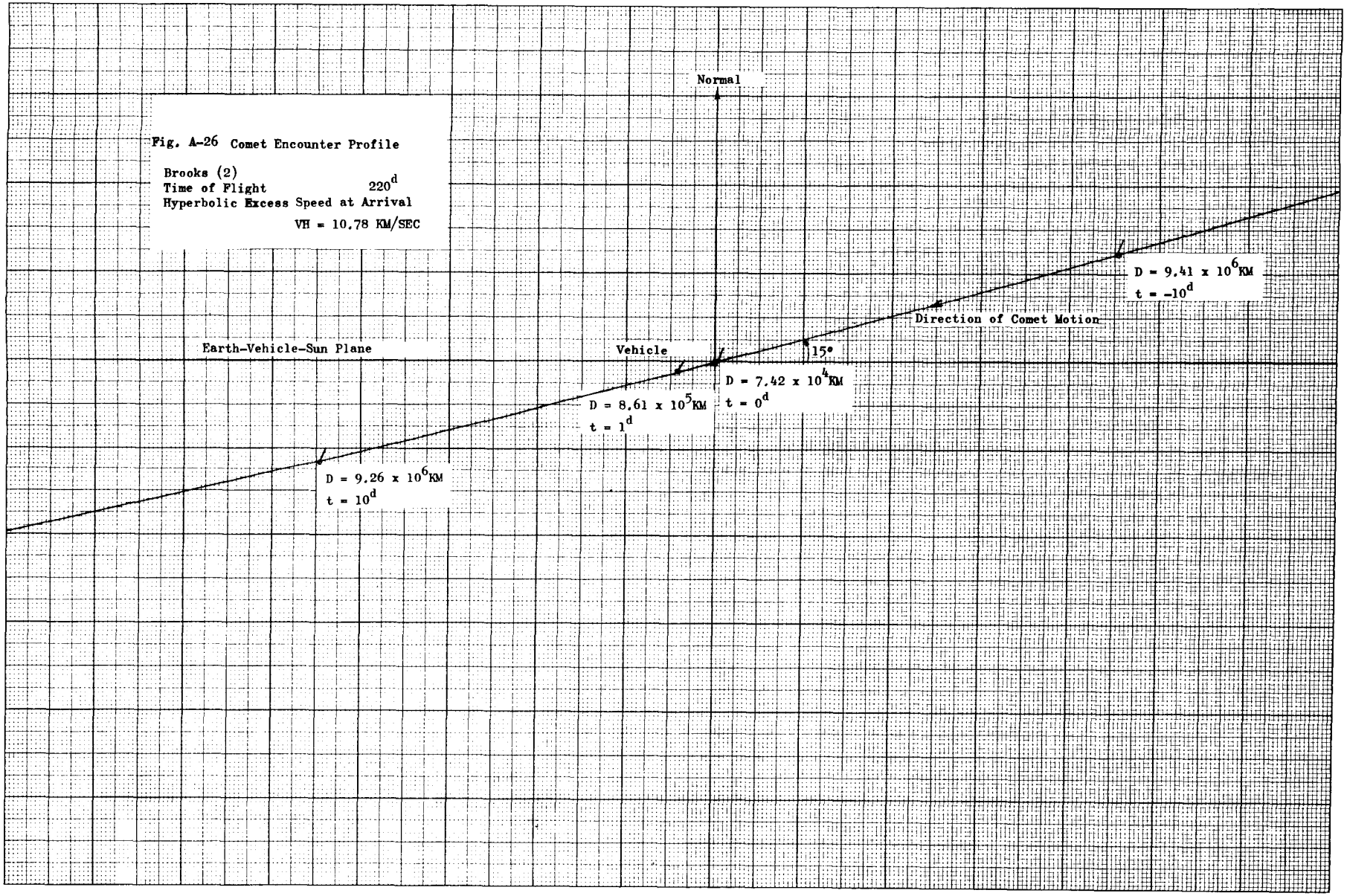

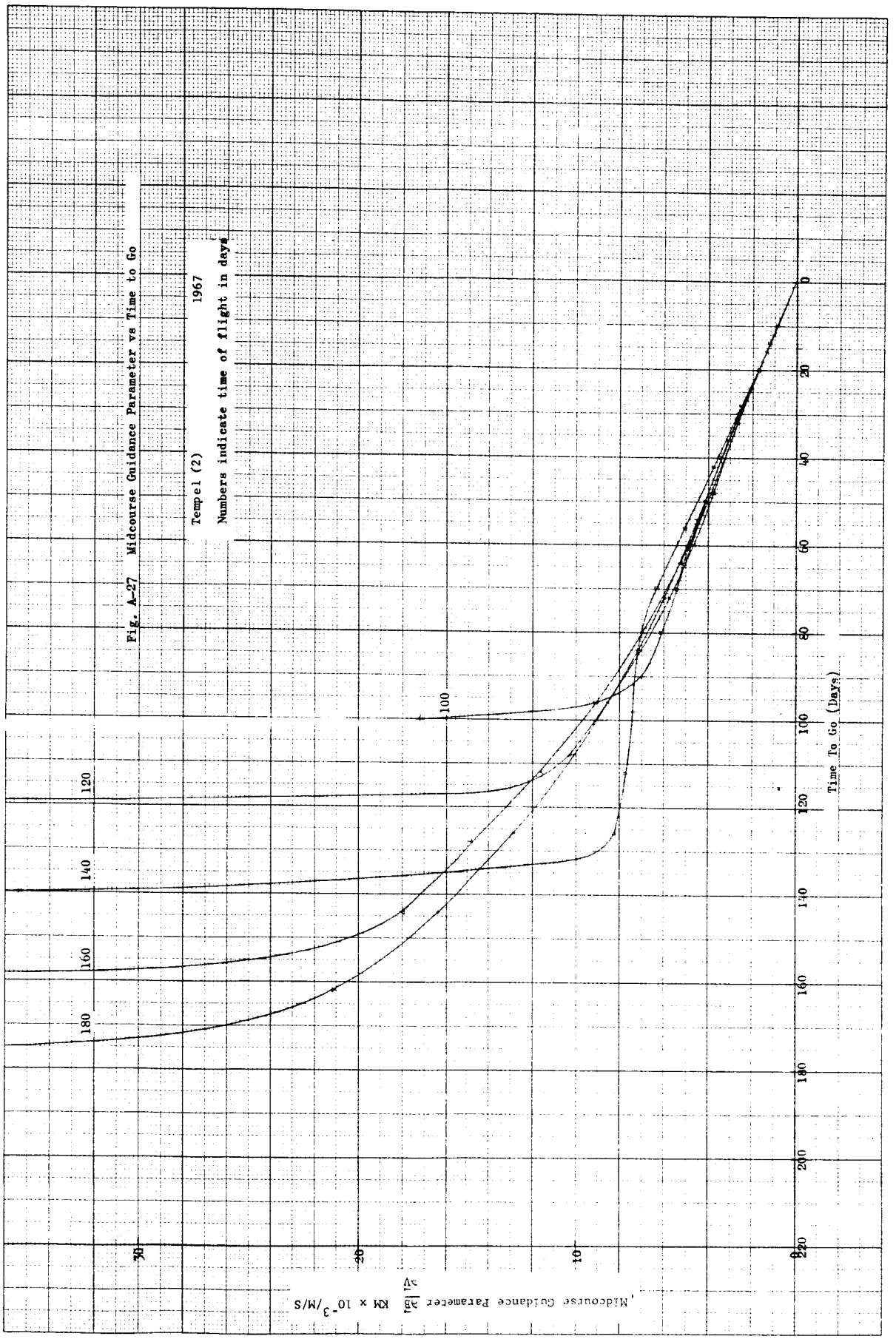

Fig. A-27. Midcourse Guidance Parameter vs. Time to Go for Tempel (2)

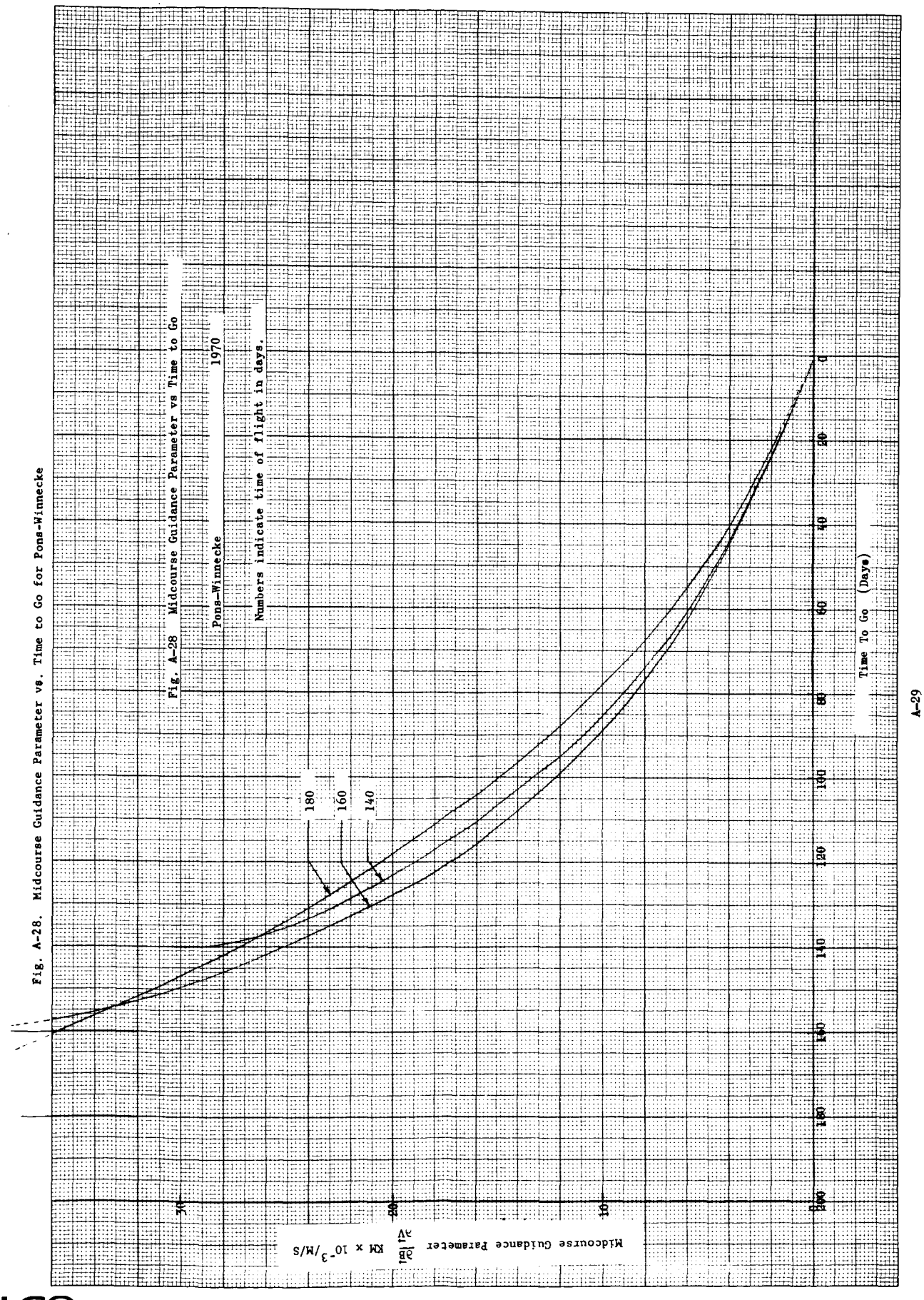

Fig. A-28. Midcourse Guidance Parameter vs. Time to Go for Pons-Winnecke

Fig. A-28 Midcourse Guidance Parameter vs Time to Go

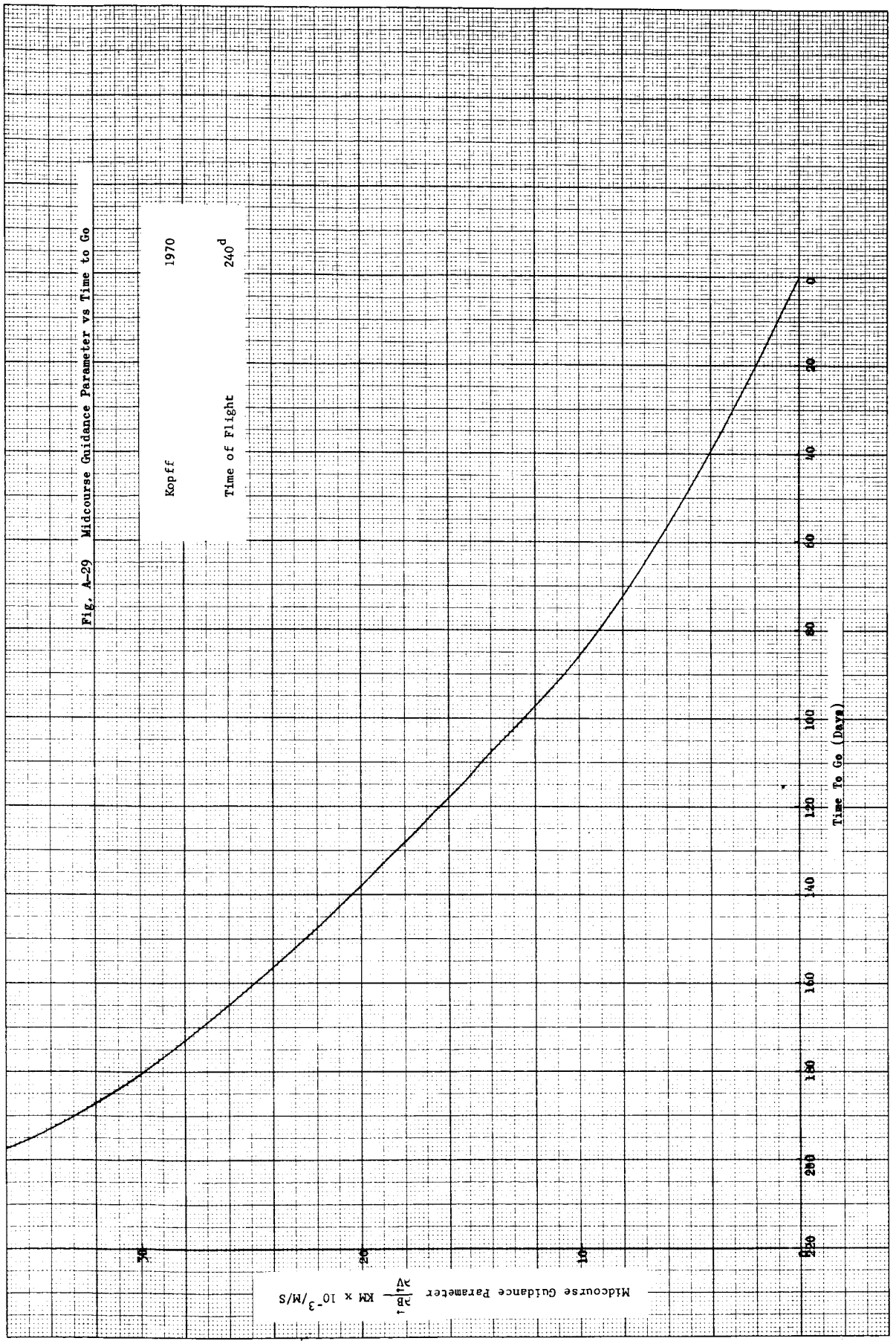

Fig. A-29. Midcourse Guidance Parameter vs. Time to Go for Kopff

Fig. A-29 Midcourse Guidance Parameter vs Time to Go

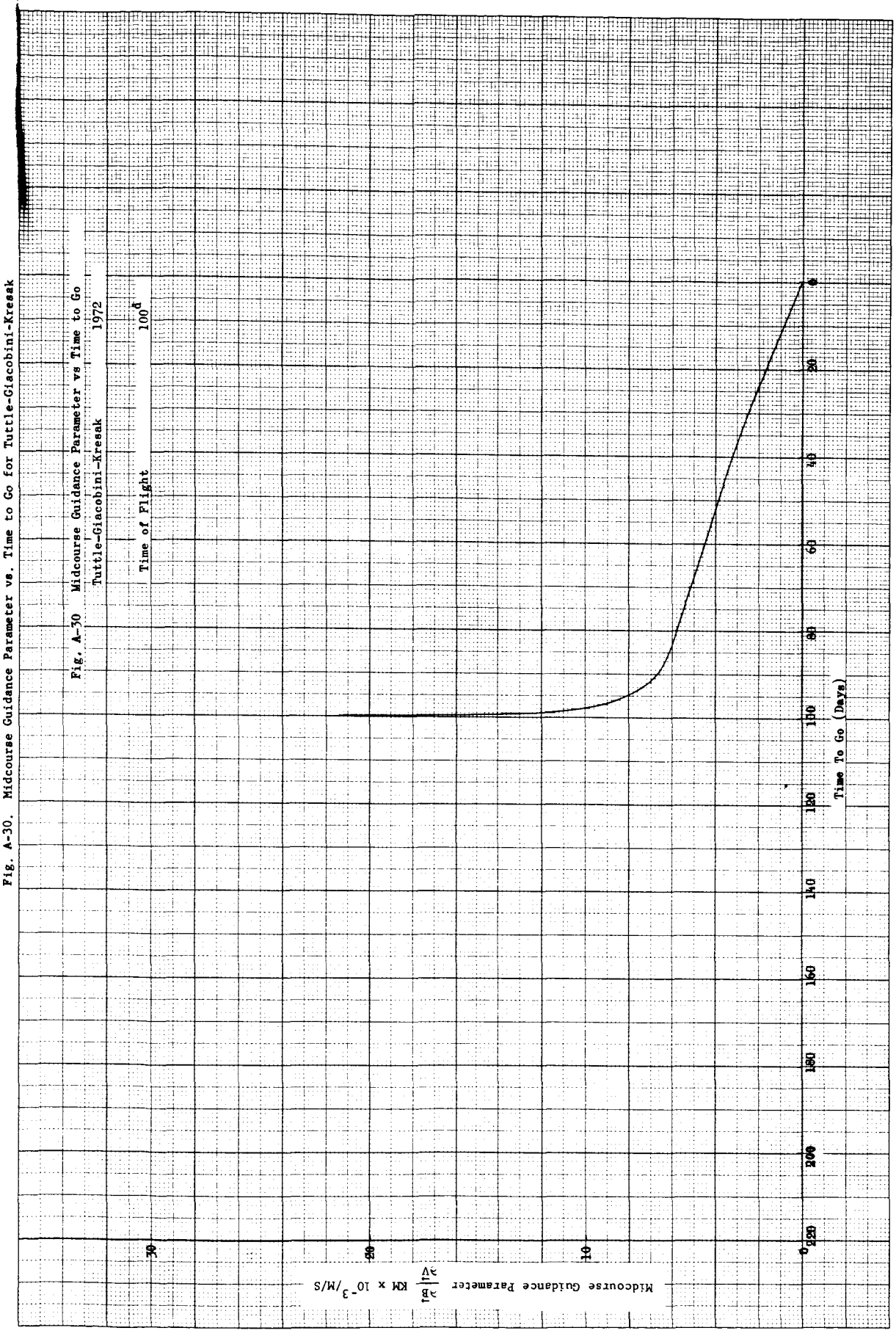

Fig. A-30. Midcourse Guidance Parameter vs. Time to Go for Tuttle-Giacobini-Kresak

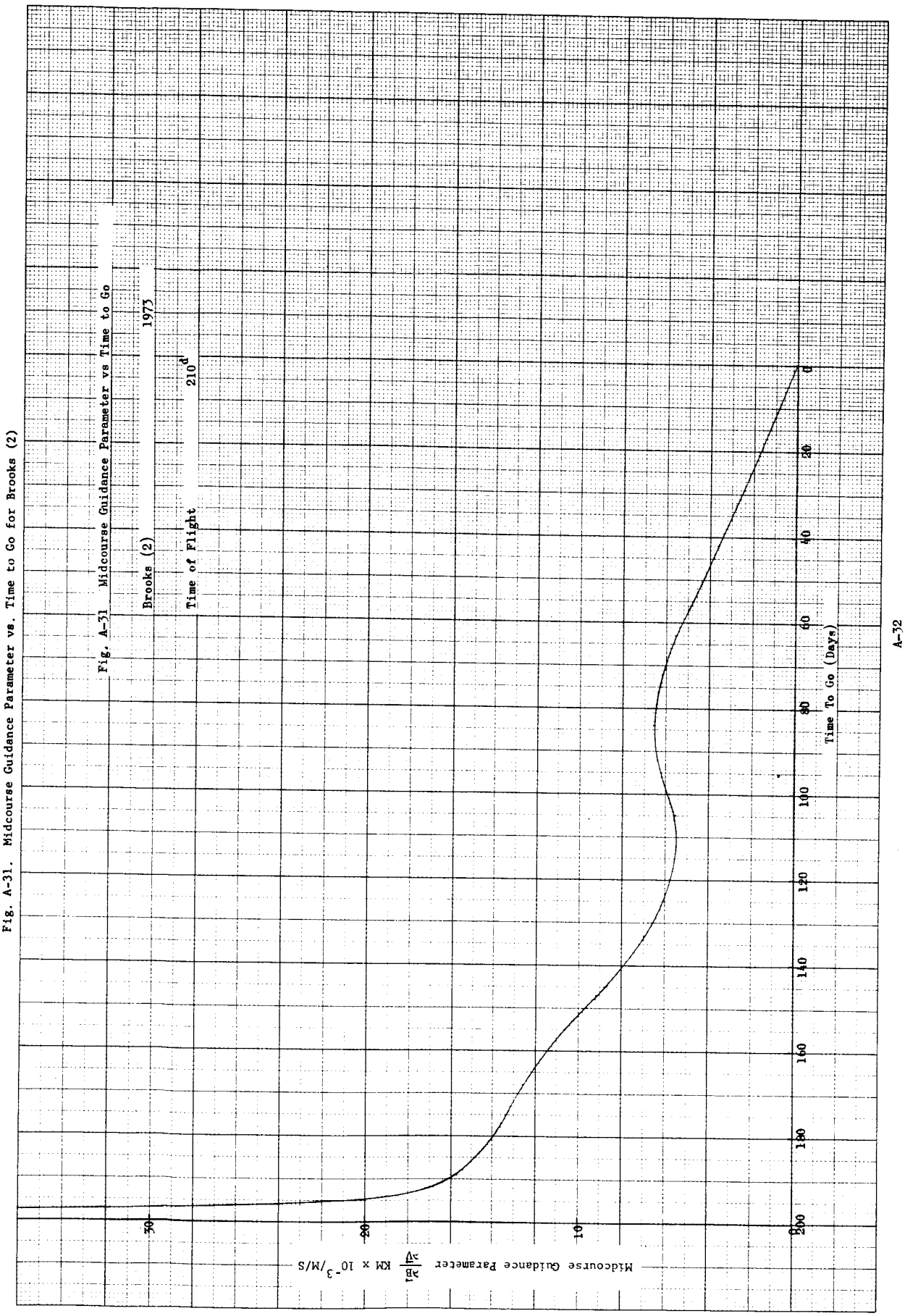

Fig. A-31. Midcourse Guidance Parameter vs. Time to Go for Brooks (2)

Fig. A-31 Midcourse Guidance Parameter vs Time to Go

Fig. A-32. Prelaunch Ephermis for Tempel (2)

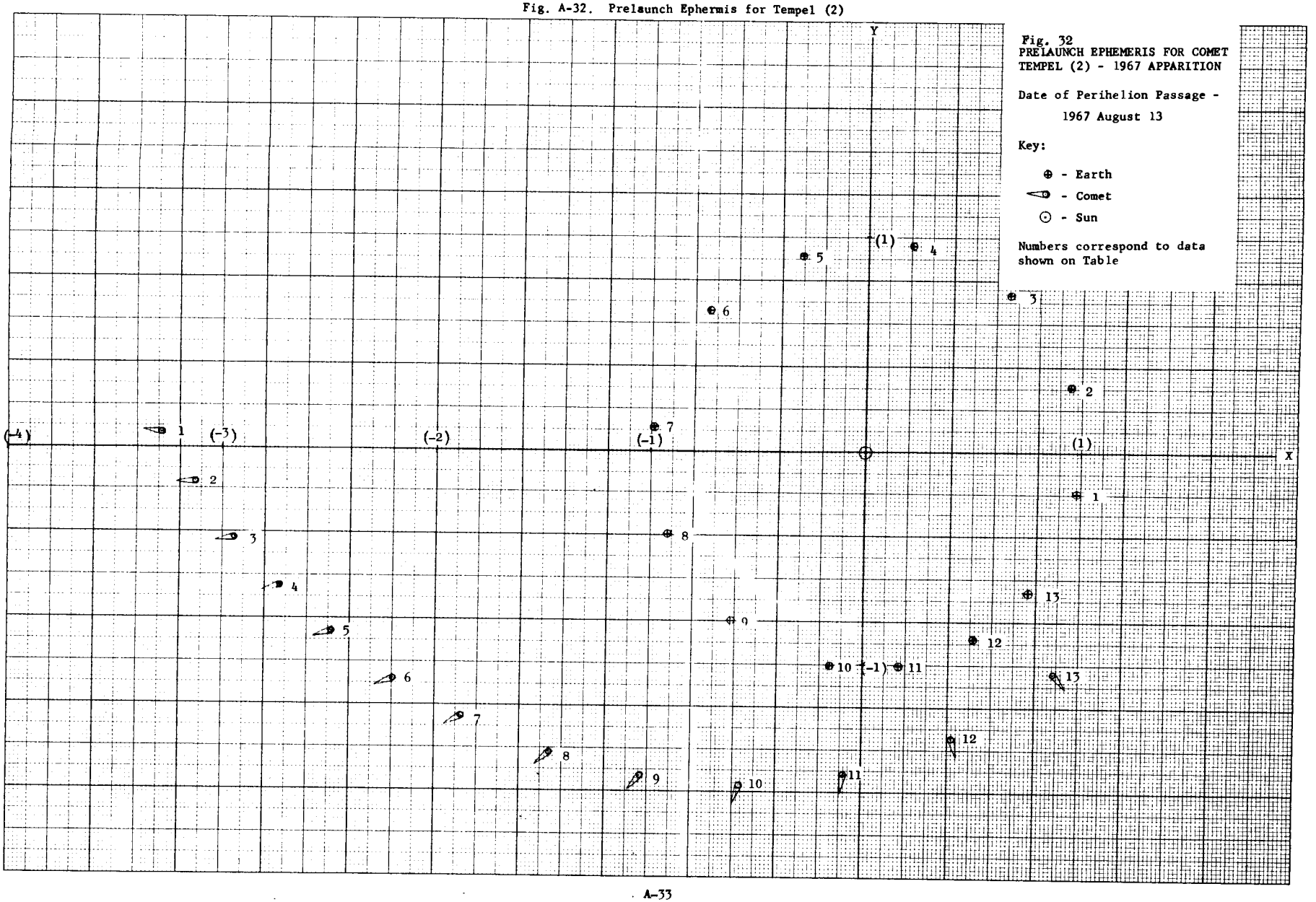

Fig. 32
PRELAUNCH EPHEMERIS FOR COMET TEMPEL (2) - 1967 APPARITION

Date of Perihelion Passage - 1967 August 13

Key:

⊕ - Earth
Comet
⊙ - Sun

Numbers correspond to data shown on Table

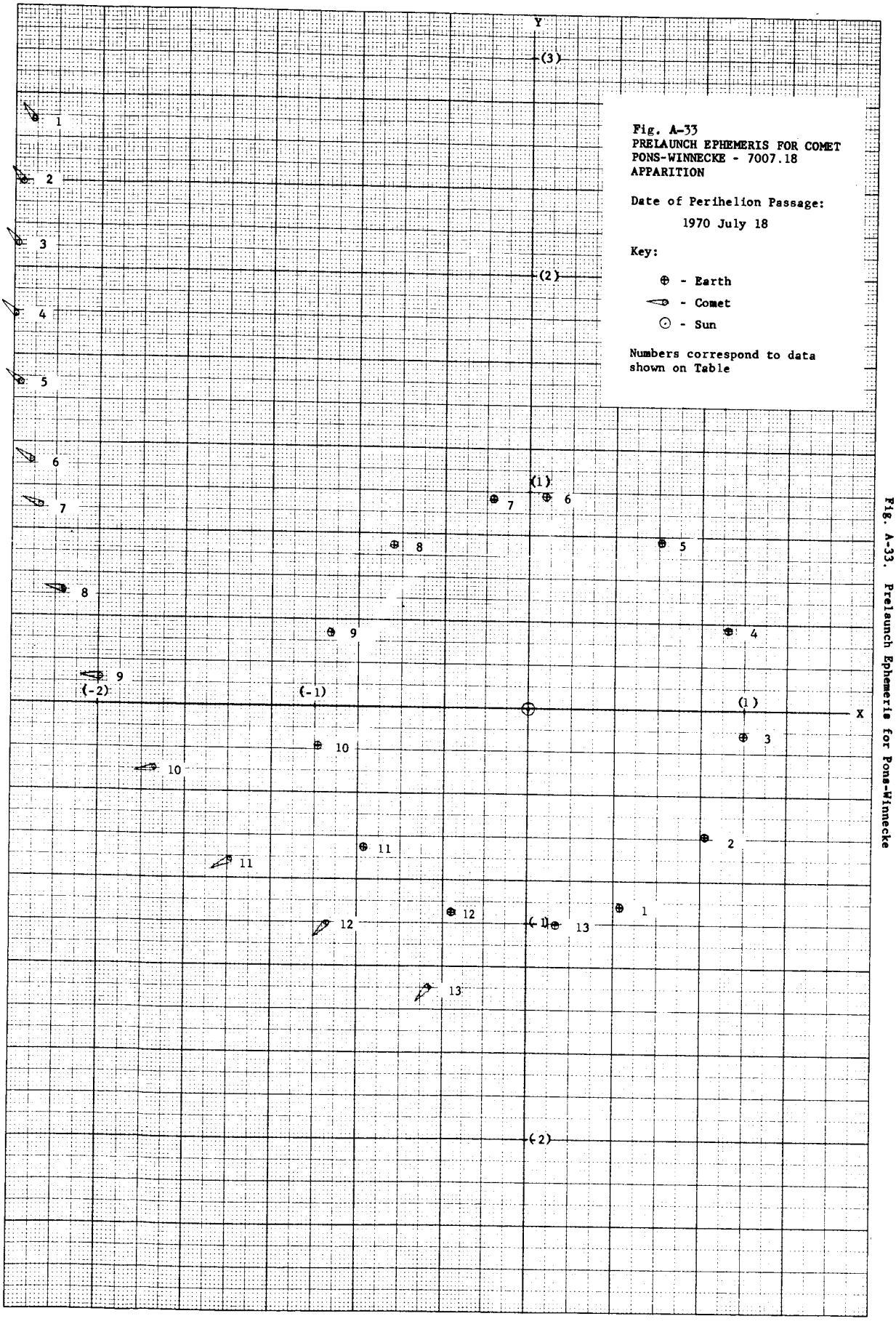

Fig. A-33. Prelaunch Ephemeris for Pons-Winnecke

Fig. A-34. Prelaunch Ephemeris for Kopff

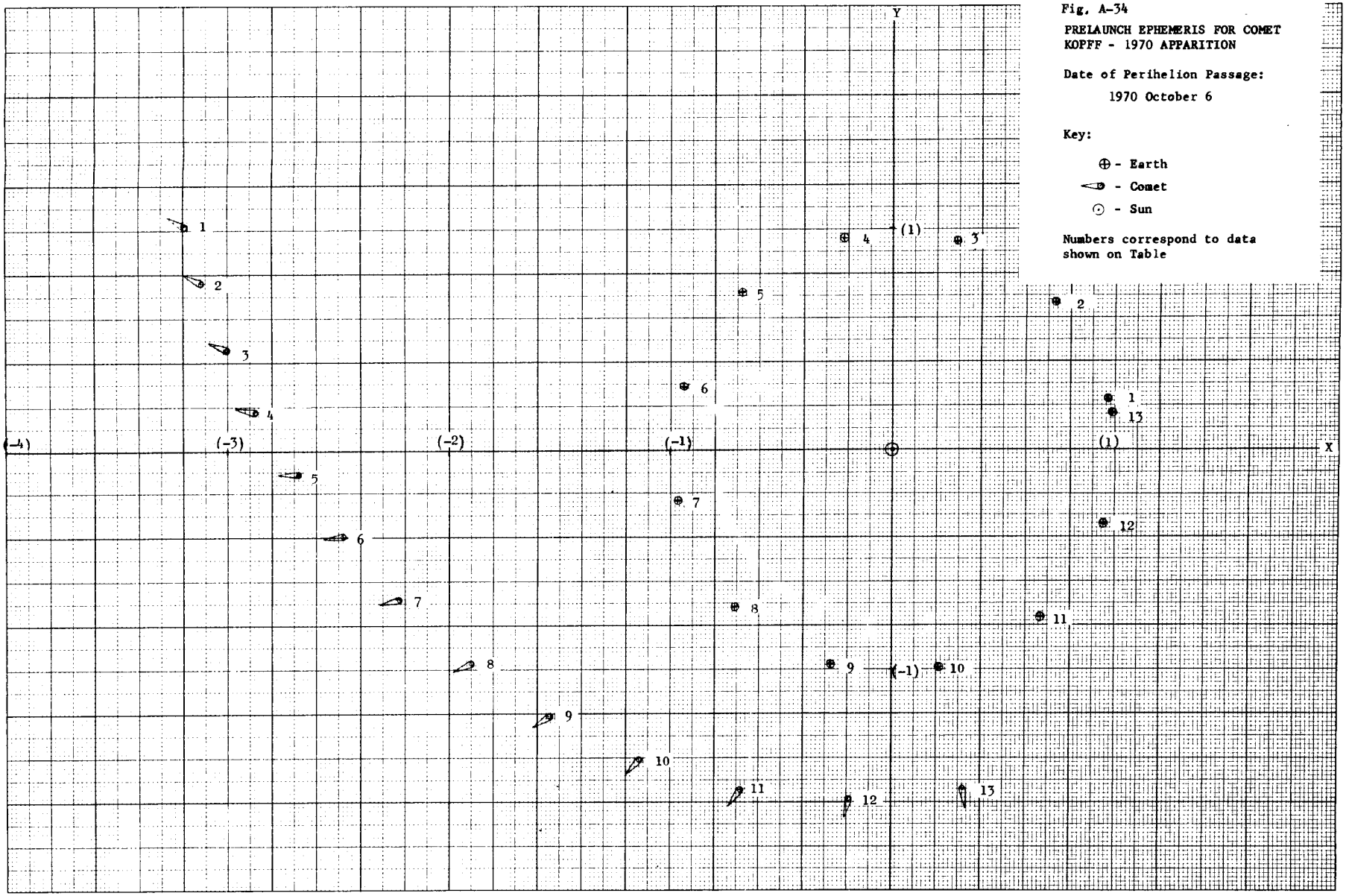

Fig. A-34

PRELAUNCH EPHEMERIS FOR COMET KOPFF - 1970 APPARITION

Date of Perihelion Passage:

1970 October 6

Key:

⊕ - Earth

- Comet

⊙ - Sun

Numbers correspond to data shown on Table

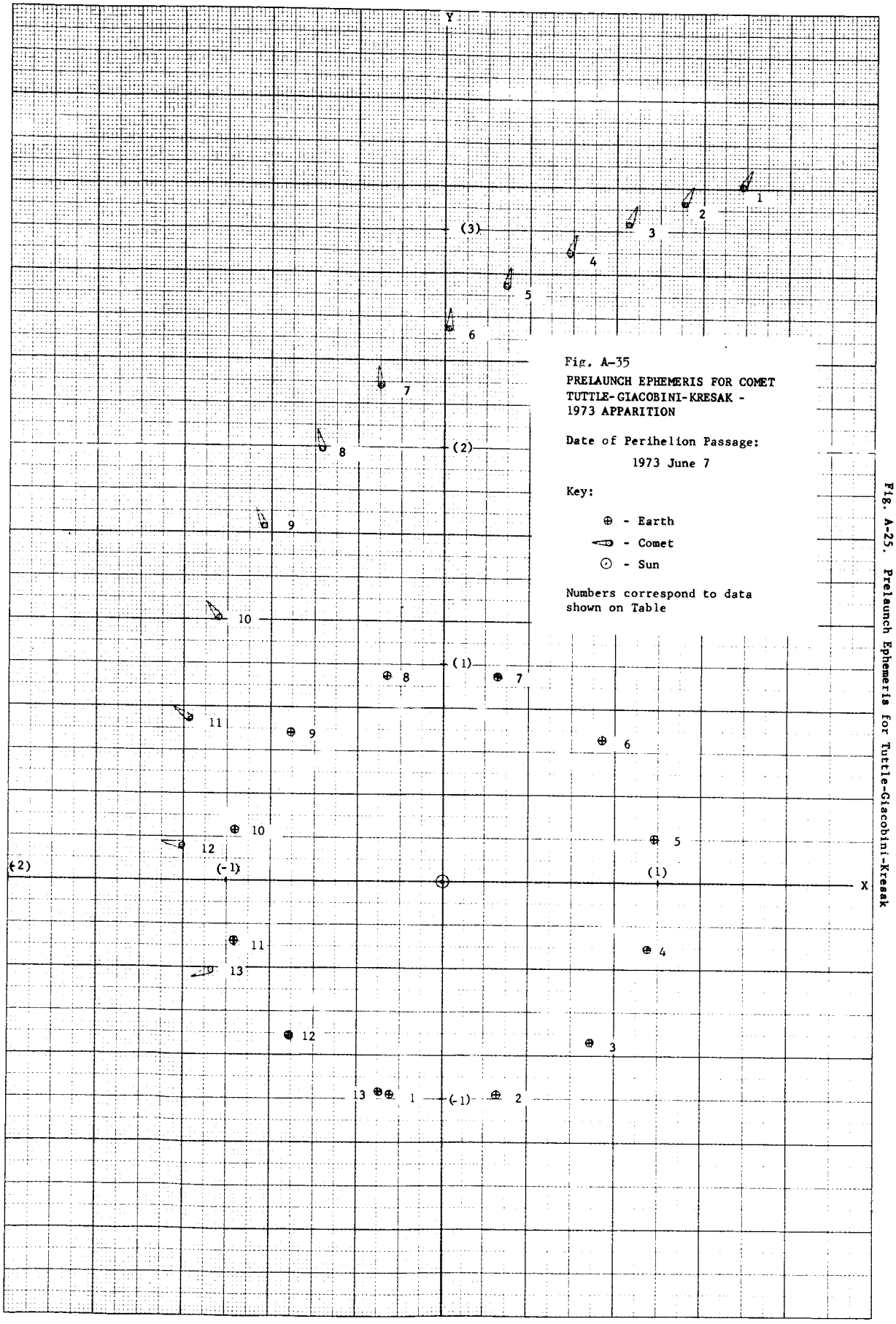

Fig. A-25. Prelaunch Ephemeris for Tuttle-Giacobini-Kresak

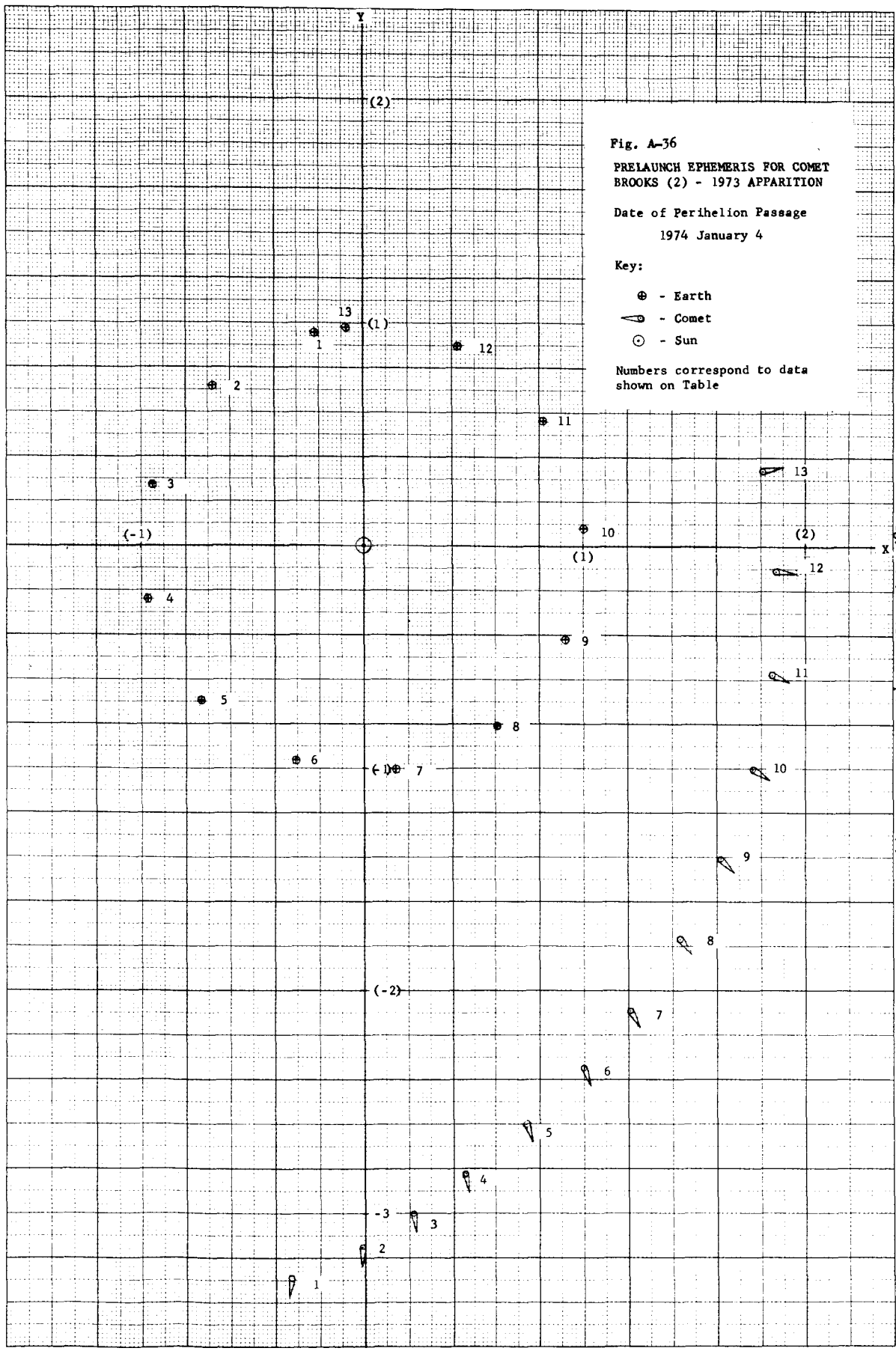

Fig. A-36

PRELAUNCH EPHEMERIS FOR COMET BROOKS (2) - 1973 APPARITION

Date of Perihelion Passage

1974 January 4

Key:

⊕ - Earth

- Comet

⊙ - Sun

Numbers correspond to data shown on Table

Fig. A-36. Prelaunch Ephemeris for Brooks (2)

Fig. A-37 Ecliptic Latitude of Comet vs Date
Tempel (2) 1967
Perihelion Date 6708.13
Ecliptic Declination of Comet (Deg.)
Date
Perihelion Passage
Jun 19
Jul 9
29
Aug 8
29
Sep 7
17
27
Oct 7
17
27
Nov 6
16
26
8
7
6
5
4
3
2
1
0
-1
-2
-3
-4
-5
-6

Fig. A-38 Ecliptic Latitude of Comet vs Date

Pons-Winnecke 1970

Perihelion Date 7007.18

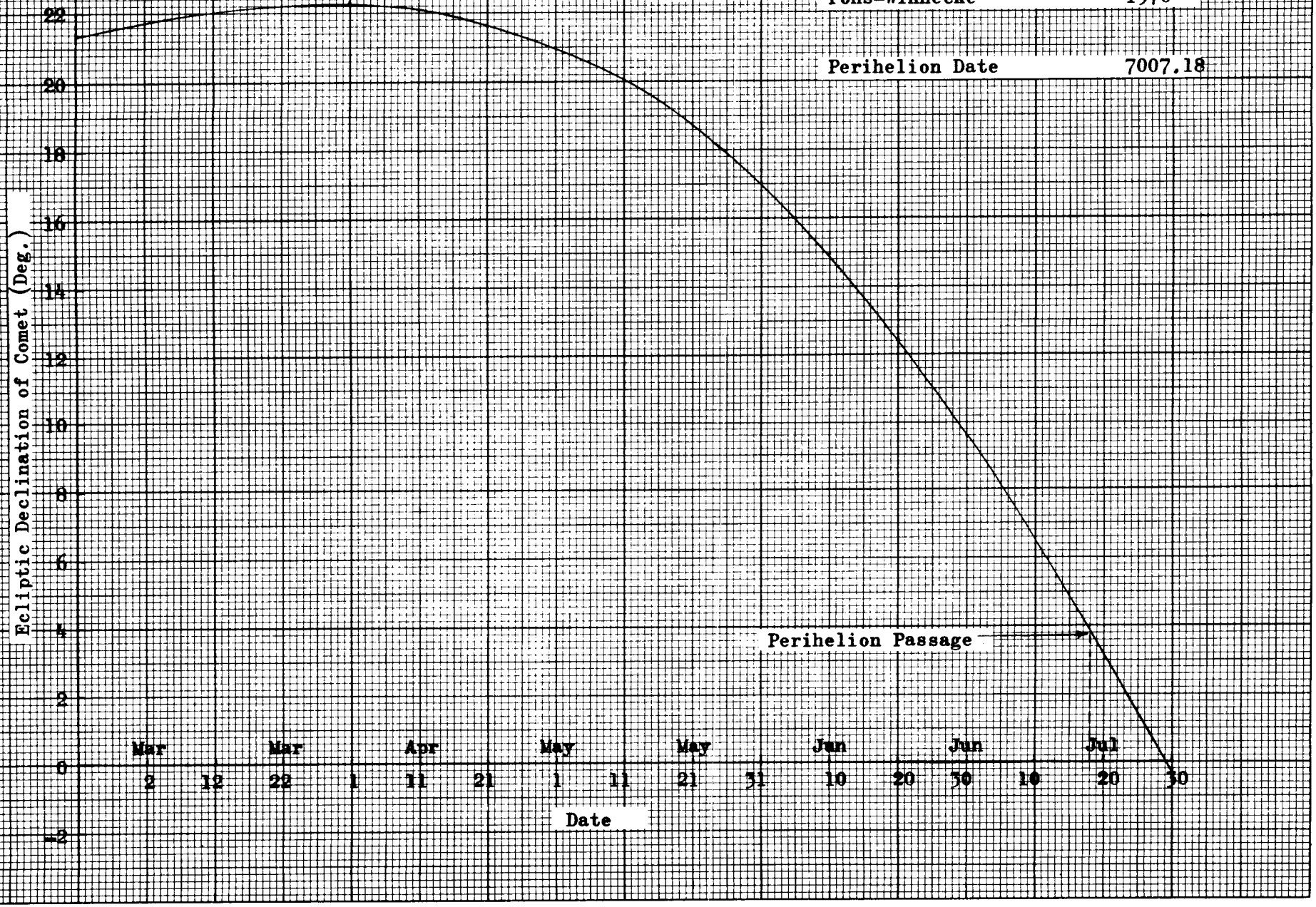

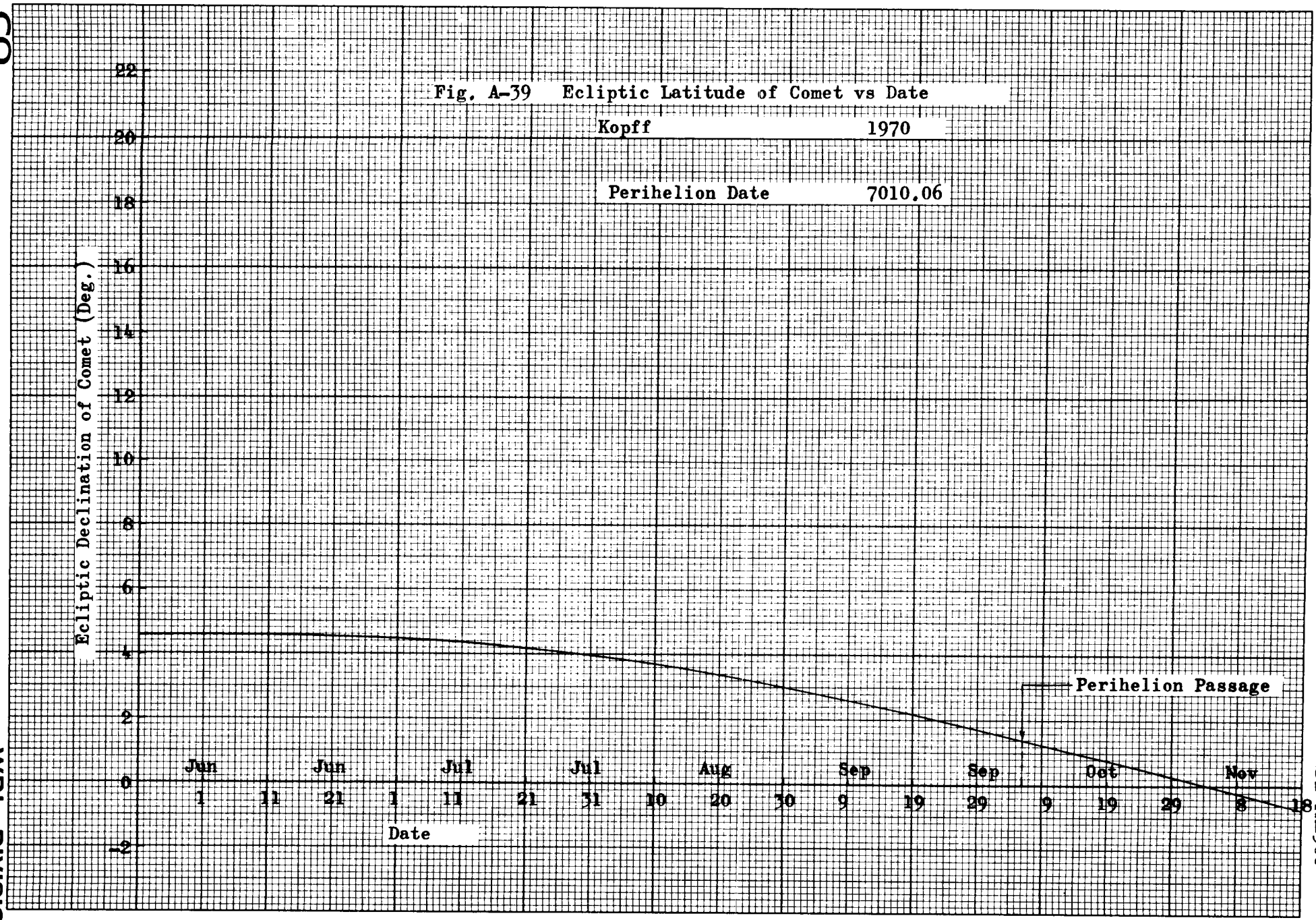

Fig. A-39 Ecliptic Latitude of Comet vs Date

Fig. A-40 Ecliptic Latitude of Comet vs Date
Tuttle-Giacobini-Kresak 1972
Perihelion Date 7306.07
Ecliptic Declination of Comet (Deg.)
-12
-10
-8
-6
-4
-2
0
2
4
6
8
10
12
Jan 27
Feb 16
6
26
Mar 8
18
28
Apr 7
17
27
May 7
17
27
Jun 6
16
26
Date
Perihelion Passage

Fig. A-41 Ecliptic Latitude of Comet vs Date

Brooks(2) 1973

Perihelion Date 7401.04

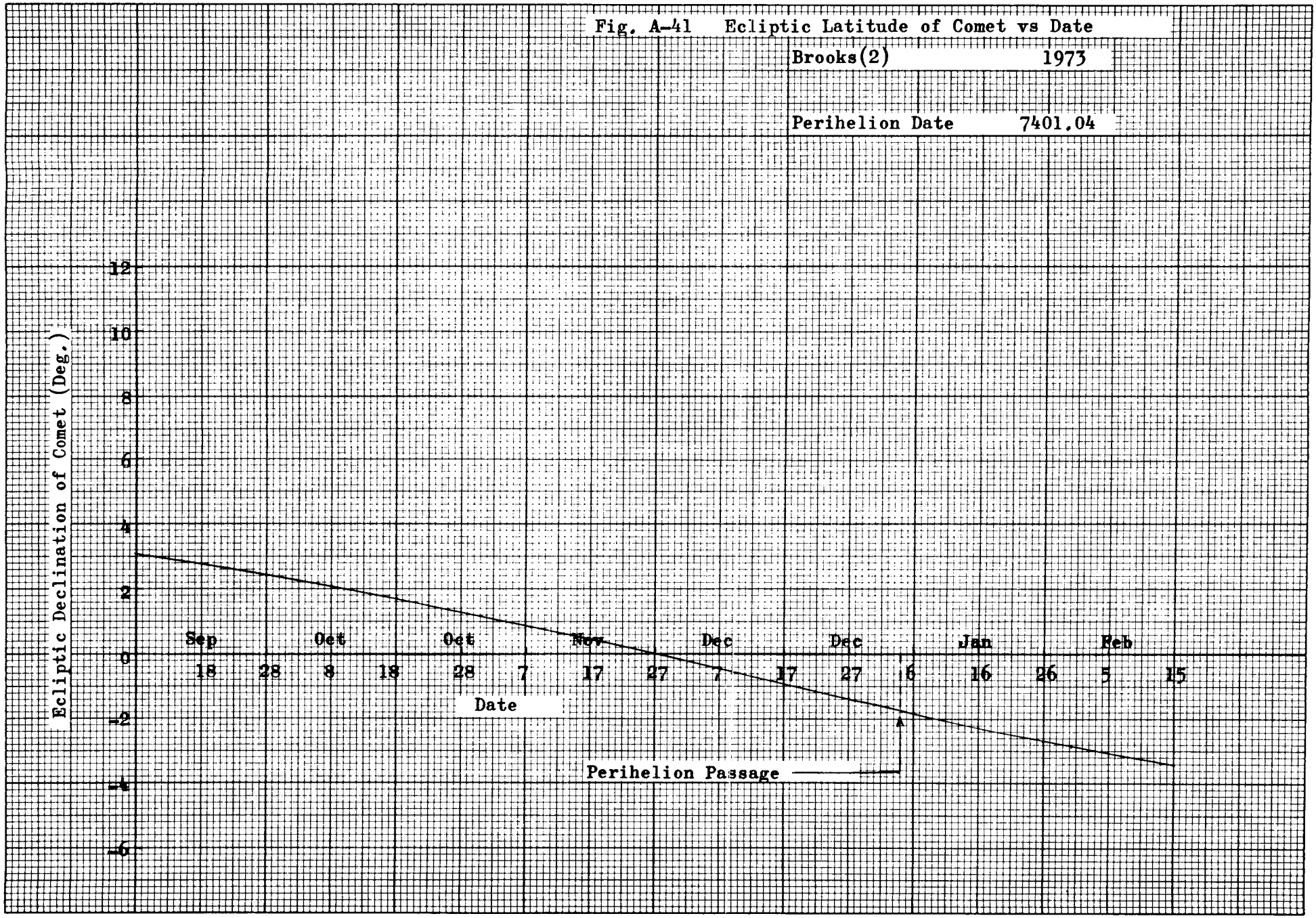

APPENDIX B

COMET TRAJECTORY AND GUIDANCE CHARACTERISTICS

Tempel (2)	B1	B2	B7
Pons-Winnecke	B1	B3	--
Kopff	B1	B4	B8
Tuttle-Giacobini-Kresak	B1	B5	--
Brooks (2)	B1	B6	--

Table No.

B1	Orbital Element Comparisons
B2-B6	Prelaunch Ephemeris Tables
B7-B8	Detailed Orbital Comparisons Obtained from Numerical Integrations
B9-B10	Orbital Element Comparisons

Table B-1 Orbital Element Comparisons

COMET		a (km)	e	i (Deg)	Ω (Deg)	ω (Deg)	T_P	ΔT_P (Days)
Tempel (2)	a	3.02	0.548	12.5	119.3	191.0	1967 Aug 18	-5
	b	3.025	0.548	12.48	119.27	190.95	1967 Aug 13	
Pons-Winnecke	a	3.35	0.653	21.7	94.4	170.2	1970 Jul 9	9
	b	3.426	0.636	22.32	92.79	172.23	1970 Jul 18	
Kopff	a	3.42	0.556	4.7	121.0	161.7	1970 Sep 7	29
	b	3.456	0.547	4.73	120.45	162.72	1970 Oct 6	
Arend-Rigaux	a	3.56	0.611	17.2	124.6	326.4	1971 Feb 9	51
	b	3.601	0.599	17.84	121.56	328.94	1971 Apr 1	
Tuttle-Giacobini-Kresak	a	3.11	0.641	13.8	165.6	37.9	1973 Apr 13	55
	b	3.141	0.634	13.61	165.17	38.76	1973 Jun 7	
Brooks (2)	a	3.56	0.505	5.6	176.9	197.1	1973 Nov 26	39
	b	3.616	0.491	5.55	176.29	198.16	1974 Jan 4	

a - JPL E.P.D. 224

b - IITR Report No. T-7

Fig. B-1 Schematic of Sun-Earth-Comet Geometry

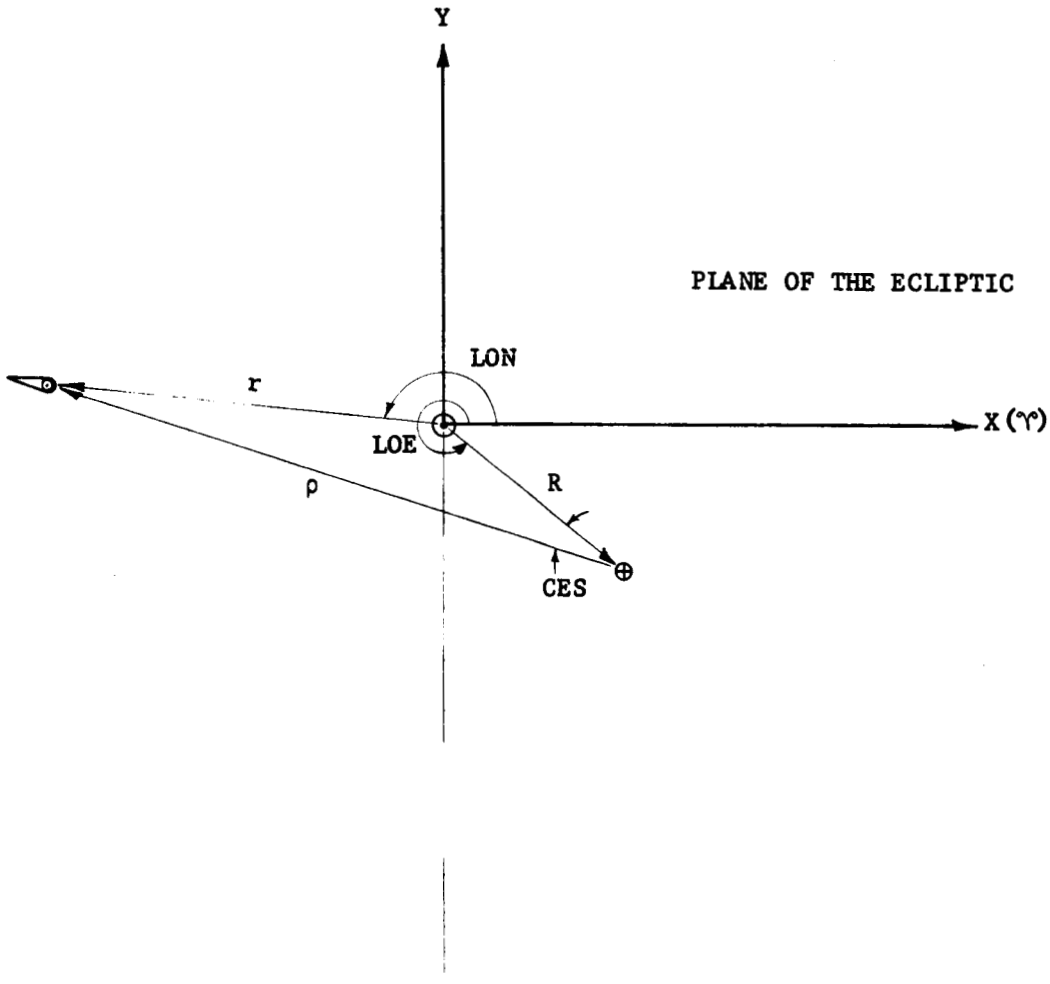

RAC - RT. Ascension of Comet

RAS - RT. Ascension of Sun

RAM - RT. Ascension of Moon

TEMPEL (2)

Table B-2 Prelaunch Ephemeris Data

No. On Graph	Date	Distances (A.U.)			Predicted Comet Magnitude	Angle Data (Deg.)							Comments
						Equatorial				Ecliptic			
		R	r	ρ		RAC	RAS	RAM	DECC	LOE	LON	CES	
	1966												
1	Aug 13	1.014	3.296	4.120	21.4	174.06	141.20	91.86	11.97	319.58	178.84	-40.49	
2	Sep 2	1.007	3.144	4.113	21.3	182.97	169.48	132.75	8.05	348.56	183.05	-25.18	
3	Oct 12	0.998	2.984	3.955	21.1	192.92	196.59	170.28	3.96	17.99	187.71	11.68	
4	Nov 11	0.990	2.814	3.657	20.8	203.75	225.45	204.92	-0.02	47.92	192.94	36.73	
5	Dec 11	0.985	2.636	3.242	20.4	215.36	257.24	241.38	-3.55	78.26	198.86	60.17	
	1967												
6	Jan 10	0.984	2.452	2.747	19.8	227.61	290.37	280.94	-6.23	108.81	205.67	83.30	Acquisition
7	Feb 9	0.987	2.261	2.214	19.2	240.24	321.73	318.24	-7.67	139.41	213.62	105.31	
8	Mar 15	0.995	2.041	1.632	18.3	254.33	354.02	325.39	-7.40	173.48	224.44	128 02	
9	Apr 14	1.003	1.849	1.171	17.4	265.58	21.40	65.47	-5.55	203.13	236 06	145 42	Launch
10	May 14	1.011	1.669	0.80	16.3	274.31	49.88	104.02	-3.24	232.29	250.17	159.83	Opposition
11	Jun 13	1.016	1.516	0.54	15.3	279.04	80.29	143.34	-3.90	261.08	267.20	-170.93	
12	Jul 13	1.017	1.408	0.40	14.5	280.81	111.31	179.15	-13.63	289.70	287.18	-176.34	
13	Aug 12	1.014	1.367	0.40	14.4	287.70	140.81	214.48	-29.97	319.30	309.95	-170.60	Perihelion

Table B-3 Prelaunch Ephemeris Data

No. On Graph	Date	Distances (A.U.)			Predicted Comet Magnitude	Angle Data (Deg.)							Comments
						Equatorial				Ecliptic			
		R	r	ρ		RAC	RAS	RAM	DECC	LOE	LON	CES	
	1969												
1	Jul 18	1.017	3.547	4.510	22.4	132.93	116.87	155.01	29.20	294.93	130.94	-21.30	
2	Aug 17	1.013	3.371	4.347	22.2	143.02	145.97	185.54	27.05	323.64	134.43	17.77	
3	Sep 16	1.006	3.186	4.030	21.9	153.67	173.28	219.08	24.66	352.68	138.37	37.57	
4	Oct 16	0.997	2.991	3.584	21.5	164.65	200.51	259.93	22.30	22.18	142.85	60.89	
5	Nov 15	0.990	2.787	3.047	21.0	175.76	229.77	303.47	20.41	52.18	148.04	84.45	
6	Dec 15	0.985	2.575	2.468	20.4	186.78	261.91	340.96	19.71	85.57	154.15	107.30	Acquisition
	1970												
7	Jan 1	0.984	2.450	2.143	20.0	192.81	280.75	188.67	20.20	99.88	158.13	119.54	
8	Jan 31	0.986	2.225	1.617	19.2	202.39	312.87	221.24	23 43	130.42	166.37	138.87	Launch
9	Mar 2	0.992	1.995	1.200	18.3	208.85	342.20	261.10	30.27	160.71	176.60	152.93	Opposition
10	Apr 1	1.000	1.768	0.922	17.5	208.78	9.72	303.84	38.70	190.57	189.57	-157.80	
11	May 1	1.008	1.555	0.765	16.8	201.56	37.52	341.50	41.45	219.93	206.06	-155.29	
12	May 31	1.015	1.377	0.668	16.2	197.15	67.14	15.66	31.99	248.86	226.59	-152.54	
13	Jun 30	1.017	1.267	0.609	15.8	203.06	98.19	51.52	10.46	277.51	250.49	-151.67	Perihelion

Table B-4 Prelaunch Ephemeris Data

No. On Graph	Date	Distance (A.U.)			Predicted Comet Magnitude	Angle Data (Deg.)							Comments
						Equatorial				Ecliptic			
		R	r	ρ		RAC	RAS	RAM	DECC	LOE	LON	CES	
	1969												
1	Oct 6	1.000	3.366	4.26		170.86	191.30	133.36	6.65	12.29	162.23	30.21	
2	Nov 5	0.992	3.207	3.85		180.01	219.69	163.60	3.09	42.13	166.50	55.70	
3	Dec 5	0.986	3.041	3.34	21.5	188.87	250.93	192.91	-0.19	72.41	171.22	81.20	
	1970												
4	Jan 4	0.984	2.870	2.76	20.9	196.83	284.06	226.21	-2.74	102.94	176.50	106.4	Acquisition
5	Feb 3	0.987	2.694	2.18	20.5	202.75	315.93	266.66	-3.97	133.47	182.47	130.86	Launch
6	Mar 5	0.993	2.514	1.68	19.6	204.82	345.00	308.72	-3.22	163.72	189.29	154.08	
7	Apr 4	1.001	2.332	1.34	18.7	201.40	12.45	345.40	-0.35	193.53	197.17	174.13	Opposition
8	May 6	1.009	2.142	1.22	18.3	194.58	42.31	45.71	2.74	224.78	207.05	-161.67	
9	Jun 5	1.015	1.971	1.29		192.51	72.26	83.51	2.40	253.65	218.01	-144.10	
10	Jul 5	1.017	1.815	1.42		197.72	103.35	120.21	-1.42	282.29	230.95	-128.53	
11	Aug 4	1.015	1.688	1.56		209.20	133.38	152.10	-7.50	310.93	246.07	-115.08	
12	Sep 3	1.009	1.601	1.69		225.80	161.35	181.23	-14.44	339.80	263.20	-103.39	
13	Oct 3	1.001	1.567	1.82		246.80	188.34	212.22	-20.40	9.08	281.64	-92.56	Perihelion

TUTTLE-GIACOBINI-KRESAK

Table B-5 Prelaunch Ephemeris Data

No. On Graph	Date	Distances (A.U.)			Predicted Comet Magnitude	Angle Data (Deg.)							Comments
						Equatorial				Ecliptic			
		R	r	ρ		RAC	RAS	RAM	DECC	LOE	LON	CES	
	1972												
1	Jun 7	1.015	3.501	5.823		68.79	74.83	10.61	11.43	256.03	66.73	-16.32	
2	Jul 7	1.017	3.333	4.193		78.25	105.91	49.26	12.23	284.66	70.30	36.63	
3	Aug 6	1.015	3.155	3.766		87.90	135.78	92.06	12.06	313.31	74.27	60.00	
4	Sep 5	1.009	2.965	3.235		97.18	163.59	131.31	10.84	342.21	78.73	83.66	
5	Oct 5	1.001	2.764	2.647		105.30	190.60	164.45	8.55	11.53	83.81	107 21	Launch
6	Nov 4	0.992	2.553	2.055		110.98	218.92	195.35	5.41	41.35	89.71	130.31	
7	Dec 7	0.986	2.307	1.484		111.88	253.36	266.84	1.83	74.67	97.46	154.11	
	1973												
8	Jan 6	0.984	2.074	1.129	20.7	105.63	286.51	302.21	0.60	105.21	106.08	168.24	(Acquisition) Opposition
9	Feb 5	0.986	1.836	0.986		96.35	318.19	335.33	3.94	135.73	116.82	-158.58	
10	Mar 7	0.990	1.601	0.990		94.03	347.08	8.59	10.68	165.96	130.59	-143.88	
11	Apr 6	1.001	1.385	1.018		102.83	144.92	46.22	17.54	195.73	148.64	-132.78	
12	May 6	1.009	1.219	1.009		121.97	42.54	88.57	22.31	225.01	172.24	-127.21	
13	Jun 7	1.015	1.150	0.978		149.76	72.51	128.71	22.46	253.87	201.07	-126.76	Perihelion

BROOKS (2)

Table B-6 Prelaunch Ephemeris Data

No. On Graph	Date	Distance (A.U.)			Predicted Comet Magnitude	Angle Data (Deg.)							Comments
						Equatorial				Ecliptic			
		R	r	ρ		RAC	RAS	RAM	DECC	LOE	LON	CES	
	1973												
1	Jan 4	0.984	3.310	4.249		268.34	284.31	276.50	-19.12	103.17	264.06	19.87	
2	Feb 3	0.987	3.165	3.922		279.50	316.17	311.01	-18.68	133.70	268.76	45.21	
3	Mar 5	0.993	3.015	3.480		290.42	345.22	343.48	-17.31	163.96	273.92	70.13	
4	Apr 4	1.001	2.864	2.965	21.3	300.42	126.66	171.32	-15.18	193.76	279.63	94.12	(Acquisition)
5	May 4	1.009	2.711	2.426	20.7	308.70	40.62	55.88	-12.67	223.07	285.47	116.98	Launch
6	Jun 3	1.015	2.559	1.918		314.11	70.45	98.28	-10.41	251.96	293.06	138.65	
7	Jun 30	1.017	2.424	1.539		315.25	98.43	90.92	-9.40	277.74	300.19	157.10	
8	Jul 30	1.016	2.281	1.272		311.68	128.75	130.93	-10.35	306.36	309.08	175.11	Opposition
9	Aug 29	1.011	2.148	1.213		306.54	157.01	165.69	-13.08	335.19	319.10	-163.57	
10	Sep 28	1.003	2.031	1.326		306.65	184.03	198.45	-15.35	4.39	330.33	-145.86	
11	Oct 28	0.994	1.937	1.528		314.23	211.84	232.53	-15.56	34.09	342.78	-128.67	
12	Nov 27	0.987	1.873	1.760		327.22	242.28	267.90	-13.22	64.27	356.28	-112.01	
13	Dec 27	0.984	1.843	2.002		343.11	275.18	301.86	-8.55	94.76	10.46	-95.71	Perihelion

Table B-7 Orbital Element Comparisons for Tempel (2)

EPOCH	T_{PW} Date	T_{PF} Hours	Min.	SMA KM x 10^9	ECC	LAN DEG.	INC DEG.	APF DEG.	COMMENTS
Feb 11, 1957	Feb 4, 1957	22	35	0.4528 3067	0.5475 7533	119. 27799	12. 470098	191. 012888	Program Starter Data (WDL)
Feb 11, 1957	Feb 4, 1957	22	35	0.4528 317	0.5475 763	119. 2780	12. 4701	191. 0129	Data taken from BAA Handbook 1956
May 12, 1962	May 12, 1962	04	17	0.4523 7915	0.5488 7873	119. 27374	12. 481857	191. 03197	Computed Perihelion (WDL)
May 16, 1962	May 12, 1962	05	39						Predicted Perihelion by Marsden (BAA Handbook, 1962, UAIC 1747)
	May 12, 1962	14	24						Observed Perihelion by Miss Roemer (UAIC 1757)
Aug 13, 1967	Aug 13, 1967	11	47	0.4526 3162	0.5482 8814	119. 26879	12. 473889	190. 95732	Computed Perihelion (WDL)
	Aug 13, 1967			0.4522	0.548	119. 27	12. 48	190. 95	Computed Perihelion from IITR, Report No. T-7
Nov 14, 1972	Nov 14, 1972	00	38	0.4524 2662	0.5487 8443	119. 26707	12. 480415	190. 85239	Computed Perihelion (WDL)
	Nov 13, 1972			014520	0.549	119. 27	12. 48	190. 85	Computed Perihelion from IITR, Report No. T-7
Feb 19, 1978	Feb 19, 1978	11	15	0.4530 2217	0.5472 2835	119. 24015	12. 467990	190. 91372	Computed Perihelion (WDL)

A.U. to KM Conversion Used = .149599 x 10^9 KM/A.U.

Table B-8 Orbital Element Comparisons for Kopff

EPOCH	T_{PW} Date	T_{PF} Hours	Min.	SMA KM x 10^9	ECC	LAN DEG.	INC DEG.	APF DEG.	COMMENTS
Sept 14, 1958	Jan 20, 1958	11	01	0.5108 0383	0.5555 2526	120. 91165	4.70 65945	161. 80780	Program Starter Data (WDL)
Sept 14, 1958	Jan 20, 1958	11	01	0.5108 045	0.5555 257	120. 91167	4.70 6586	161. 80786	Data taken from ACTA Astronomica 13, 87, 1963
May 16, 1964	May 16, 1964	00	43	0.5108 7769	0.5550 1427	120. 86889	4.70 74632	161. 92584	Computed Perihelion (WDL)
May 5, 1964	May 16, 1964	00	55	(Not given in standard form)					Predicted Perihelion by Kepinsk, ACTA Astronomica 13, 195, 1963
	May 16, 1964	03	40						Observed Perihelion by Miss Roemer (UAIC 1854)
Oct 2, 1970	Oct 2, 1970	03	36	0.5165 0055	0.5461 5861	120. 38276	4.72 38458	162. 76317	Computed Perihelion (WDL)
	Oct 6, 1970			0.5166	0.547	120. 45	4.73	162. 72	Computed Perihelion from IITR, Report No. T-7
Mar 7, 1977	Mar 7, 1977	20	15	0.5172 7307	0.5453 8846	120. 33073	4.72 40894	162. 91017	Computed Perihelion (WDL)

A.U. TO KM Conversion Used = .149599 x 10^9 KM/A.U.

APPENDIX C

EROS TRAJECTORY CHARACTERISTICS

Figure No.

All data presented was generated using orbital element data provided by Dr. L. E. Cunningham, WDL consultant.

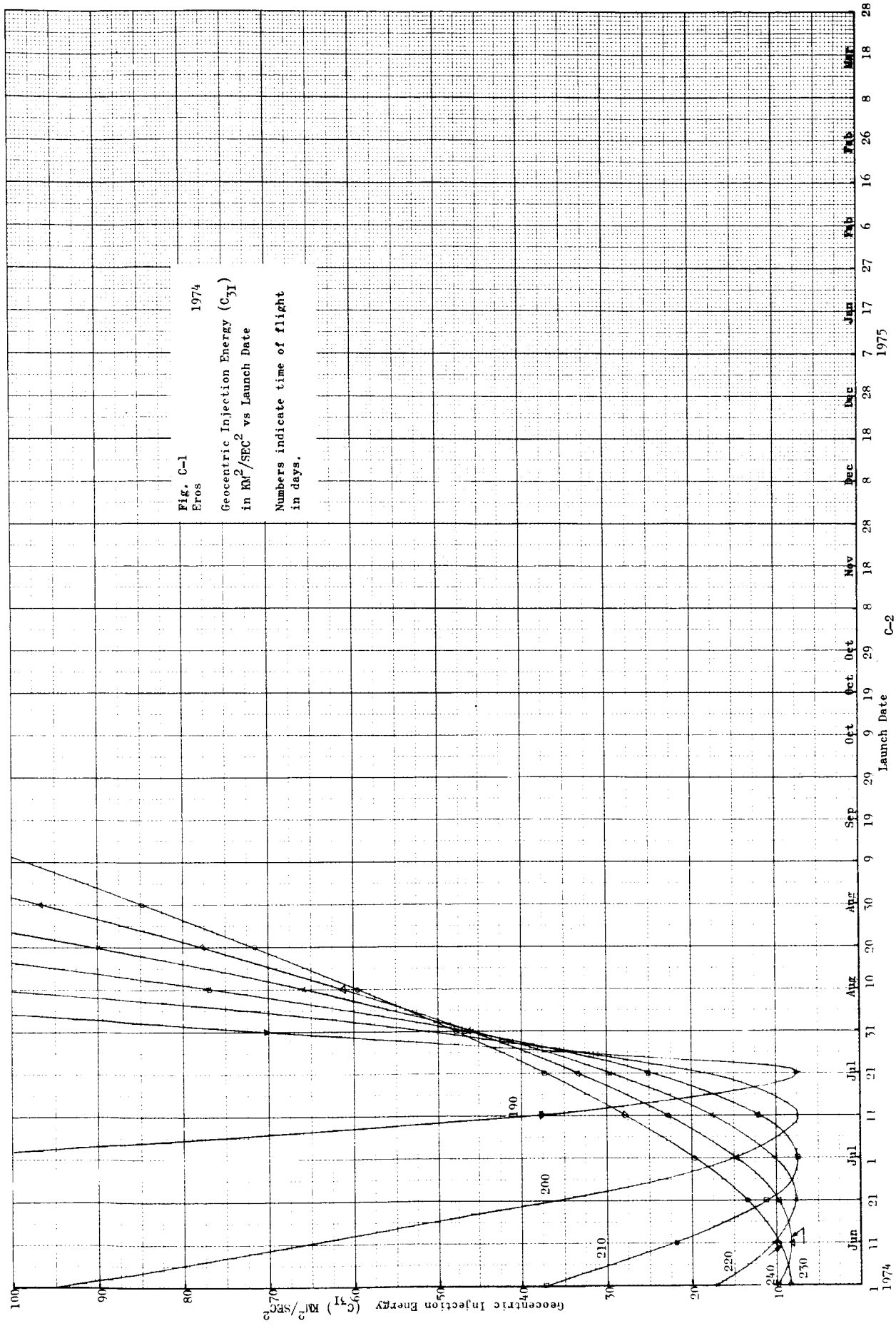
Fig. C-1
Eros
1974
Geocentric Injection Energy (C_{3I})
in KM^2/SEC^2 vs Launch Date
Numbers indicate time of flight
in days.
Geocentric Injection Energy (C_{3I}) KM^2/SEC^2
Launch Date
1974
1975
Jun
Jul
Aug
Sep
Oct
Nov
Dec
Jan
Feb
Mar
190
200
210
220
230
240

Fig. C-2 Target Arrival Conditions vs Launch Date for Eros 1974

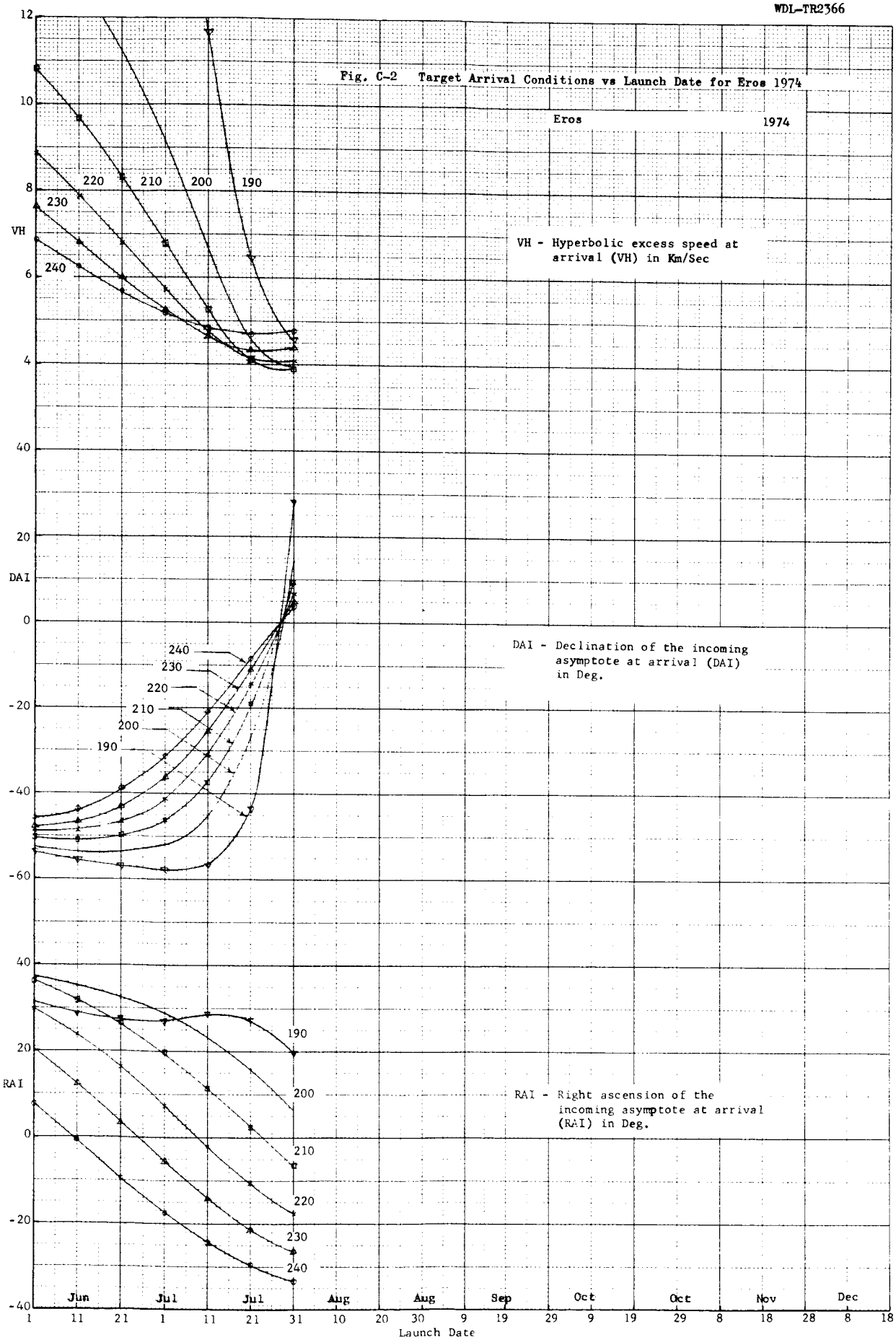

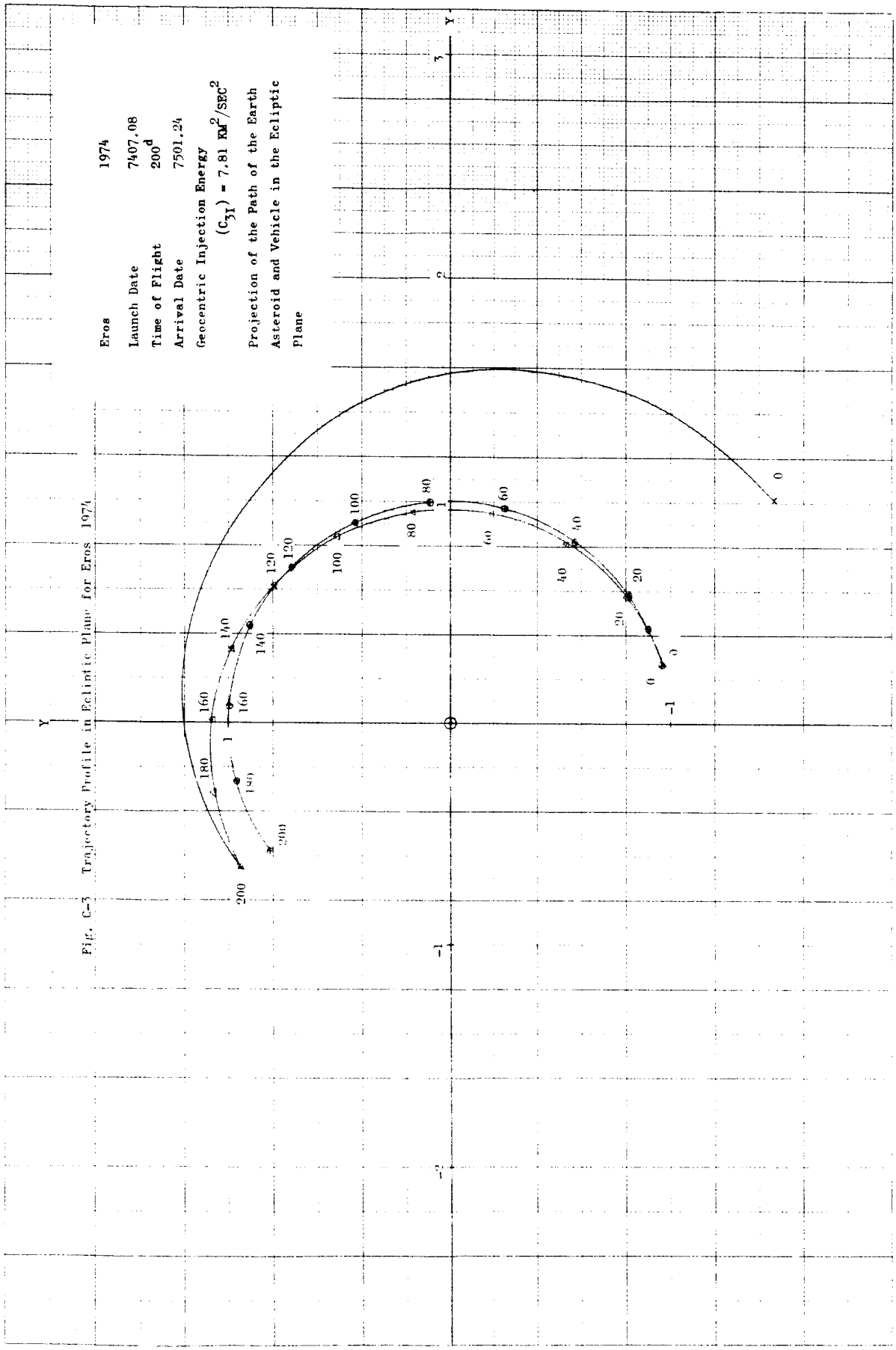

Fig. C-3 Trajectory Profile in Ecliptic Plane for Eros 1974